Internal Note No. 69-FM-127

NATIONAL AERONAUTICS AND SPACE ADMINISTRATION

MSC INTERNAL NOTE NO. 69-FM-127

May 12, 1969

APOLLO 10 (MISSION F) VEHICLE AND TRAJECTORY RESPONSE TO THE CSM POWERED FLIGHT MANEUVERS

Guidance and Performance Branch

MISSION PLANNING AND ANALYSIS DIVISION

MANNED SPACECRAFT CENTER
HOUSTON, TEXAS

MSC INTERNAL NOTE NO. 69-FM-127

PROJECT APOLLO

APOLLO 10 (MISSION F) VEHICLE AND TRAJECTORY RESPONSE TO THE CSM POWERED FLIGHT MANEUVERS

By James L. Wells, Jr.
Guidance and Performance Branch

May 12, 1969

MISSION PLANNING AND ANALYSIS DIVISION
NATIONAL AERONAUTICS AND SPACE ADMINISTRATION
MANNED SPACECRAFT CENTER
HOUSTON, TEXAS

Approved: Marlowe D. Cassetti
Marlowe D. Cassetti, Chief
Guidance and Performance Branch

Approved: for O. L. Owens
John P. Mayer, Chief
Mission Planning and Analysis Division

CONTENTS

FIGURES

APOLLO 10 (MISSION F) VEHICLE AND TRAJECTORY RESPONSE TO THE CSM POWERED FLIGHT MANEUVERS

By James L. Wells, Jr.

1.0 SUMMARY

These simulations were generated to determine what typical response could be expected on the onboard displays, DSKY displays, and ground trajectory displays during each SPS burn.

For each maneuver, the primary guidance system (G&N) performed the maneuver and drove the FDAI-1. The SCS system was alined at the beginning of each burn and drove the FDAI-2 during the burn for monitoring purposes. For each SPS maneuver, time histories are presented for SPS engine angles, vehicle body rates, IMU gimbal angles, attitude angles, SCS rates, SCS attitudes and attitude errors, t_{GO}, V_{GO}, V_g components in control coordinates, EMS decremented ΔV, cross-axis velocity errors, predicted apogee and perigee, altitude, and V_i versus γ_i.

Each burn is discussed separately to explain the characteristic responses that are shown in the figures. The discussion also includes an explanation of the velocity residuals at the end of each burn.

2.0 INTRODUCTION

The intent of this document is to present time histories of the G&N control response that drives the FDAI-1, the DSKY parameters that are generated during and after the burn, the SCS monitoring parameters available on FDAI-2, and the trajectory parameters that can be monitored on the ground. The updated DAP as defined in reference 1 was used for this study.

These trajectory simulations were initiated by use of the operational reference trajectory. These six-degree-of-freedom cases simulated the G&N guidance and control system, the SCS system, and the EMS system. These simulations did not contain slosh and bending effects. Each time history figure represented in this document is referenced to SPS ignition for that particular burn.

Each maneuver consisted of the following sequence.

a. Coast

b. Guidance precomputation

c. Realinement and reorientation

d. Average g ON at t_{IG} = 30 seconds

e. SPS burn

The IMU was alined so that the FDAI-1 read 0°, 0°, 0° (roll, pitch, and yaw) at SPS ignition (preferred alinement), and the SCS was alined so that FDAI-2 read 0°, 0°, 0° (roll, pitch, and yaw) from the BMAG's at SPS ignition. Because no RCS ullage was simulated before the SPS maneuver, the displays did not show any deadband errors at SPS ignition as in previous studies. An initial SPS engine mistrim of +0.3° in pitch and +0.3° in yaw was apllied to the SPS engine pitch and yaw angles that appear in table I. The weight and balance data were obtained from reference 2.

In the figures are presented time histories of parameters that are affected by SPS engine misalinement, offset center of gravity, rotational dynamics, and control system corrections. The trajectory parameters and targets before the maneuvers are presented in table I, and the resultant conditions after the maneuvers are presented in table II.

3.0 ABBREVIATIONS

BMAG	body mounted attitude gyro
CSM	command/service modules
DAP	digital autopilot
DSKY	display keyboard
EMS	entry monitoring system
FDAI-1	flight director attitude indicator, command pilot
FDAI-2	flight director attitude indicator, CSM pilot
G&N	guidance and navigation

IMU	inertial measurement unit
LOI-1	lunar orbit insertion maneuver
LOI-2	circularization maneuver
RCS	reaction control system
SCS	stabilization control system
SPS	service propulsion system
TEI	transearth injection
TVC	thrust vector control
t_{GO}	time to go
t_{IG}	time of SPS ignition
V_g components	velocity in control coordinates
V_{GO}	total velocity to go
V_i	inertial velocity
ΔV	velocity change
γ_i	inertial flight-path angle

4.0 SPS BURN PARAMETERS

4.1 Evasive Maneuver

The evasive maneuver consists of a 19.68-fps burn to move the CSM/LM away from the booster. The SPS engine initially is mistrimmed by 0.3° in pitch and 0.3° in yaw (ref. 3). Because an RCS ullage is not required, the vehicle body rates, the IMU gimbal angles, and the attitude errors are all zero at SPS ignition. Ninety percent of full thrust is reached in 0.42 second, and the first DAP output does not occur until 0.66 second. When the TVC DAP comes on, it uses the initial vehicle attitude as a reference point to maintain attitude control and drives the SPS engine

[fig. 1(a)] to damp out the body rates [fig. 1(b)]. For the small ΔV, the onboard computer executes this maneuver with the short burn logic, and the guidance does not have enough time to issue a steering command before SPS cutoff. The body rates remain small, but the IMU gimbal angles [fig. 1(c)] and attitude errors [fig. 1(d)] continue to increase slightly until cutoff. The attitude errors at cutoff were as follows: roll = 0.06°, pitch = -0.14°, and yaw = -0.13°.

The SCS rates [fig. 1(e)], attitudes [fig. 1(f)], and attitude errors [fig. 1(g)] do not cause any noticeable differences in these short burns because guidance is not involved. The G&N body rates and the SCS body rates are obtained from the same source. The t_{GO} calculation [fig. 1(h)] is made in the guidance precomputation and is not updated because of the short evasive burn. The V_{GO} (the V_g calculated by the onboard computer) is shown in figure 1(i), and the V_g's in control coordinates are shown in figure 1(j). These figures show that V_g approaches zero at cutoff (tailoff not shown in figures). After tailoff, there was a velocity error of only 0.12 fps (table II).

The EMS ΔV counter was simulated during each burn, and the results for this maneuver are shown in figure 1(k). The desired velocity was loaded into the ΔV counter and was monitored during this burn.

The cross-axis velocity that is shown in figure 1(l) is an external method (not onboard computer) used to determine the velocity errors normal to the desired thrusting direction that are created during the evasive maneuver. For this burn, the cross-axis velocity error is approximately 0.17 fps at cutoff. The acceleration of this heavy vehicle is so small that the mistrim has very little effect on these short burns. The calculated orbital parameters (earth reference) are shown in figures 1(m), 1(n), and 1(o).

4.2 Midcourse Correction Maneuver

The second CSM/LM SPS burn is G&N controlled with a total external ΔV target of 56.97 fps. No ullage maneuvers are required for the midcourse correction burn. The SPS engine is initially misalined 0.3° in pitch and 0.3° in yaw and the SPS engine starts to damp out the rates that start to build up [fig. 2(a)]. The effects of the SPS engine on the vehicle body rates are shown in figure 2(b). The initial rates are damped out by 2 seconds, and the rates are reversed at approximately 4.5 seconds before being nulled to a constant rate at cutoff. The IMU gimbal angles [fig. 2(c)] and the attitude errors [fig. 2(d)] reflect the effect of the initial mistrim. The maximum attitude error occurred at approximately 6 seconds with a pitch reading of -0.42° and a yaw reading of -0.46°.

Monitoring the FDAI-2 [figs. 2(e), 2(f), and 2(g)] indicated that the G&N was performing normally.

The first and only t_{GO} [fig. 2(h)] is calculated at 4 seconds. It is not updated at 6 seconds because $t_{GO} \leq 4$ seconds, and cutoff occurs at 8.26 seconds. The total velocity to be gained [fig. 2(i)] is decremented from ignition until cutoff. The velocity to be gained in control coordinates is presented in figure 2(j) which shows that most of the V_g is in the X coordinate. The EMS decreases the desired velocity along the X-body axis [fig. 2(k)] from SPS thrust buildup through tailoff. This system is also used to determine whether the G&N is performing efficiently.

The total cross-axis velocity error was computed and is presented in figure 2(l). Because only one steering command was generated during this burn, the effect was not sufficient to null the cross-axis velocity error that was still increasing slightly at cutoff.

The following orbital elements are presented: predicted apogee and perigee [fig. 2(m)], altitude [fig. 2(n)], and inertial velocity versus intertial flight-path angle [fig. 2(o)].

4.3 First Lunar Orbit Insertion Maneuver (LOI-1)

The third SPS burn is a CSM/LM G&N controlled maneuver that will place the vehicle into a lunar orbit. This maneuver requires a total external ΔV target of 2978.36 fps, and a burn duration of approximately 361.4 seconds.

The SPS engine angles [fig. 3(a)] reflect the initial mistrim, its correction, and the tracking of the c.g. until cutoff. The effects of the initial mistrim can be seen during the first 20 seconds of the vehicle body rates [fig. 3(b)]. After that time, the rates are reduced and remain negligible through cutoff. The IMU gimbal angles [fig. 3(c)] show the initial mistrim effect and the turning of the vehicle to keep the thrust vector through the moving Z c.g. to meet the target conditions. The maximum pitch and yaw attitude error [fig. 3(d)] was -0.41° in pitch and -0.45° in yaw.

The SCS rates [fig. 3(e)], attitudes [fig. 3(f)], and attitude errors [fig. 3(g)] drive the FDAI-2 and give approximately the same results as the G&N.

The first good t_{GO} occurs at 4 seconds and then is updated every 2 seconds until $t_{GO} \leq 4$ seconds [fig. 3(h)]. The V_{GO} is shown in

figure 3(i), and the velocity components are shown in figure 3(j). The desired ΔV was input into the EMS, and the results are shown in figure 3(k). The cross-axis velocity error [fig. 3(l)] reached a maximum of 0.68 fps at 8 seconds and then went to zero at cutoff (361.38 sec). The effects of the SPS burn on selected trajectory parameters are shown in figures 3(m), 3(n), and 3(o).

4.4 Circularization Maneuver (LOI-2)

The fourth SPS burn is also a CSM/LM docked burn with an external ΔV target of 138.5 fps and a burn duration of 14.45 seconds. It is designed to circularize the lunar orbit at approximately 58 n. mi.

The SPS engine is misalined 0.3° in pitch and 0.3° in yaw for this burn also. Corrections made by the SPS engine for this initial error are shown in figure 4(a). The vehicle is much lighter during this burn; therefore, larger body attitude rates are obtained for LOI-2 than were obtained for the previous burns [fig. 4(b)]. The maximum rates reached are 0.27 deg/sec pitch and 0.28 deg/sec for yaw. The IMU angles show the effects of the initial mistrim in figure 4(c). The attitude errors reach a maximum deviation of -0.65° in pitch and -0.69° in yaw [fig. 4(d)].

The rates, attitudes, and attitude errors that are monitored by the SCS system on FDAI-2 are presented in figures 4(e), 4(f), and 4(g), respectively.

The t_{GO} calculation [fig. 4(h)] is updated every 2 seconds from 4 through 10 seconds; then $t_{GO} < 4$ seconds and is not updated again. The total V_g [fig. 4(i)], V_g components in control coordinates [fig. 4(j)], and velocity along the X-body axis [fig. 4(k)] were obtained from monitoring the onboard displays. The cross-axis velocity [fig. 4(l)] resulted in an error of 0.39 fps after a velocity of 1.13 fps was obtained during the burn. The trajectory effects are shown in figures 4(m), 4(n), and 4(o).

4.5 Transearth Insertion Maneuver (TEI)

The fifth SPS burn is the first undocked burn for the CSM. It is designed to direct the spacecraft on an earth return trajectory. The TEI burn consists of an external ΔV target of 3622.53 fps and a burn duration of 168.8 seconds.

The SPS engine is misalined 0.3° in pitch and 0.3° in yaw. The DAP comes on at 0.66 second and drives the SPS engine [fig. 5(a)] to damp out the vehicle rates [fig. 5(b)] that build up because of the initial mistrim. The SPS engine also tracks the c.g. during the burn, specifically in the Y direction [fig. 5(a)]. The vehicle body rates essentially are damped out after maximum rates of 0.19 deg/sec in pitch and 0.23 deg/sec in yaw are obtained. The initial engine misalinement effects on the IMU gimbal angles are shown in figure 5(c). After the misalinement is corrected, the yaw angle increases until cutoff occurs because the c.g. shifts in the yaw direction. The control system keeps the thrust direction towards the target; and, as the c.g. changes, the body attitude changes. The attitude errors [fig. 5(d)] remain small because the control system is homing in on the target.

The SCS rates [fig. 5(e)] and attitudes [fig. 5(f)] verify the G&N results, but the SCS attitude errors [fig. 5(g)] are different. This difference is attributed to the different methods by which they are computed.

The t_{GO} [fig. 5(h)], the total V_g [fig. 5(i)], the V_g components [fig. 5(j)] in control coordinates, and the EMS decremented velocity [fig. 5(k)] show the time histories of the available onboard displays.

The cross-axis velocity error is presented in figure 5(l). The vehicle configuration is much lighter than for the previous burns; therefore, higher rates and greater cross-axis velocity errors can be expected. The velocity error levels out at approximately 2.4 fps while the initial mistrim is being corrected then increases to 3.3 fps before being driven back to 0.8 fps at cutoff.

The predicted apogee and perigee plot [fig. 5(m)] shows the spacecraft leaving a circular orbit as the predicted apogee extends beyond the top of the plot. The altitude [fig. 5(n)] also increases at the end of the burn, which indicates that the spacecraft is going into a high elliptical orbit. This increase is also verified by the increasing inertial velocity versus inertial flight-path angle [fig. 5(o)].

5.0 CONCLUSIONS

The following is a summary of conclusions that were reached from this analysis.

1. These new DAP gains respond more quickly to the initial errors and prevent high cross-axis velocity errors.

2. For a fully loaded vehicle, the acceleration is small and does not build up significantly high cross-axis velocity errors.

3. The duration of the long burns such as LOI-1 gives the guidance and control system time to null practically all of the cross-axis velocity errors by cutoff.

4. The TEI burn is a CSM-only maneuver. Because this burn is done with a light vehicle configuration, higher rates and greater cross-axis velocities can be expected during the burn. However, this maneuver is of sufficient duration to null almost all of the velocity errors.

TABLE I.- SPS INITIALIZATION DATA

Input parameter	Evasive maneuver[a]	Midcourse correction[a]	LOI-1[b]	LOI-2[b]	TEI[b]
Time of ignition, day:hr:min:sec	0:04:28:47.6	0:09:38:46.4	3:03:45:43.2	3:08:10:45.5	5:17:20:22.40
Inertial velocity, fps	14 693.90	8 690.67	8 250.72	5 487.01	5 349.05
Inertial flight-path angle, deg	64.39	73.30	-10.84	-0.02	0.03
ΔV_X, fps	5.09	-42.90	-2 912.92	-138.5	3 618.07
ΔV_Y, fps	0.00	10.47	-587.45	0.0	-34.75
ΔV_Z, fps	19.01	-35.99	-200.97	0.0	176.45
Total ΔV, fps	19.68	56.97	2 978.36	138.5	3 622.53
SPS engine pitch angle, deg[c]	-1.25	-1.25	-1.26	0.61	-2.82
SPS engine yaw angle, deg[c]	0.55	0.54	0.54	0.28	1.16
Spacecraft weight, lb	94 585.60	94 391.84	92 427.90	68 821.20	36 574.90
Inclination, deg	31.61	31.61	153.17	157.39	157.34

[a]Earth reference.

[b]Moon reference.

[c]Engine gimbal angles do not include mistrim.

TABLE II.- SPS RESULTANT CONDITIONS

Resultant parameter	Evasive maneuver	Midcourse correction	LOI-1	LOI-2	TEI
Burn time, sec	2.85	8.26	361.38	14.45	168.82
V_{gx}, fps	0.35	-0.33	-0.48	-0.34	-0.84
V_{gy}, fps	0.17	0.53	0.02	0.25	0.71
V_{gz}, fps	-0.01	-0.29	-0.01	-0.15	0.08
Total cross-axis velocity, fps	0.17	0.62	0.03	0.39	0.79
Maximum pitch attitude, deg	-0.14	-0.42	-0.41	-0.65	-0.51
Maximum yaw attitude error, deg	-0.15	-0.46	-0.45	-0.69	-0.67
Inertial velocity, fps	14 679.56	8 711.32	5484.90	5348.17	8959.17
Inertial flight-path angle, deg	64.36	73.65	-0.30	0.00	3.09
Attitude, n. mi.	16 662.74	47 719.67	58.21	57.90	59.63
Inclination, deg	31.61	31.70	157.39	157.39	157.49

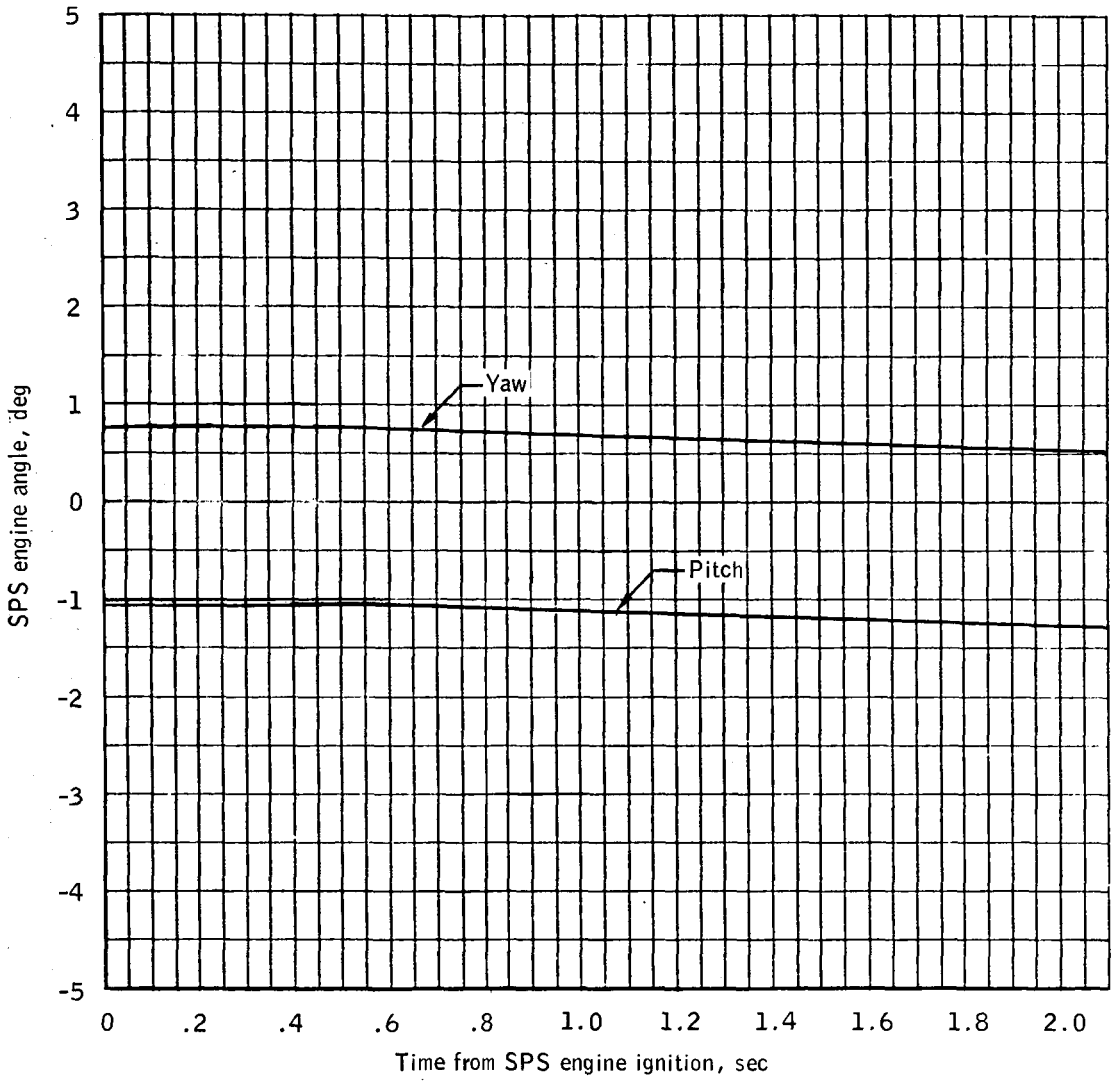

(a) SPS engine angles.

Figure 1.- Evasive maneuver burn parameters.

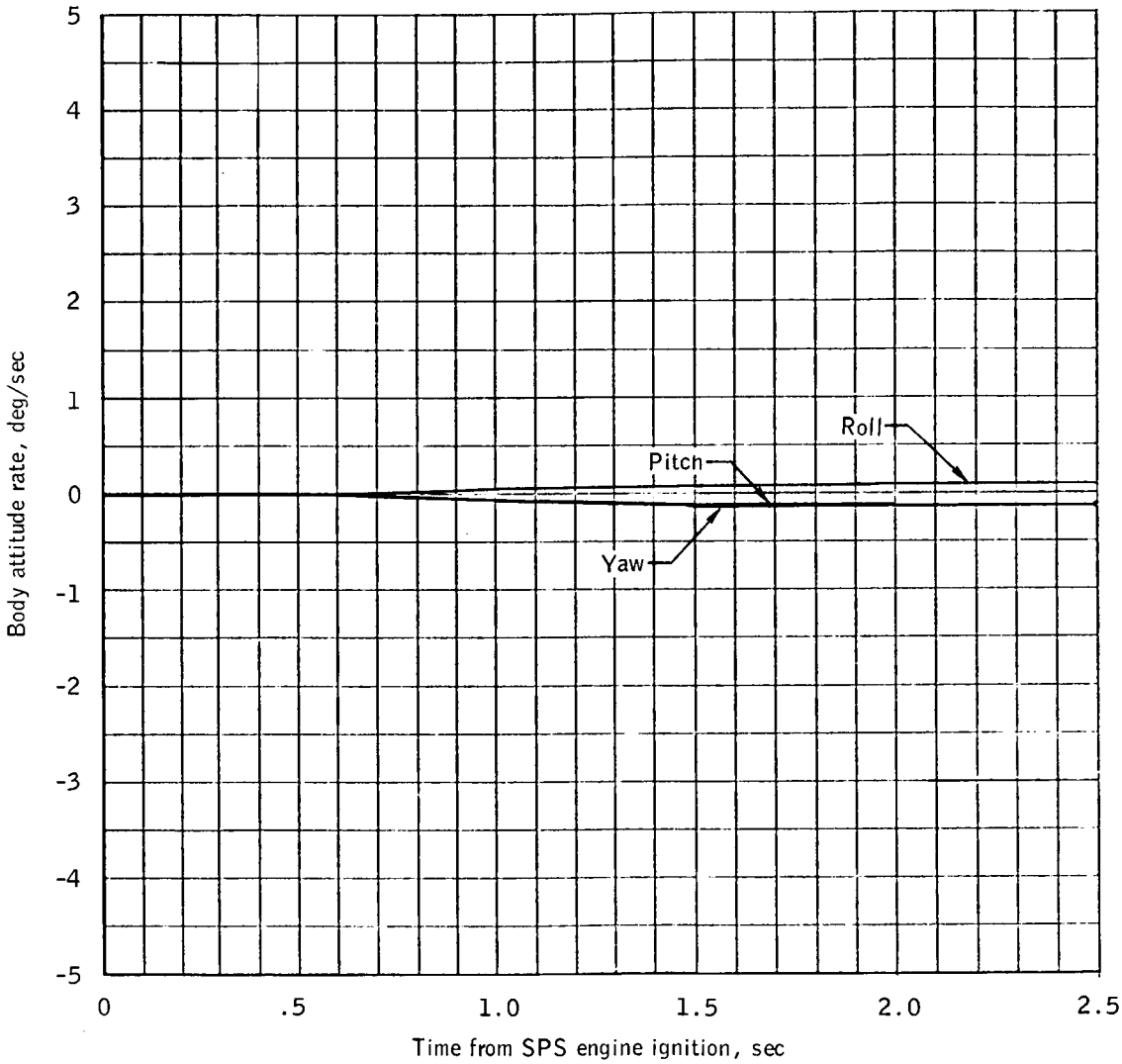

(b) Body attitude rates, FDAI-1.

Figure 1.- Continued.

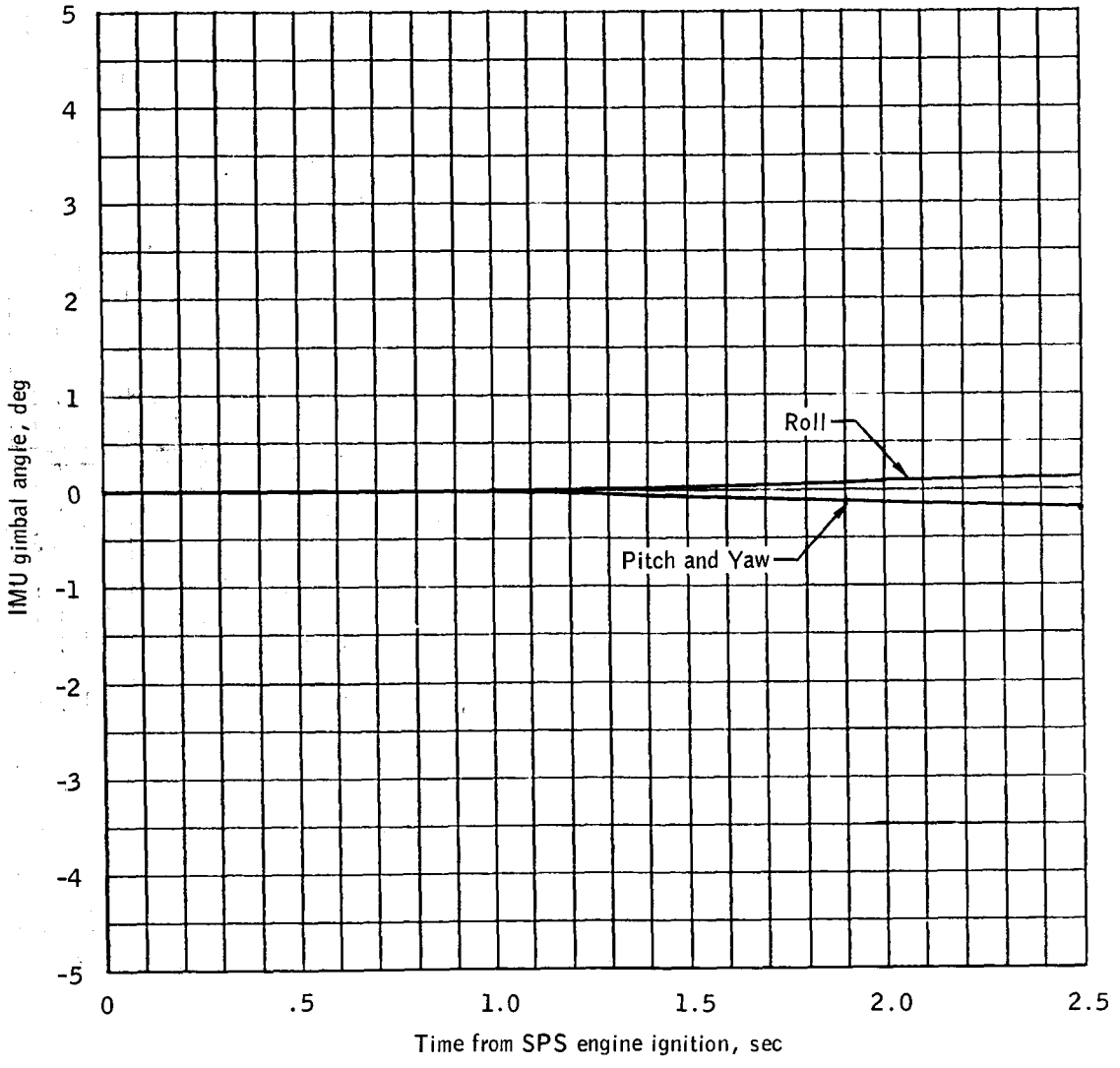

(c) IMU gimbal angles.

Figure 1.- Continued.

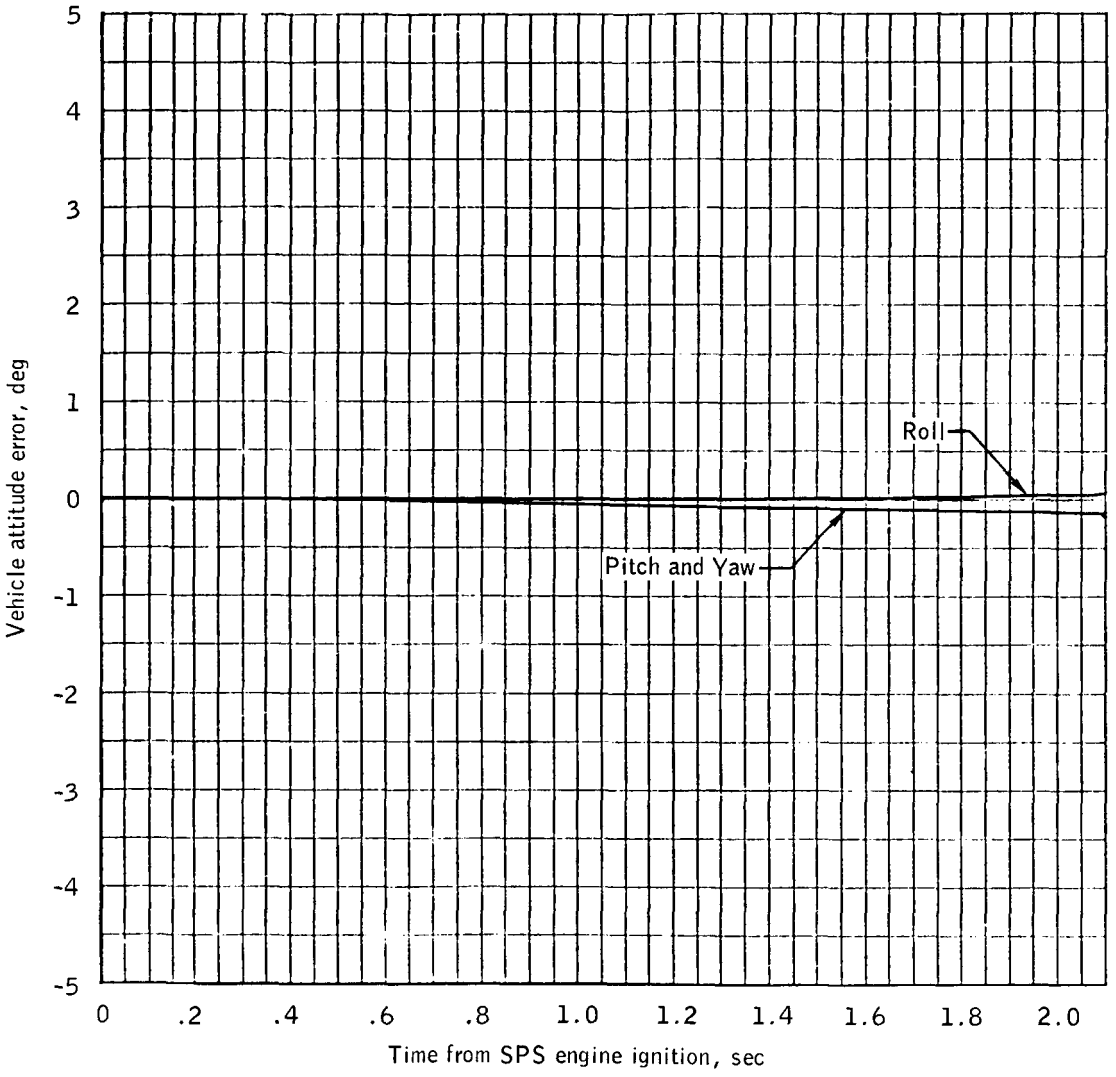

(d) Vehicle attitude errors.

Figure 1.- Continued.

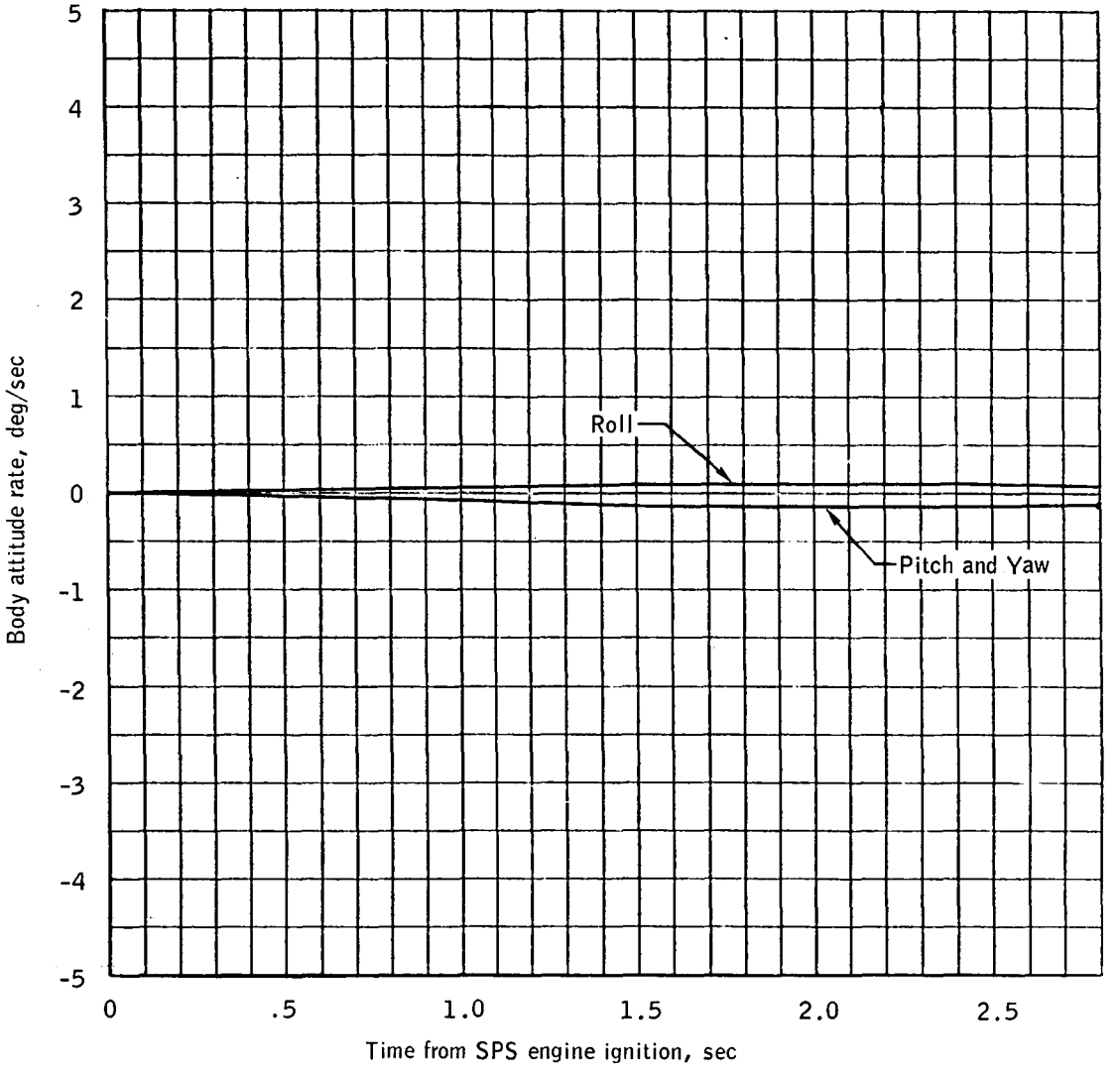

(e) Body attitude rates, FDAI-2.

Figure 1.- Continued.

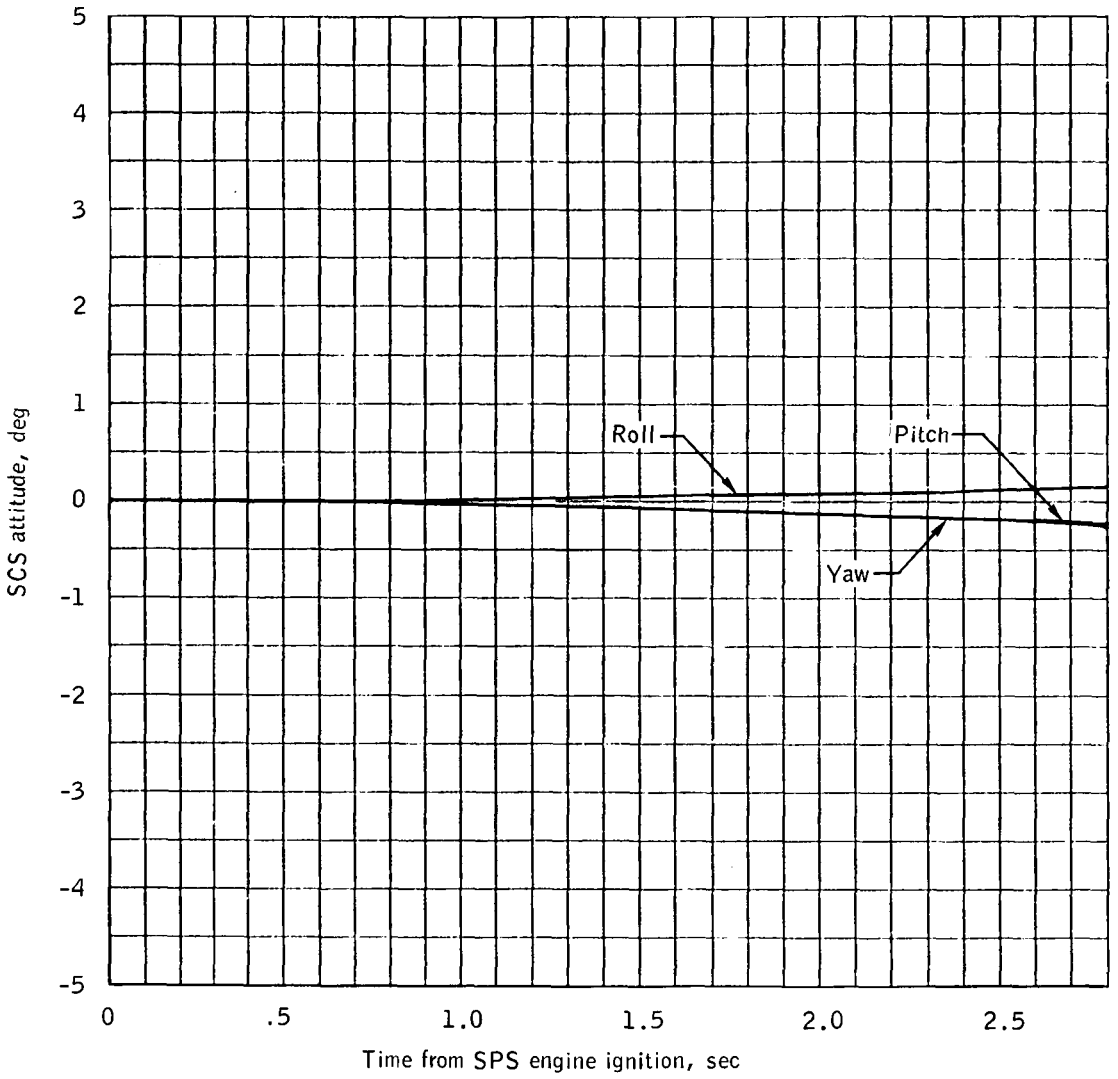

(f) SCS attitudes monitored from BMAGS.

Figure 1.- Continued.

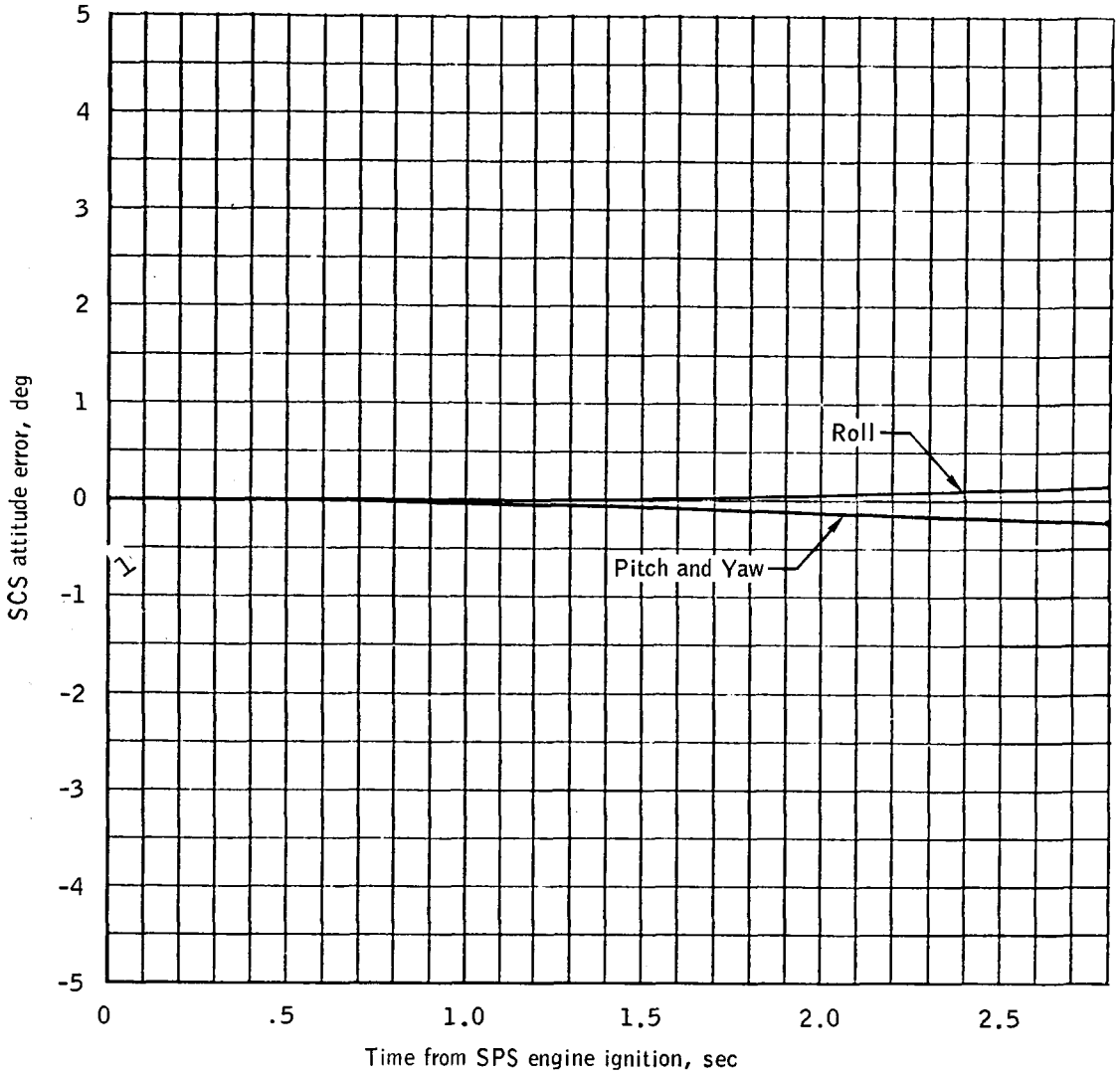

(g) SCS attitude errors monitored from BMAGS.

Figure 1.- Continued.

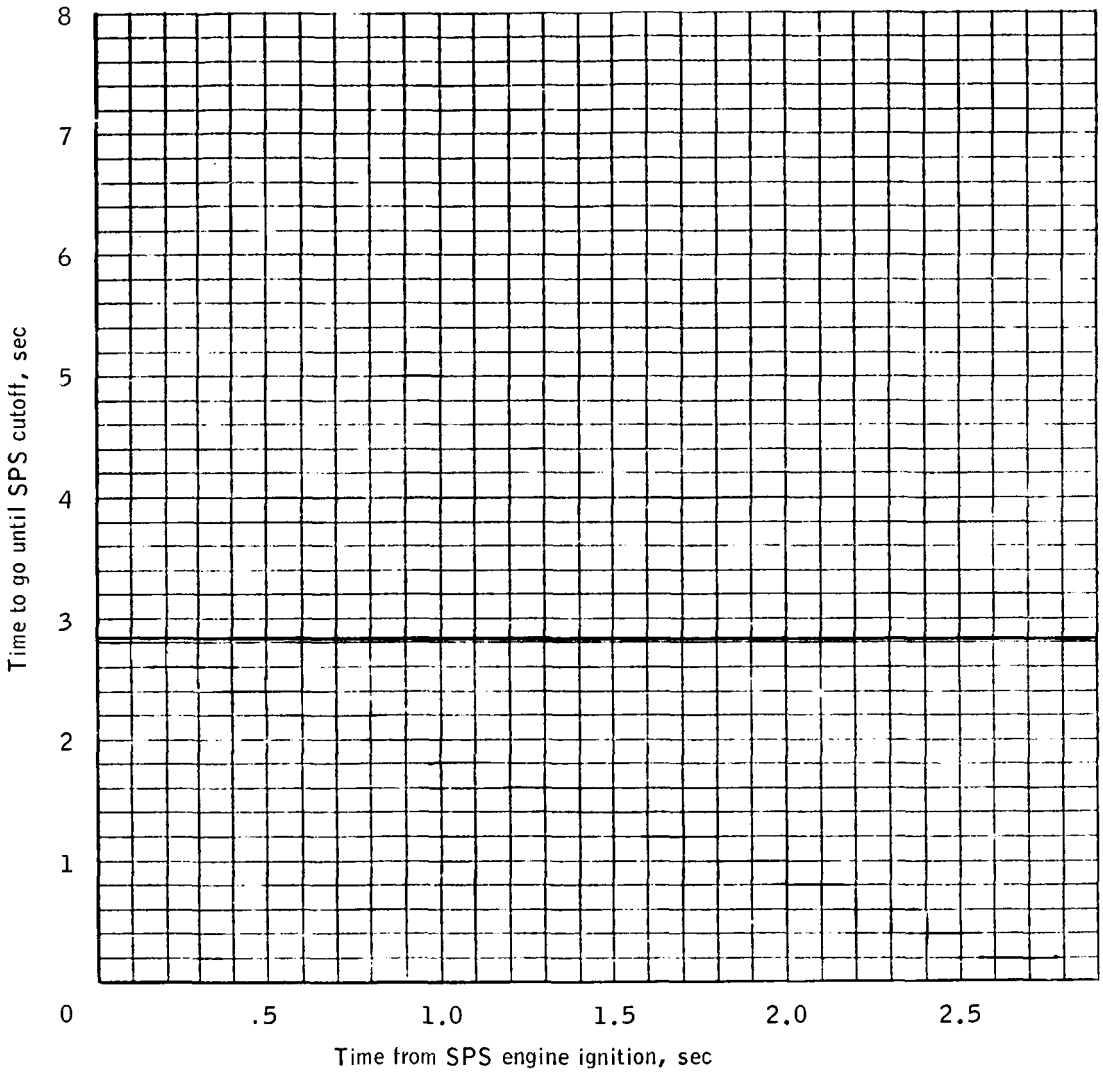

(h) Time to go until SPS cutoff.

Figure 1.- Continued.

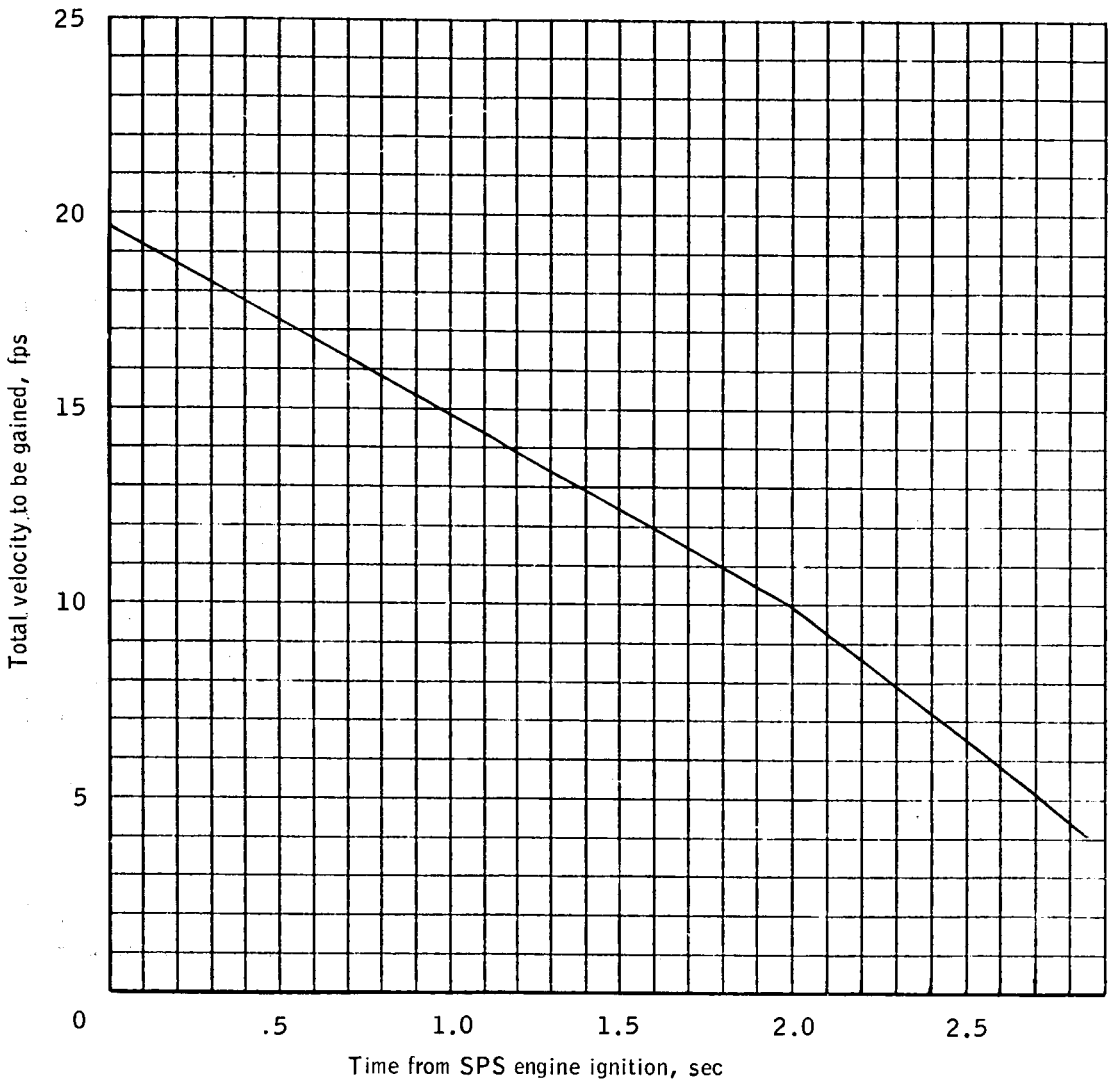

(i) Total velocity to be gained until SPS cutoff.

Figure 1.- Continued.

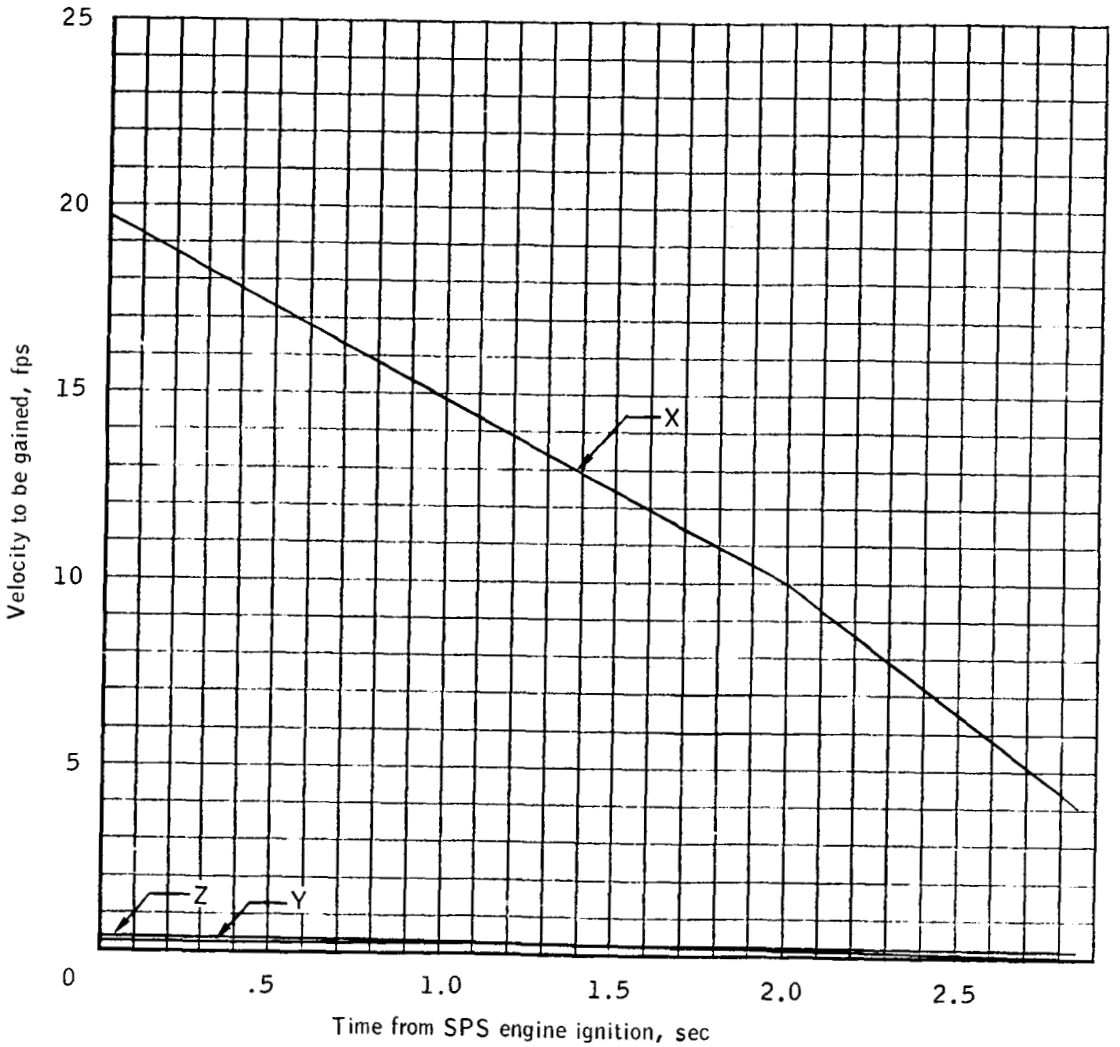

(j) Velocity to be gained in control coordinates.

Figure 1.- Continued.

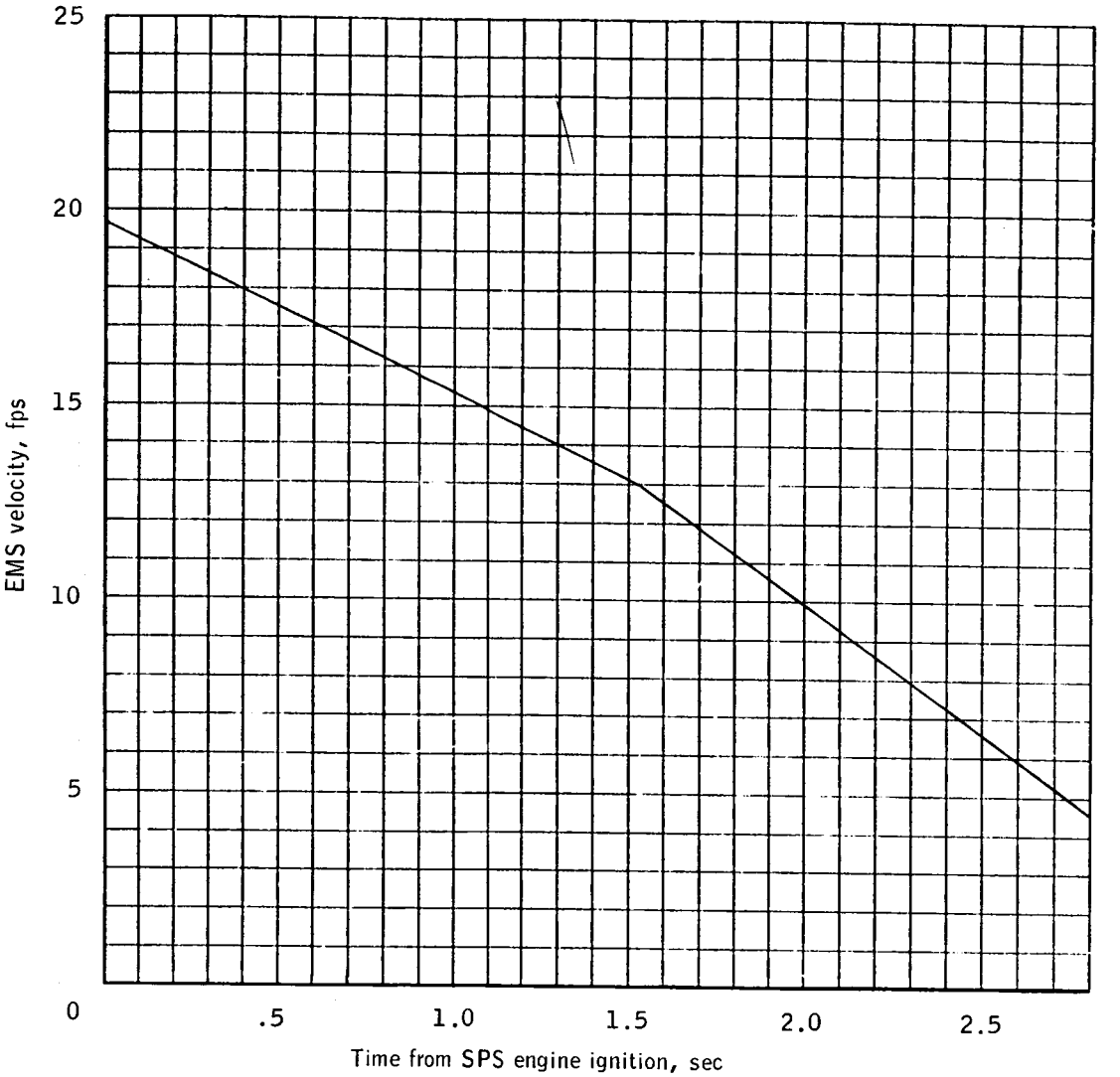

(k) EMS velocity.

Figure 1.- Continued.

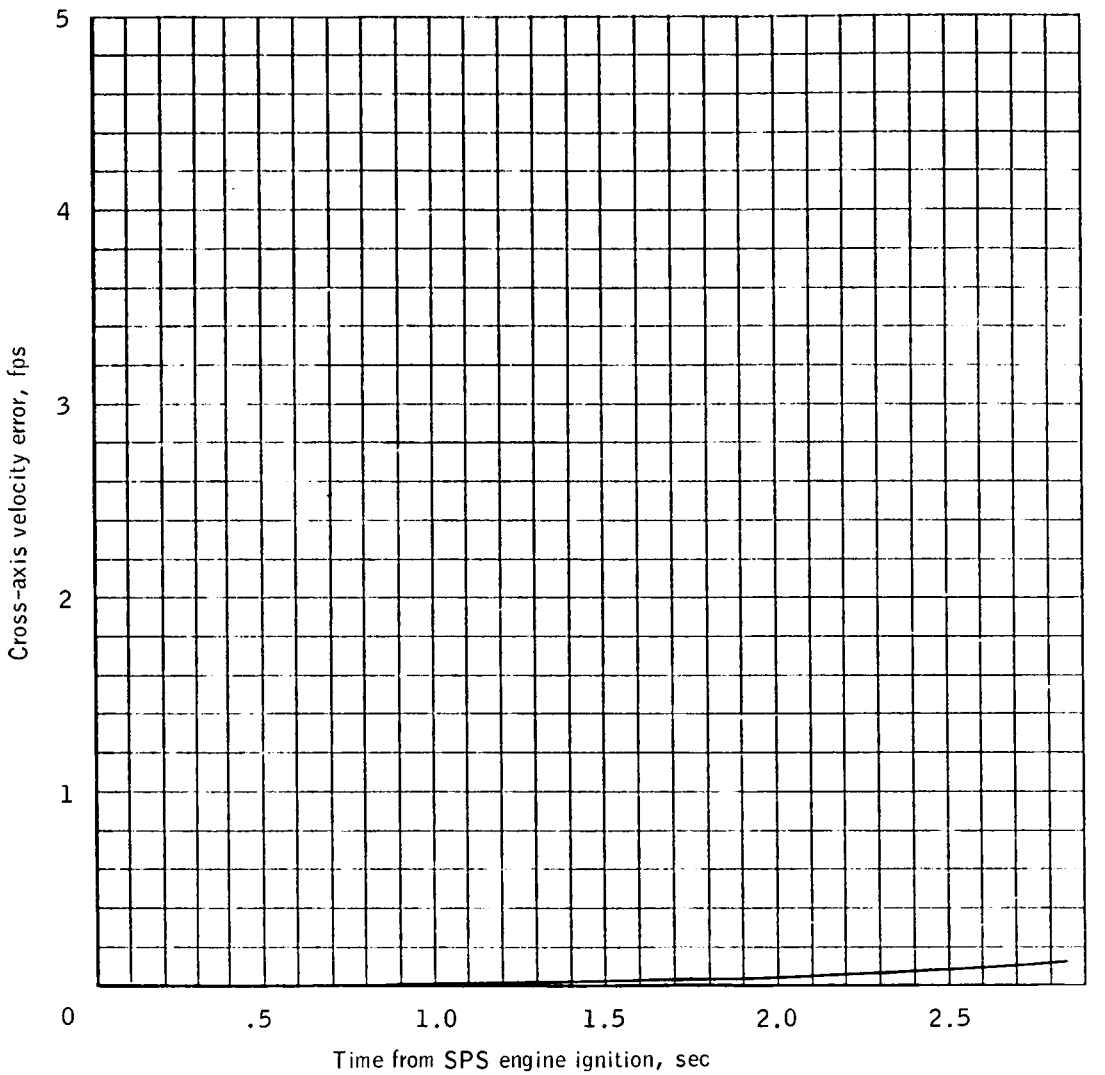

(l) Cross-axis velocity error.

Figure 1.- Continued.

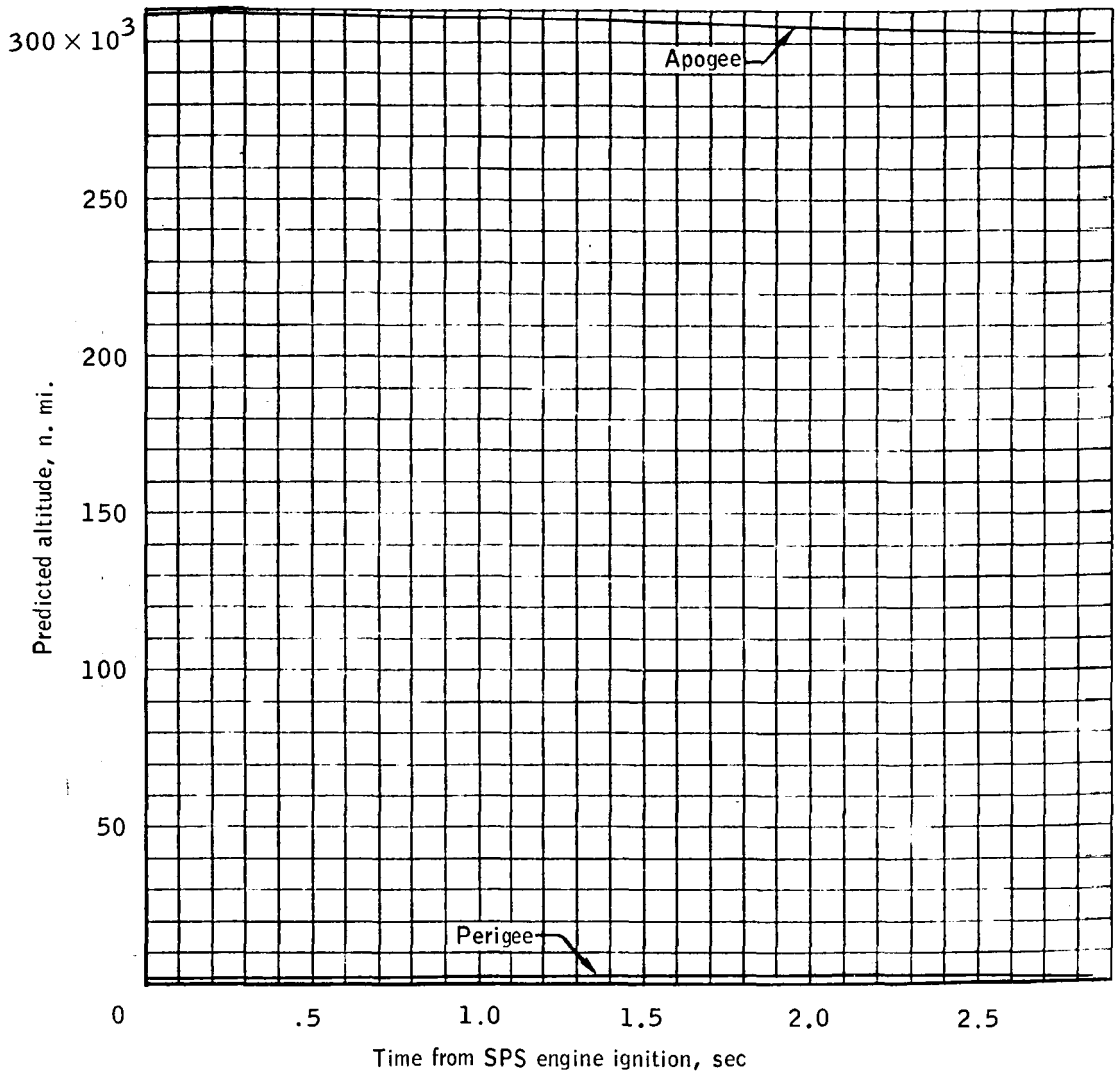

(m) Predicted apogee and perigee altitudes.

Figure 1.- Continued.

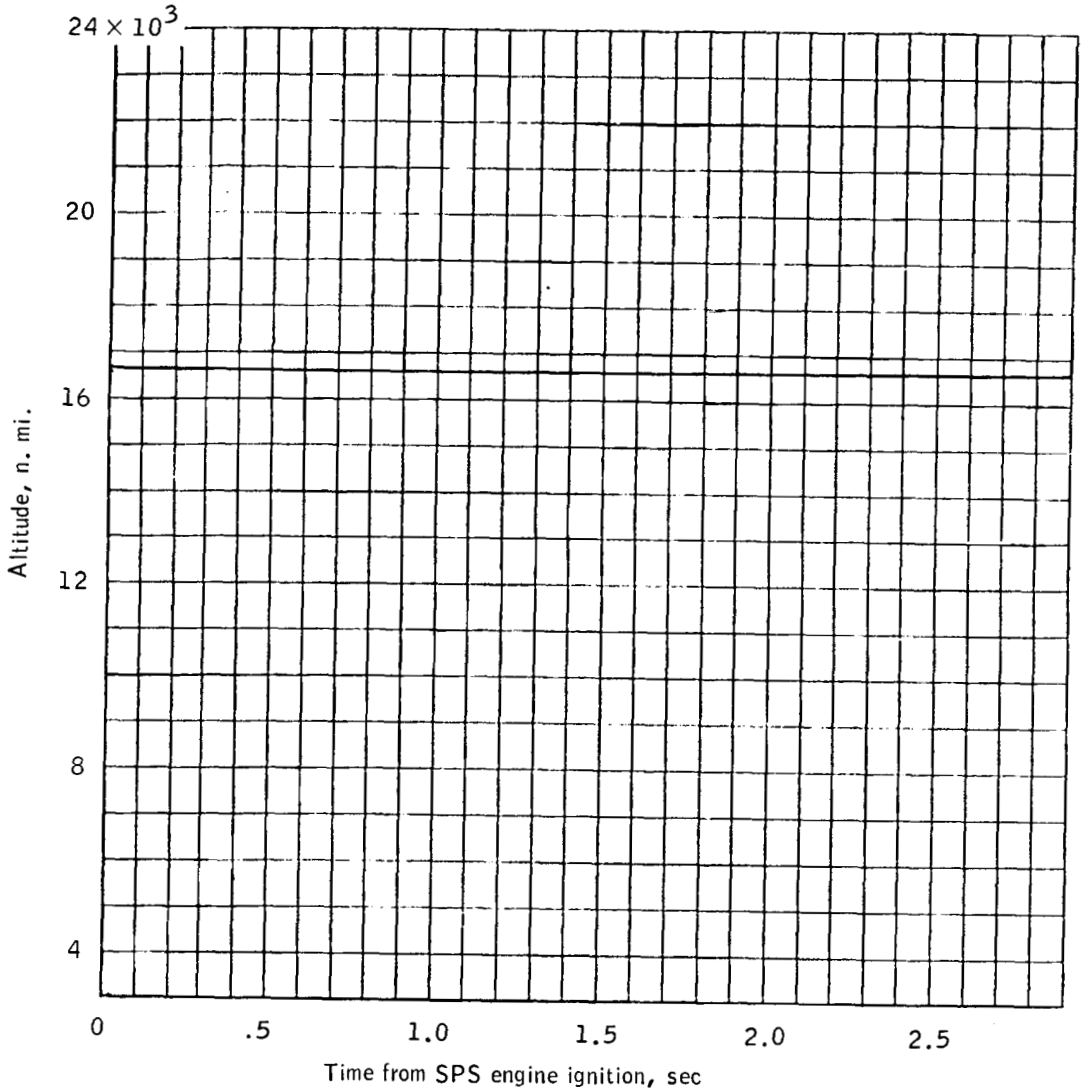

(n) Altitude.

Figure 1.- Continued.

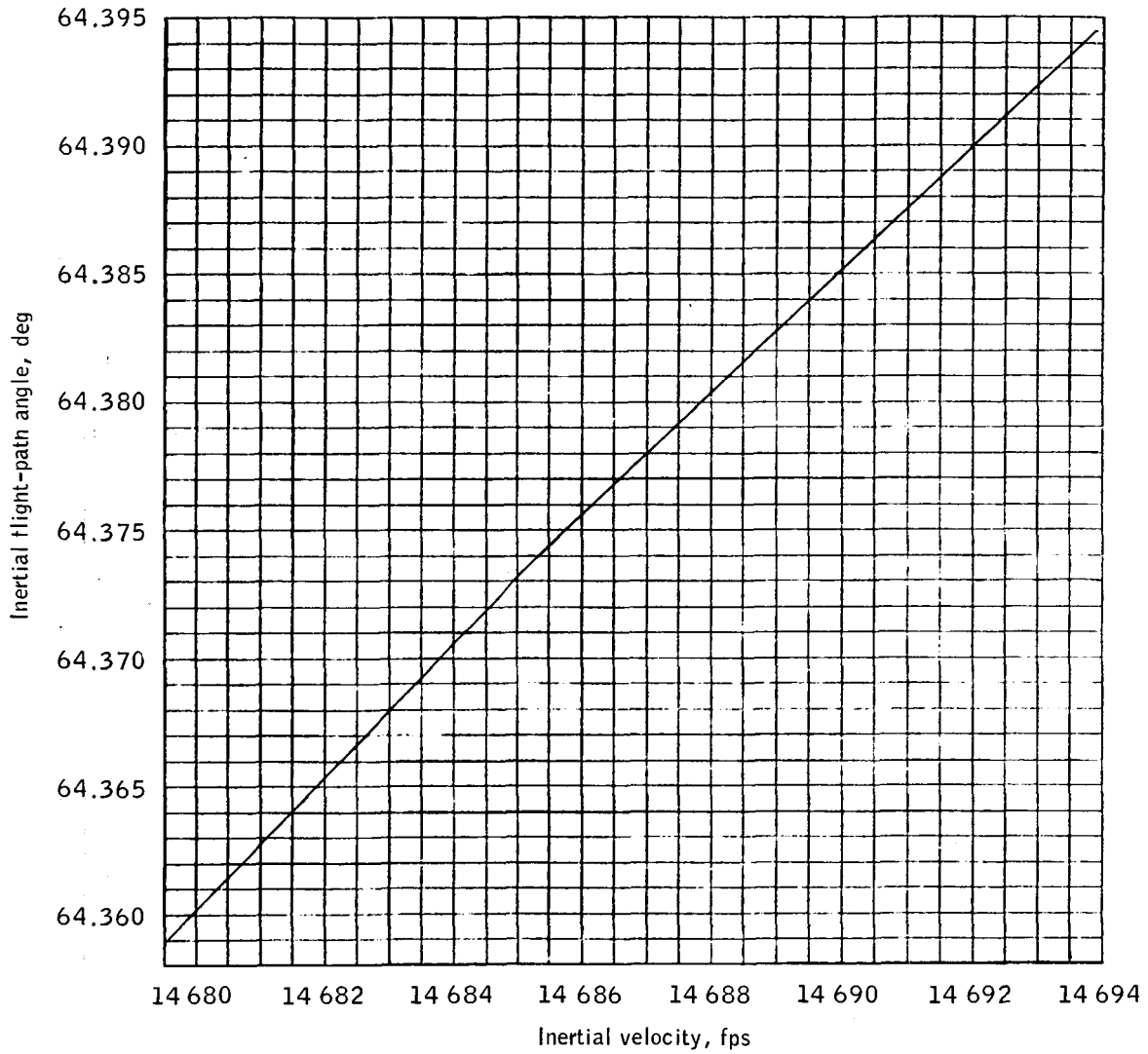

(o) Inertial flight-path angle versus inertial velocity.

Figure 1.- Concluded.

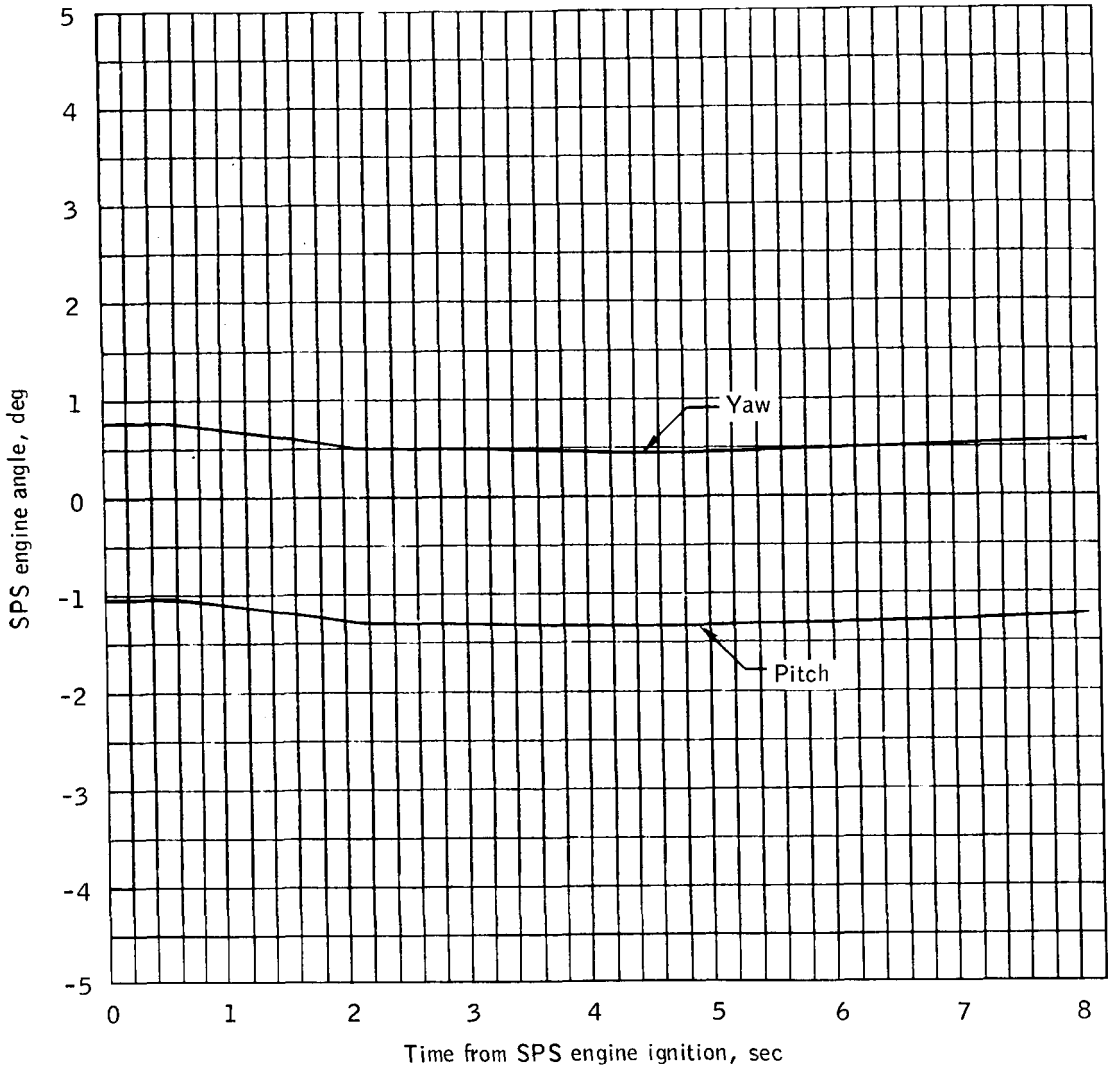

(a) SPS engine angles.

Figure 2.- Midcourse correction burn parameters.

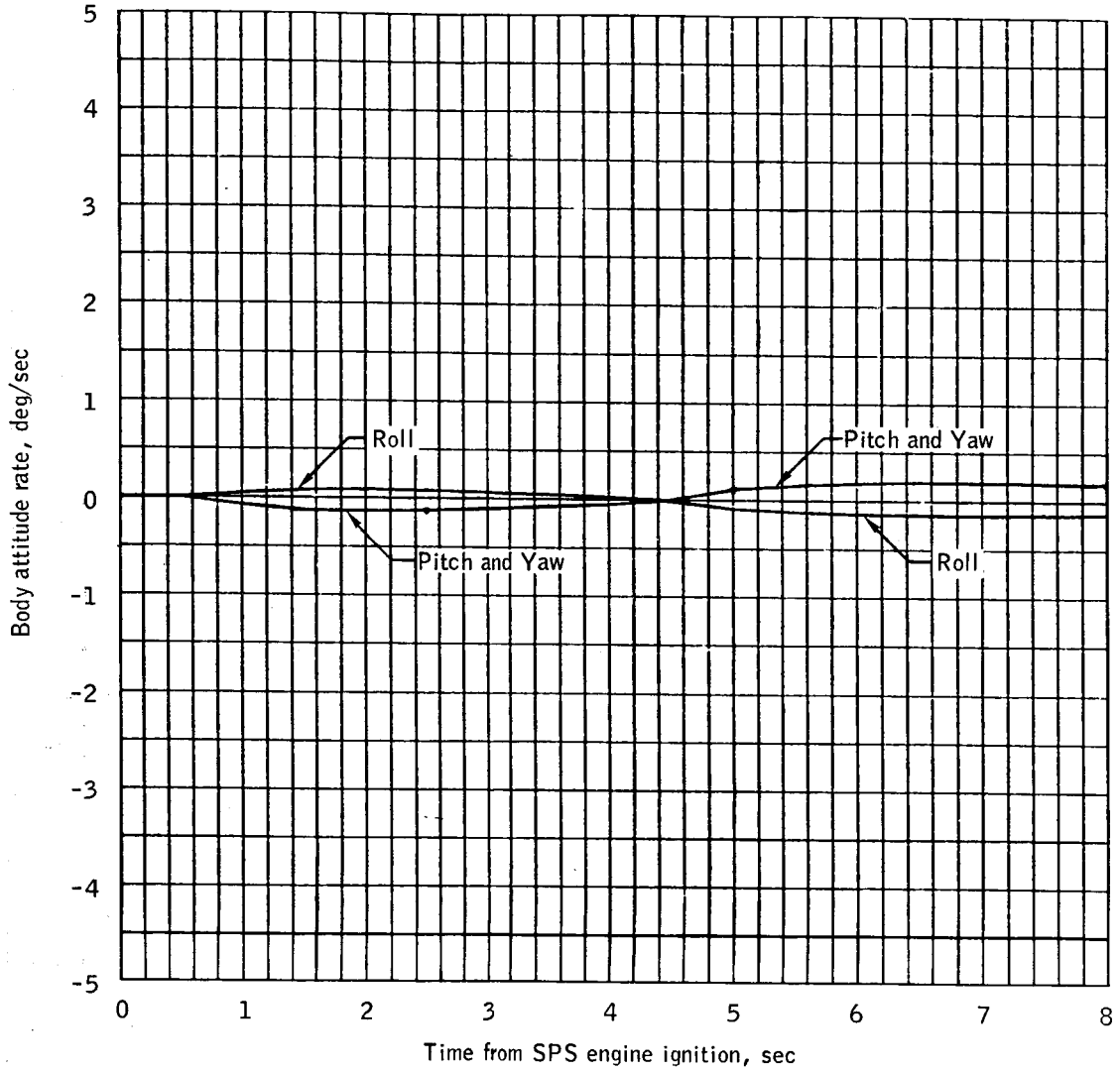

(b) Body attitude rates, FDAI-1.

Figure 2.- Continued.

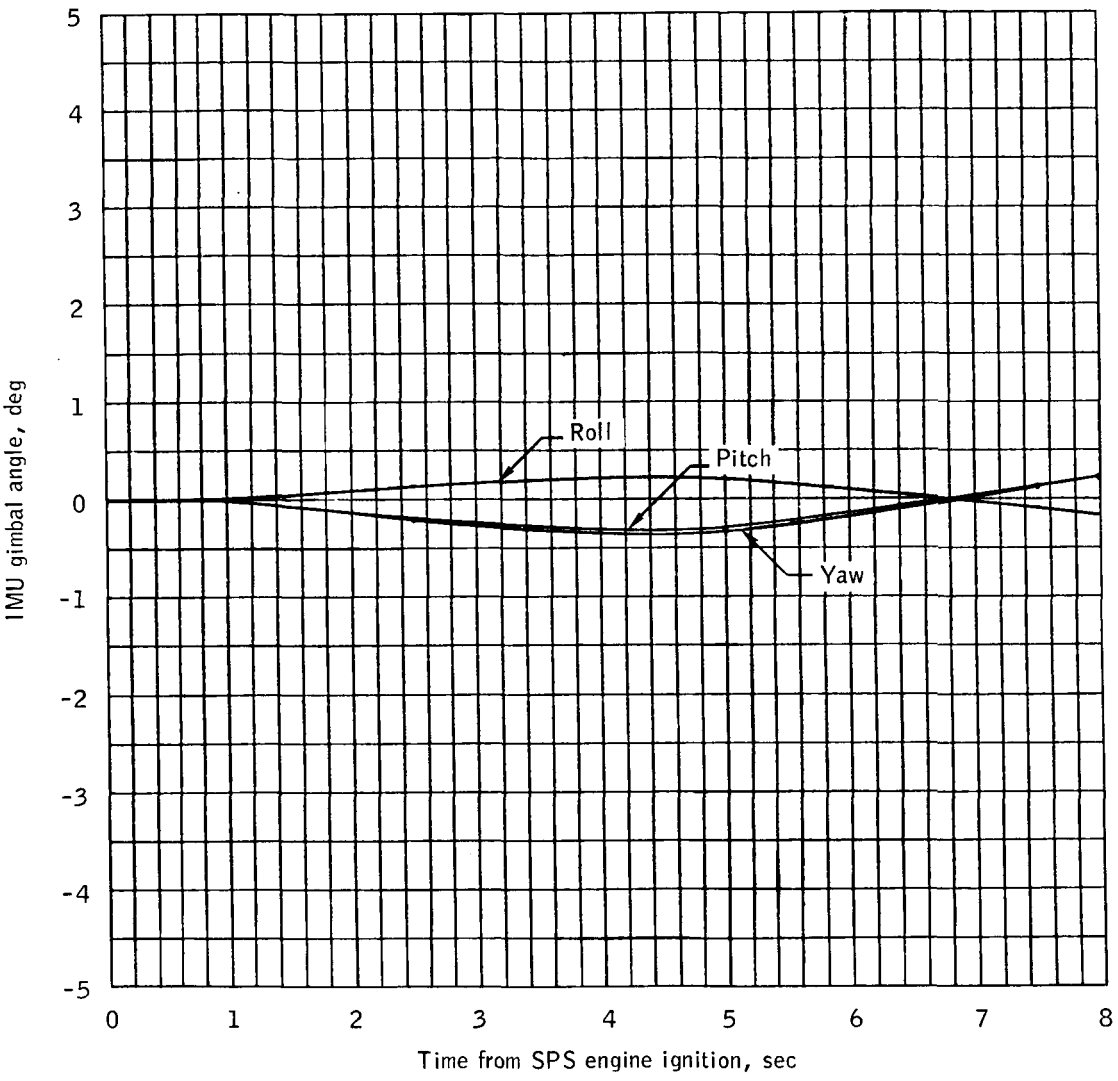

(c) IMU gimbal angles.

Figure 2.- Continued.

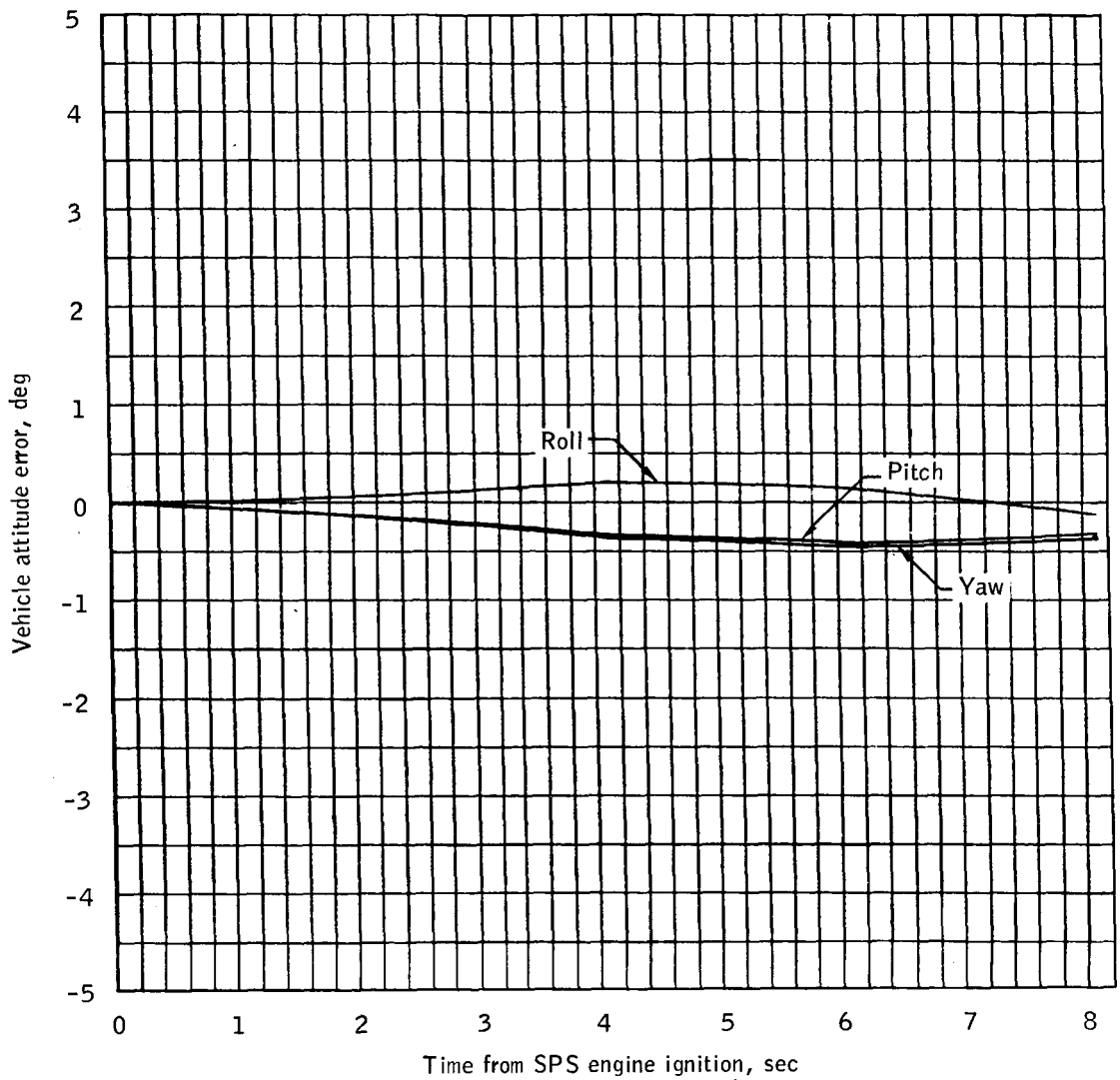

(d) Vehicle attitude errors.

Figure 2.- Continued.

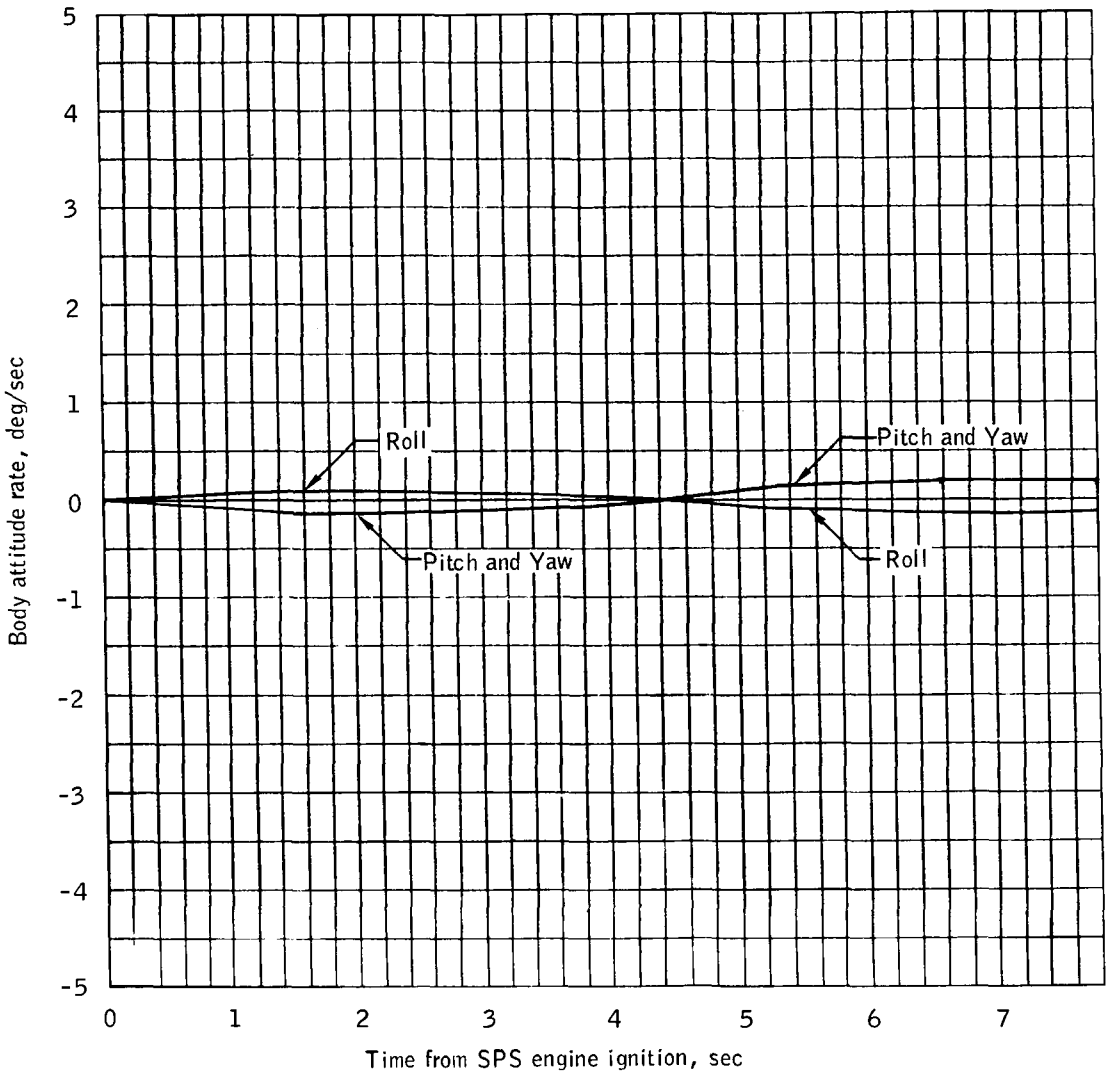

(e) Body attitude rates, FDAI-2.

Figure 2.- Continued.

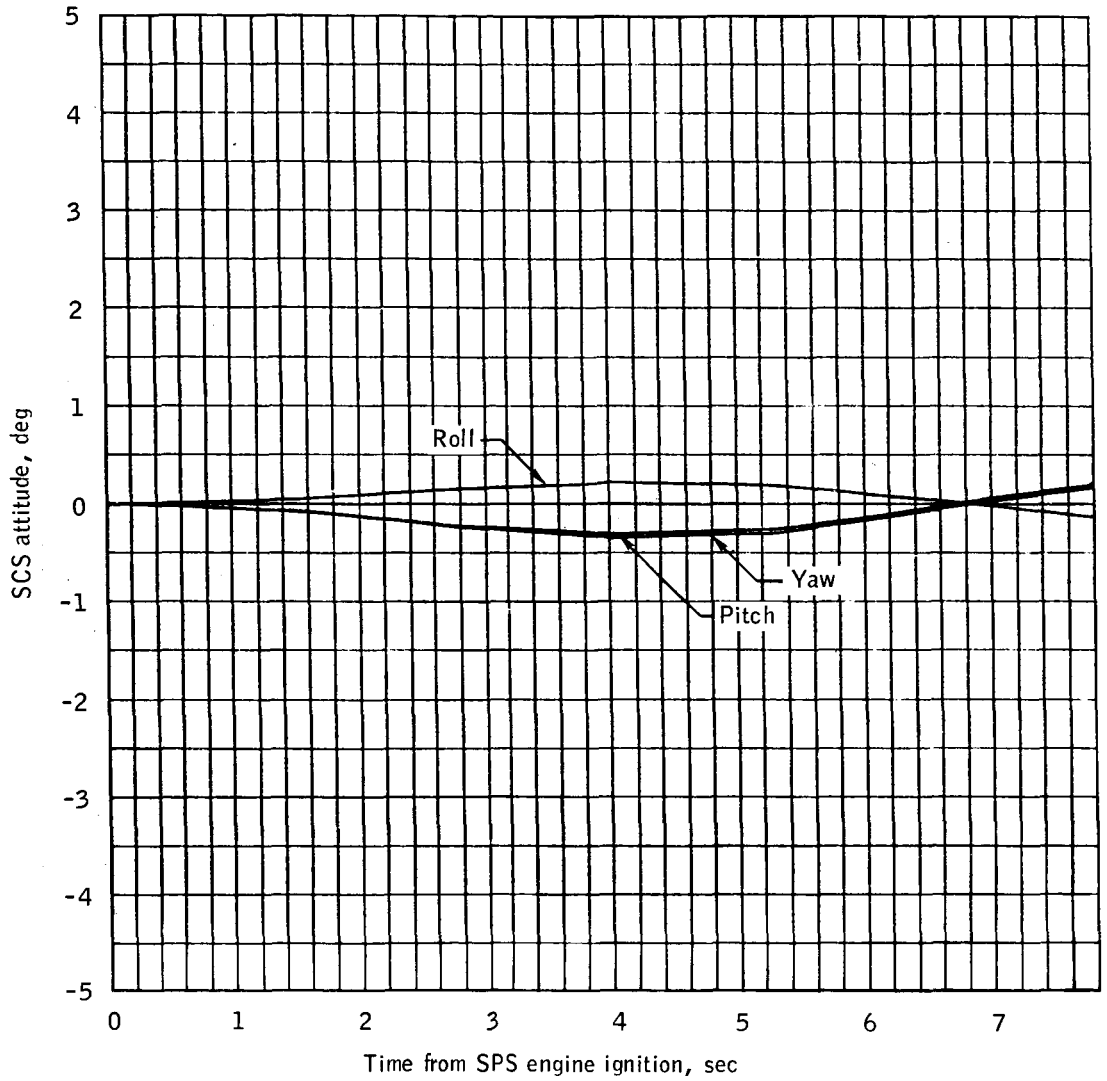

(f) SCS attitudes monitored from BMAGS.

Figure 2.- Continued.

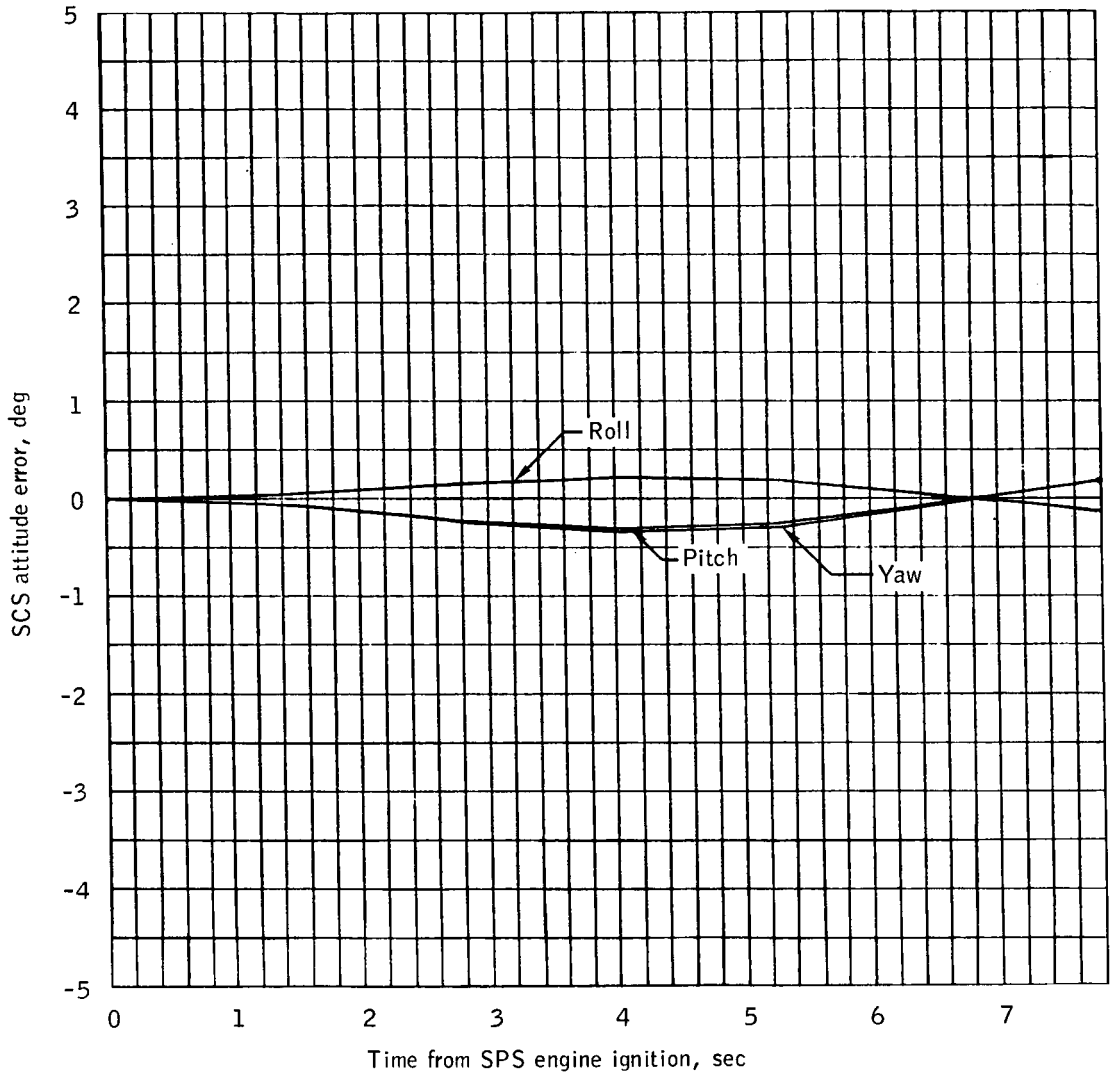

(g) SCS attitude errors monitored from BMAGS.

Figure 2.- Continued.

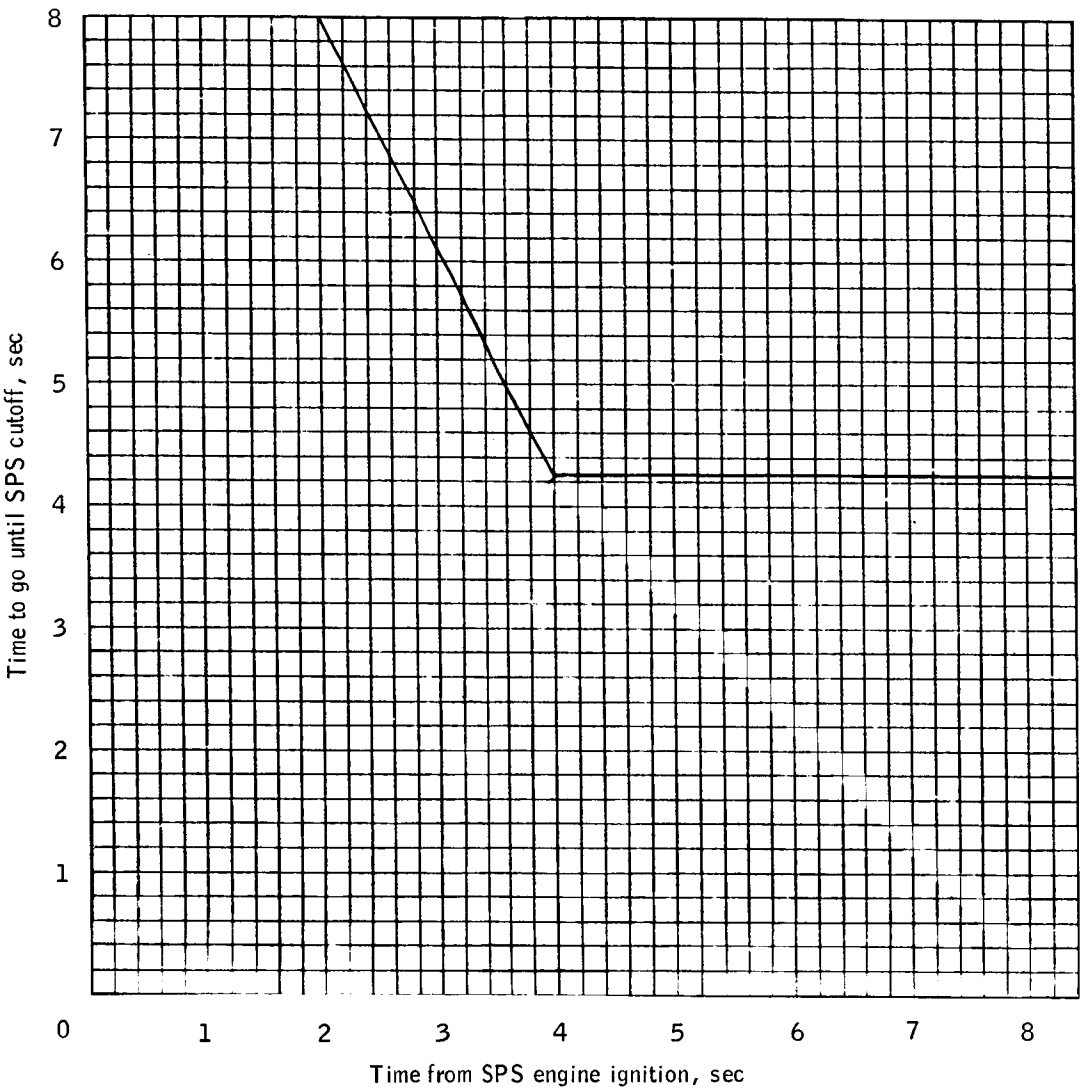

(h) Time to go until SPS cutoff.

Figure 2.- Continued.

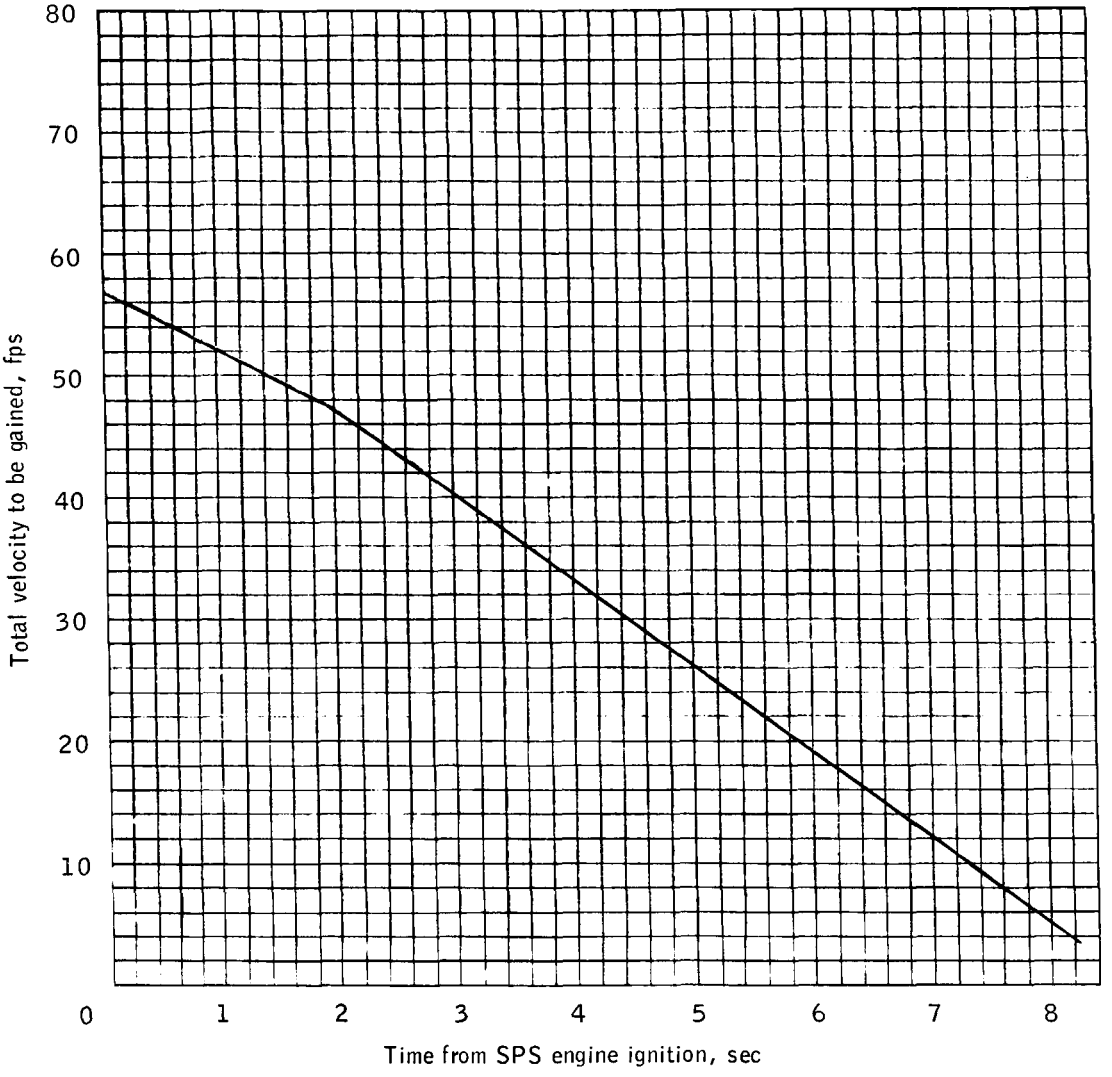

(i) Total velocity to be gained until SPS cutoff.

Figure 2.- Continued.

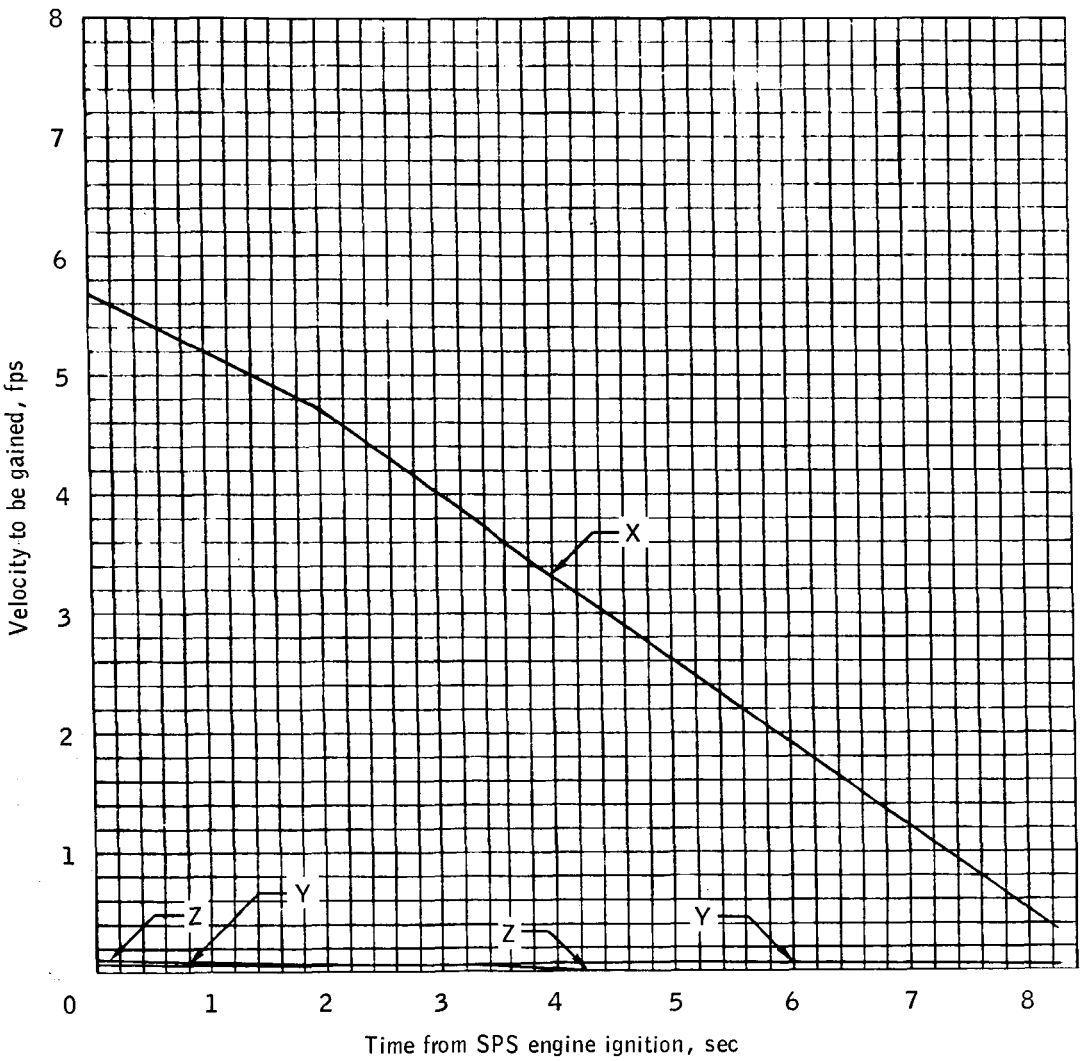

(j) Velocity to be gained in control coordinates.

Figure 2 .- Continued.

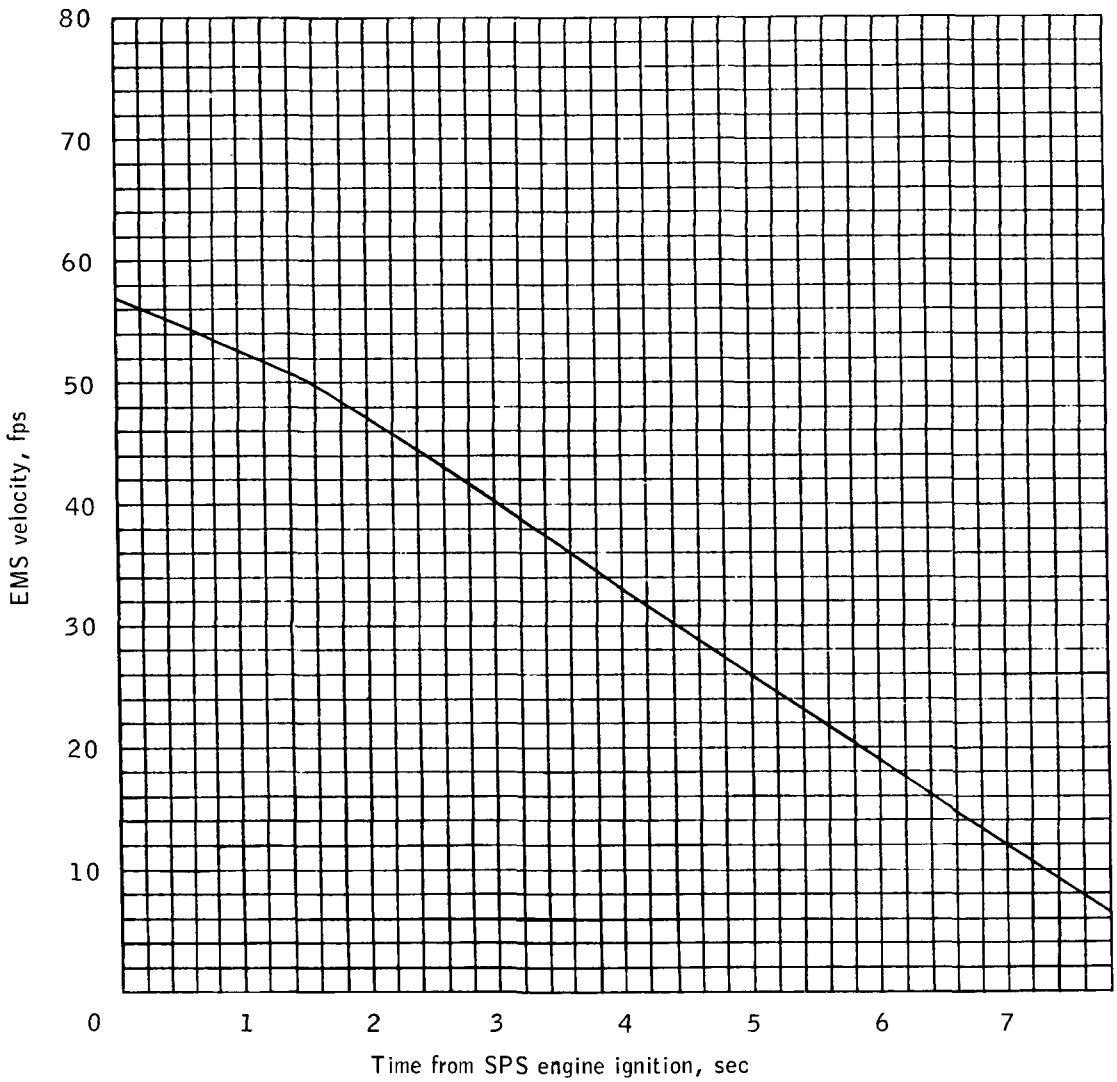

(k) EMS velocity.

Figure 2.- Continued.

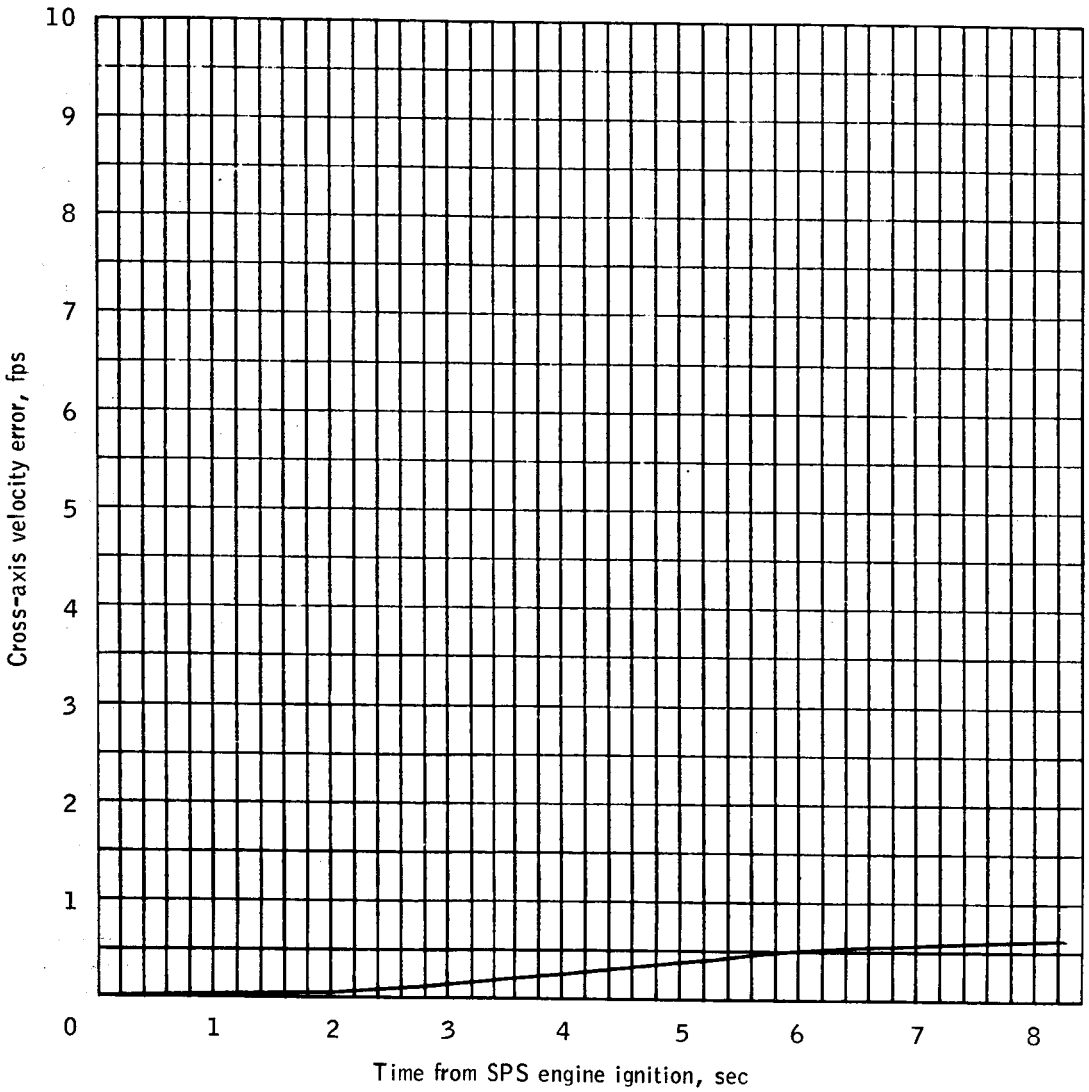

(l) Cross-axis velocity error.

Figure 2.- Continued.

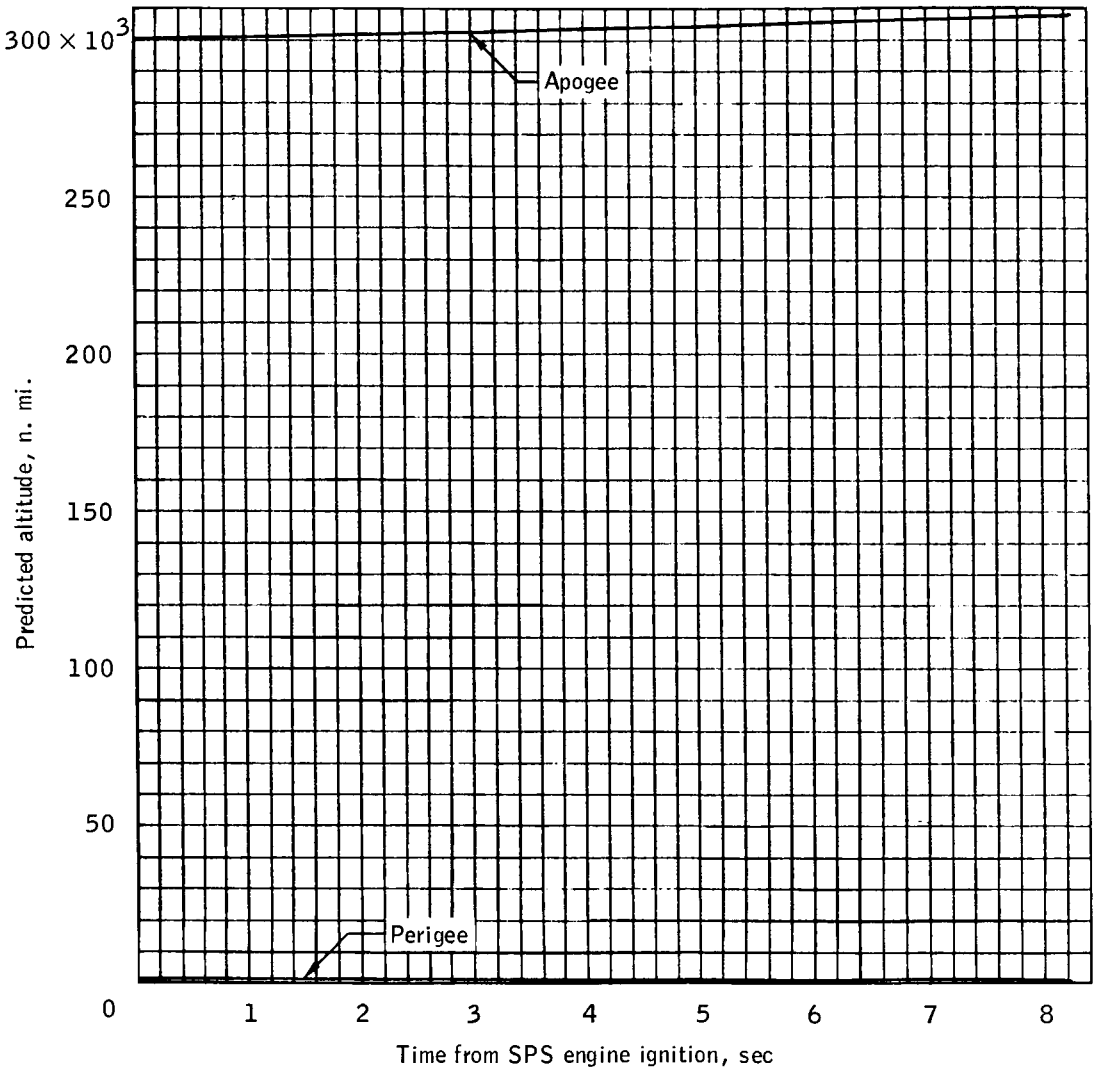

(m) Predicted apogee and perigee altitudes.

Figure 2.- Continued.

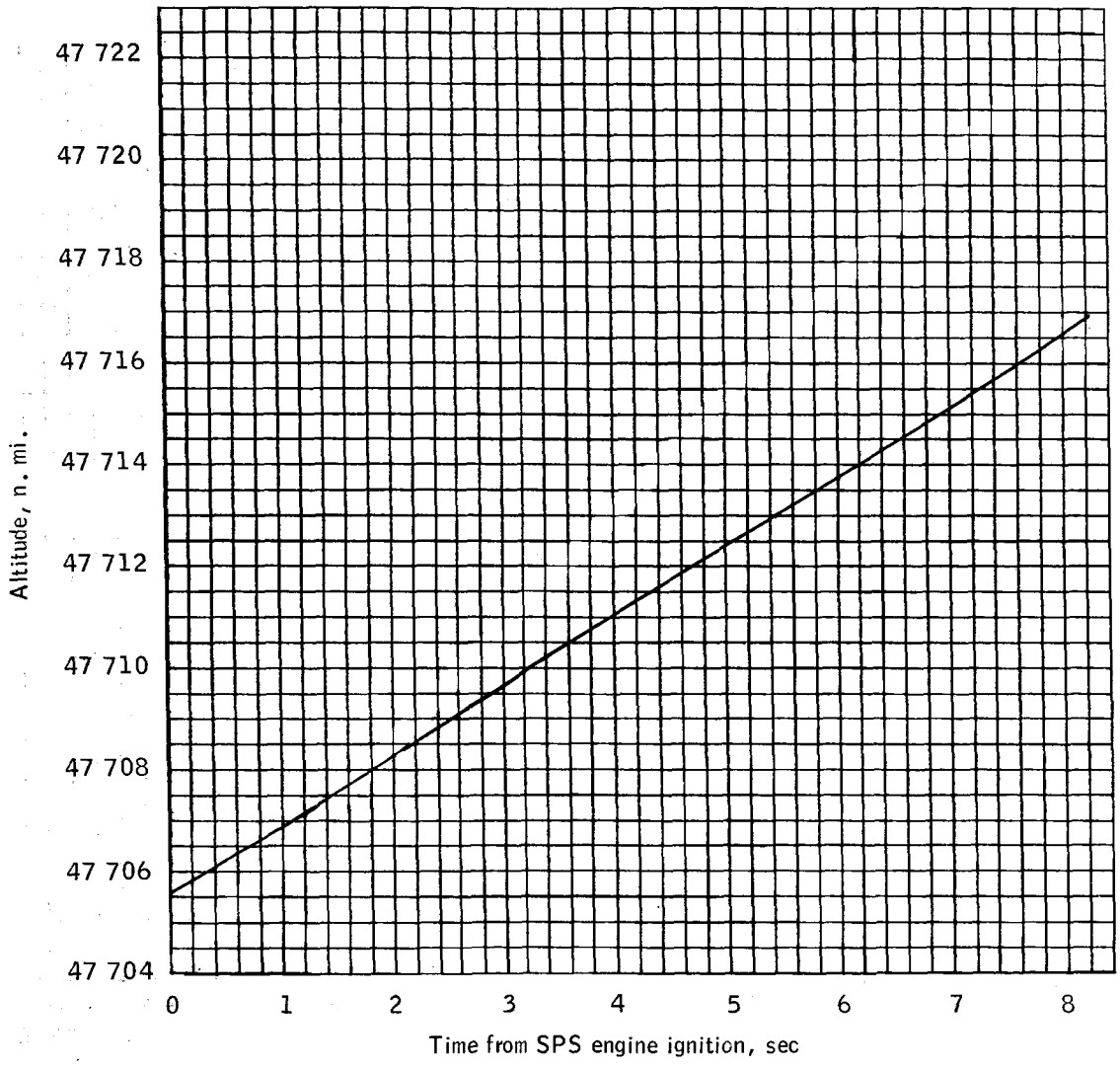

(n) Altitude.

Figure 2.- Continued.

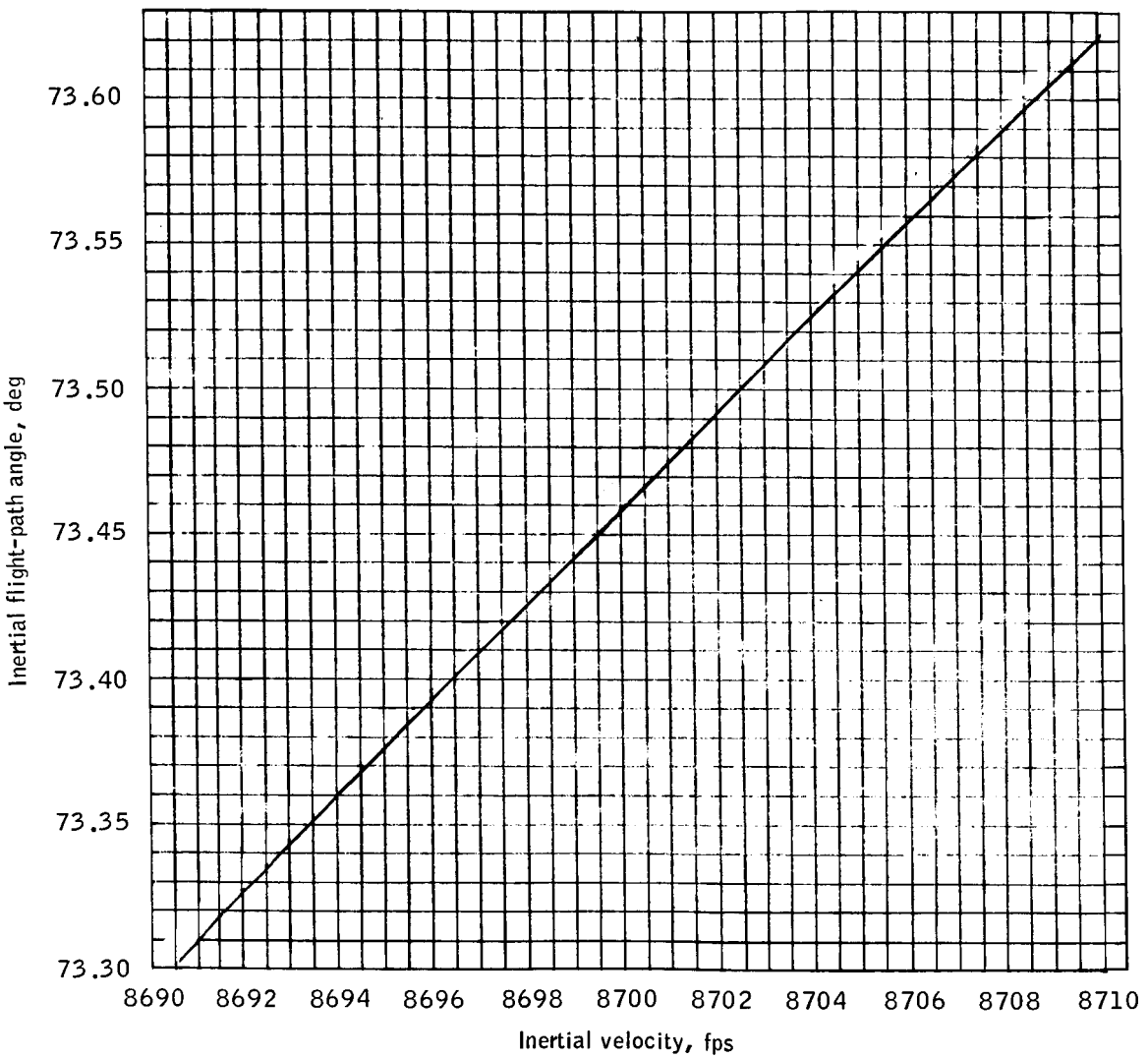

(o) Inertial flight-path angle.

Figure 2.- Concluded.

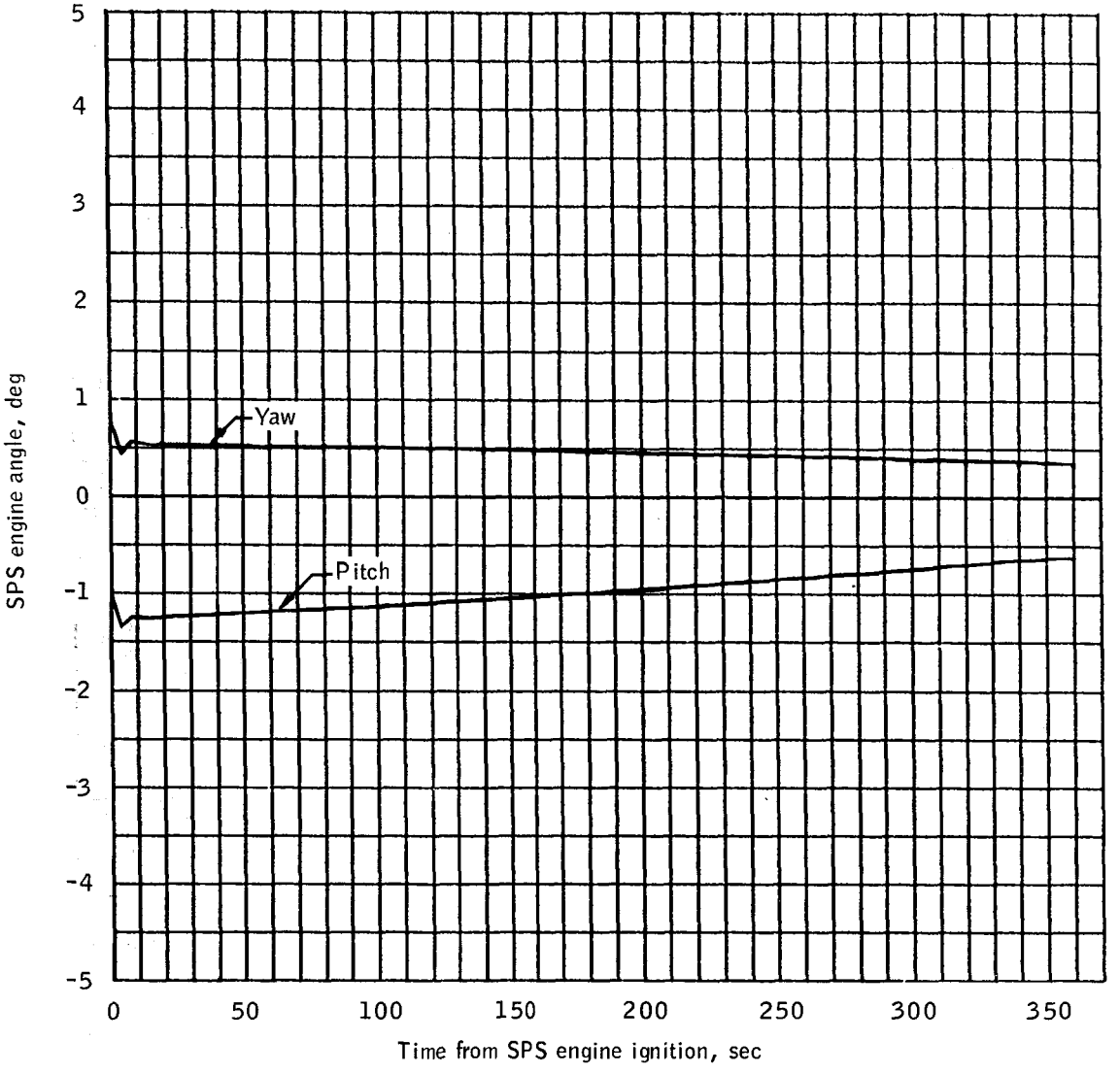

(a) SPS engine angles.

Figure 3.- LOI-1 burn parameters.

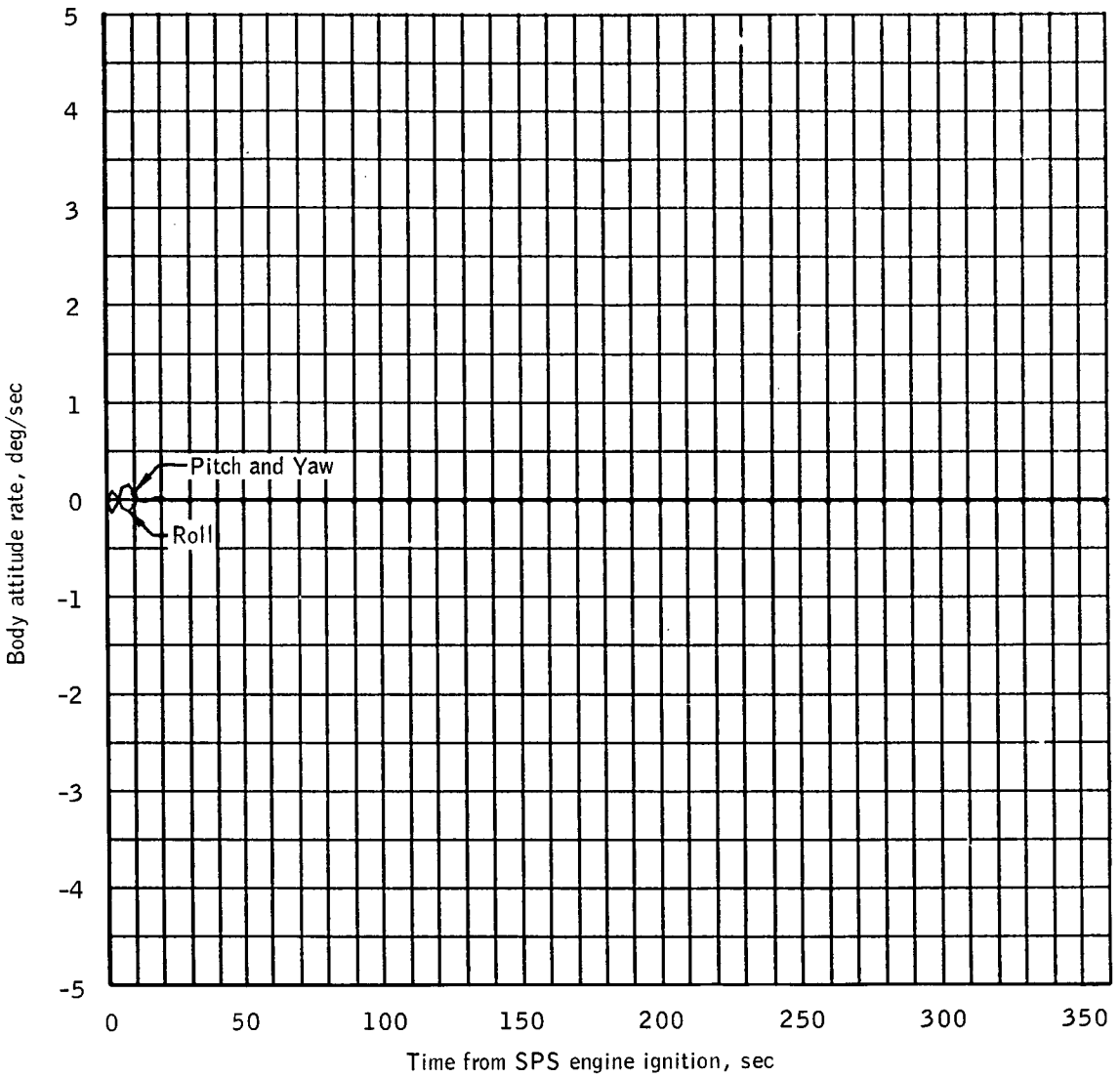

(b) Body attitude rates, FDAI-1.

Figure 3.- Continued.

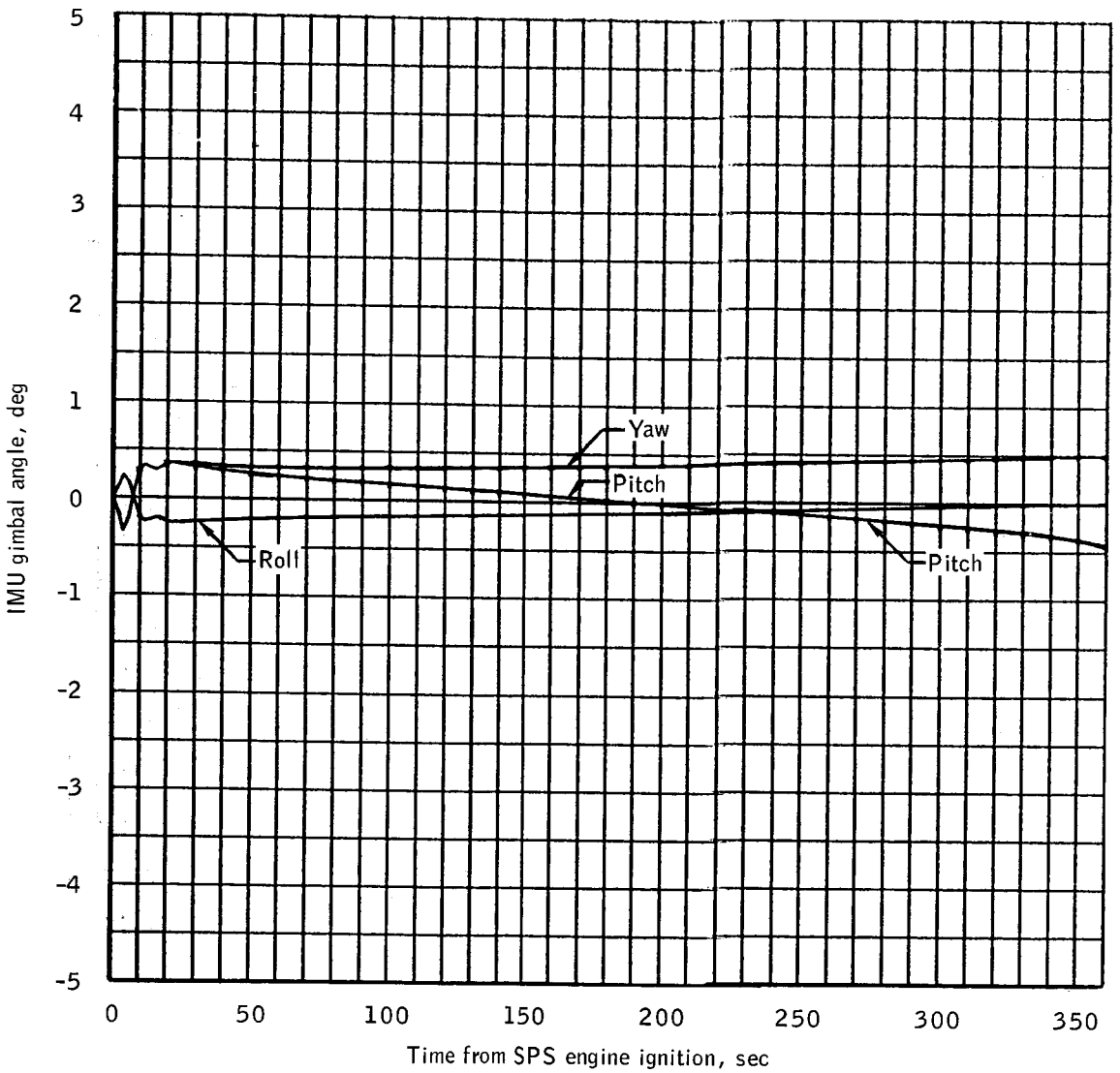

(c) IMU gimbal angles.

Figure 3.- Continued.

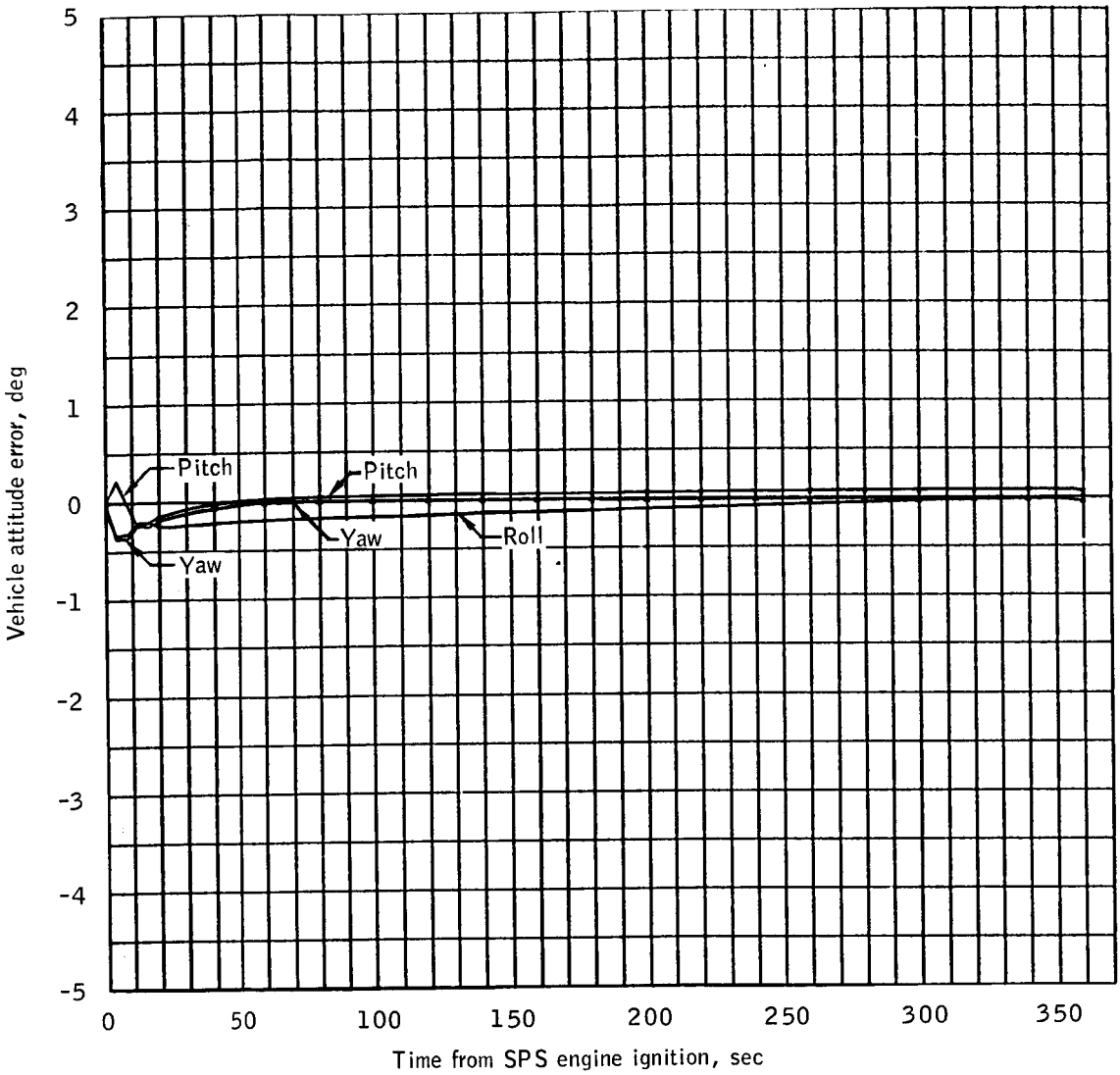

(d) Vehicle attitude errors.

Figure 3.- Continued.

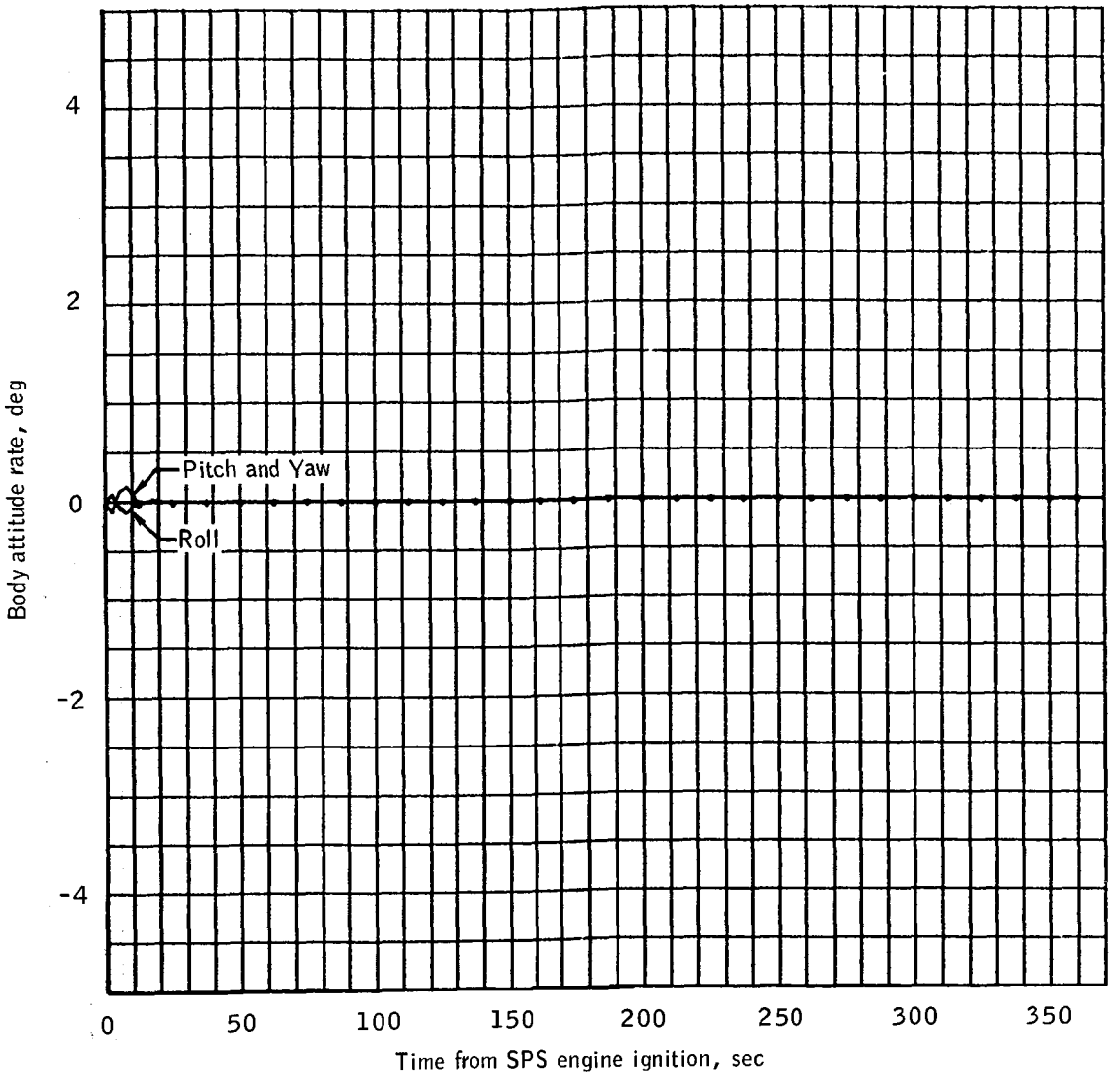

(e) Body attitude rates, FDAI-2.

Figure 3.- Continued.

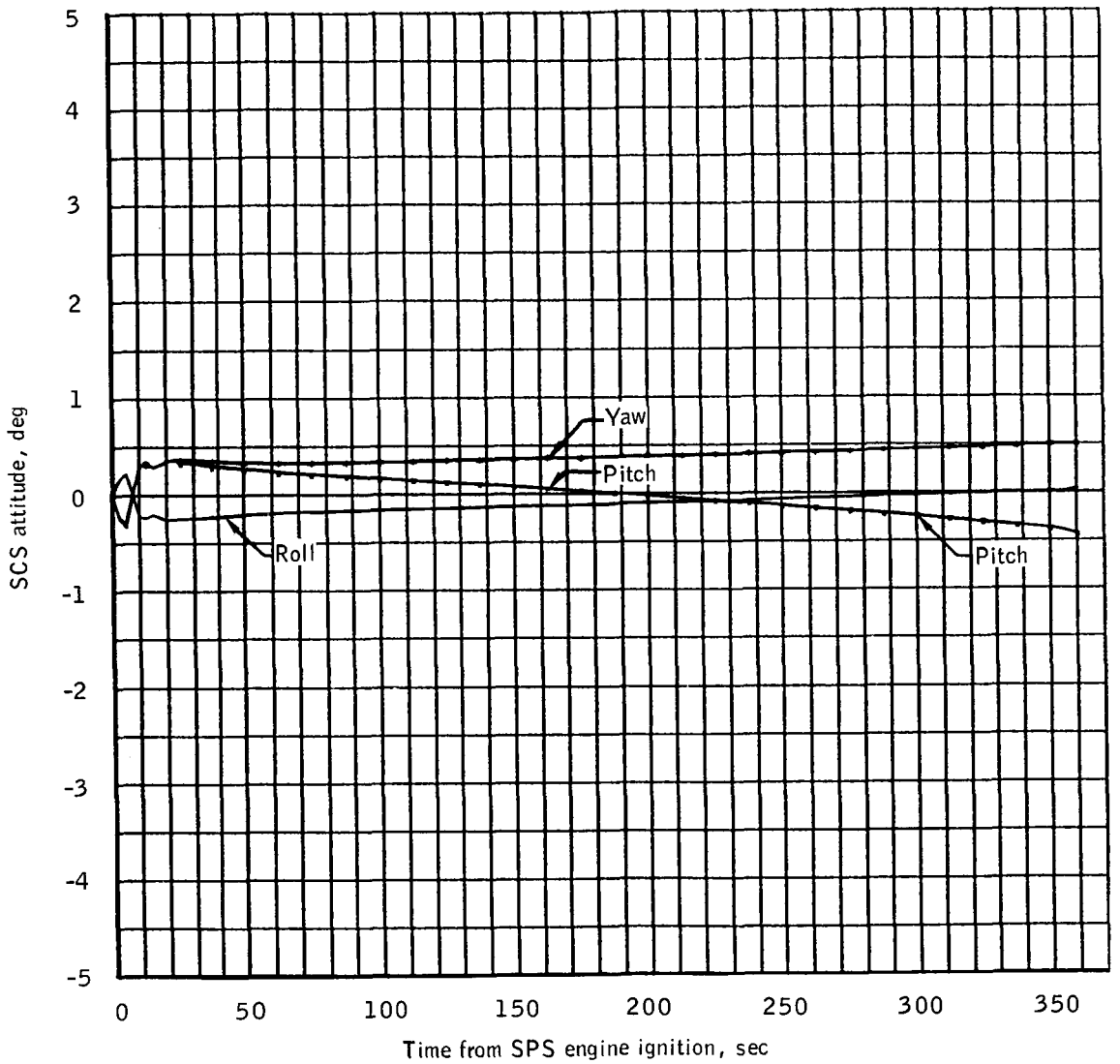

(f) SCS attitudes monitored from BMAGS.

Figure 3.- Continued.

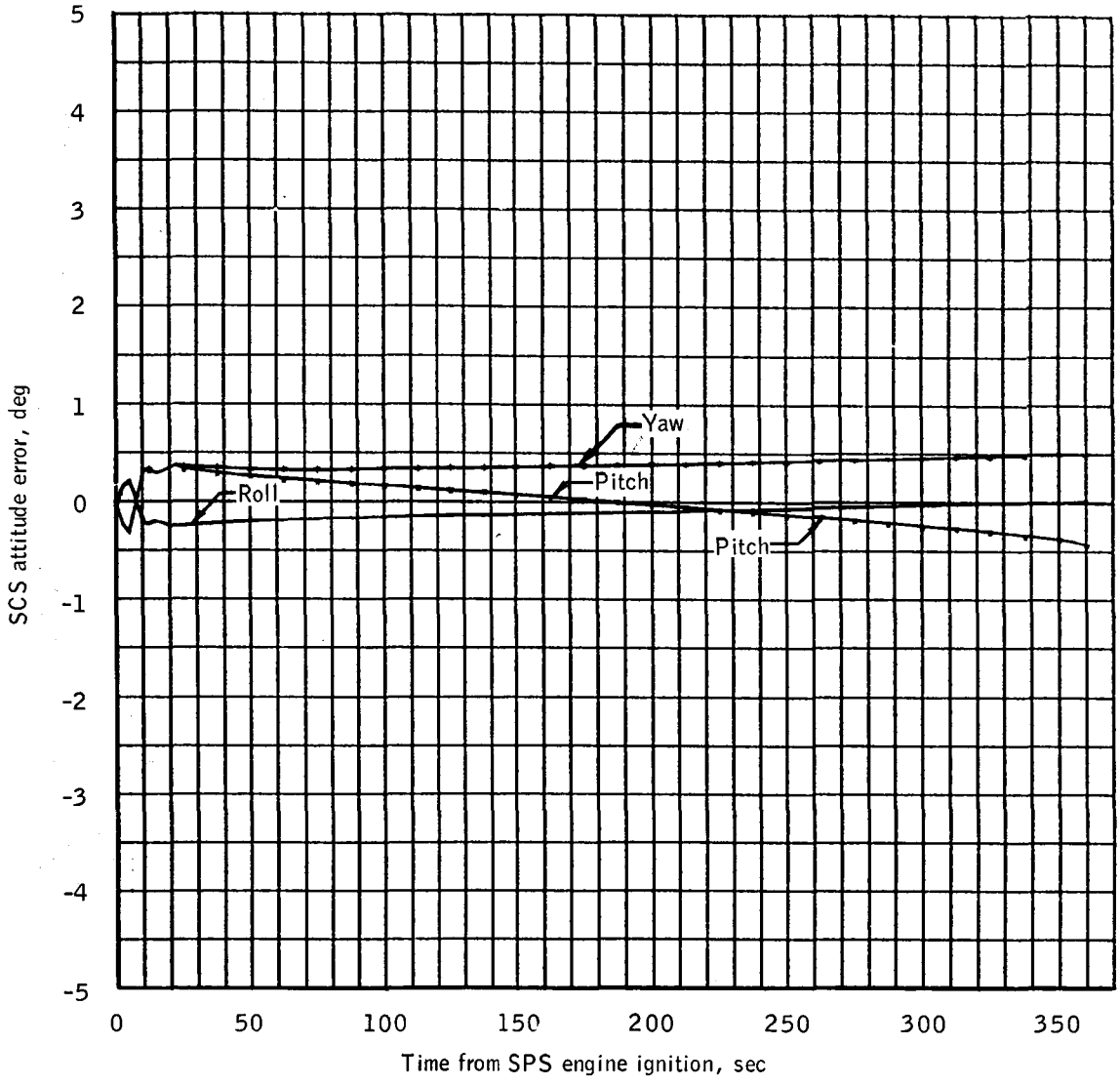

(g) SCS attitude errors monitored from BMAGS.

Figure 3.- Continued.

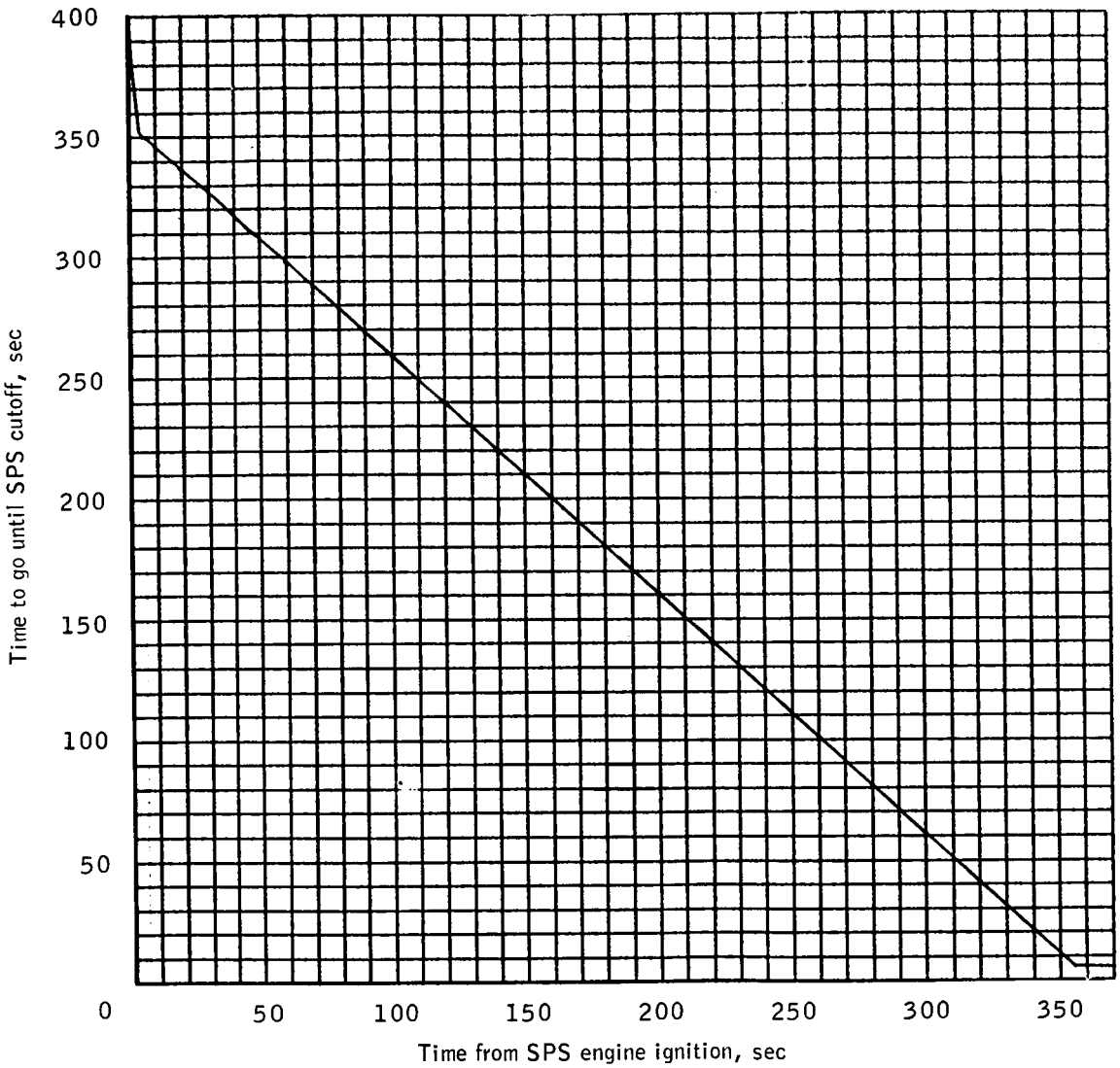

(h) Time to go until SPS cutoff.

Figure 3.- Continued.

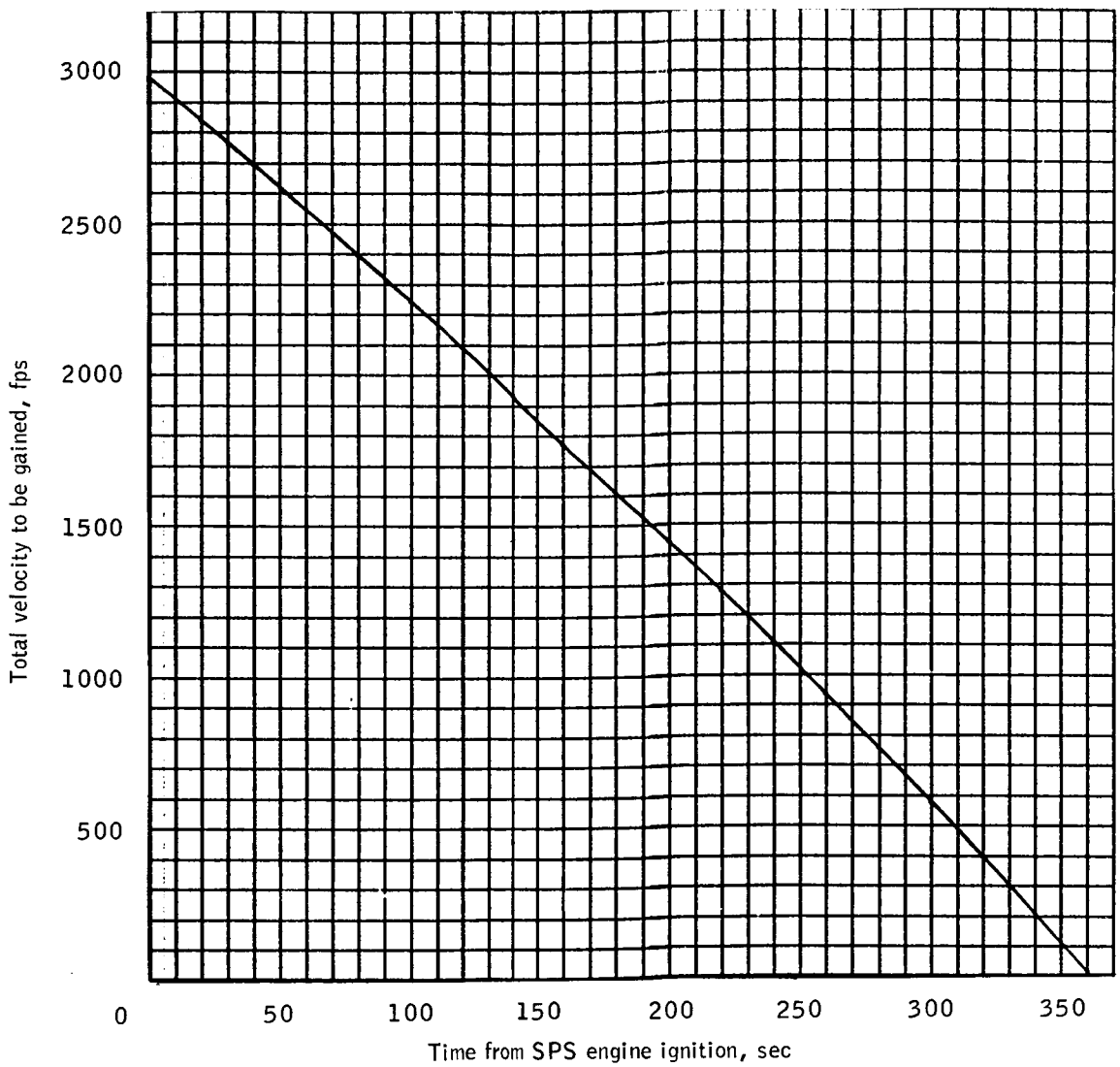

(i) Total velocity to be gained until SPS cutoff.

Figure 3.- Continued.

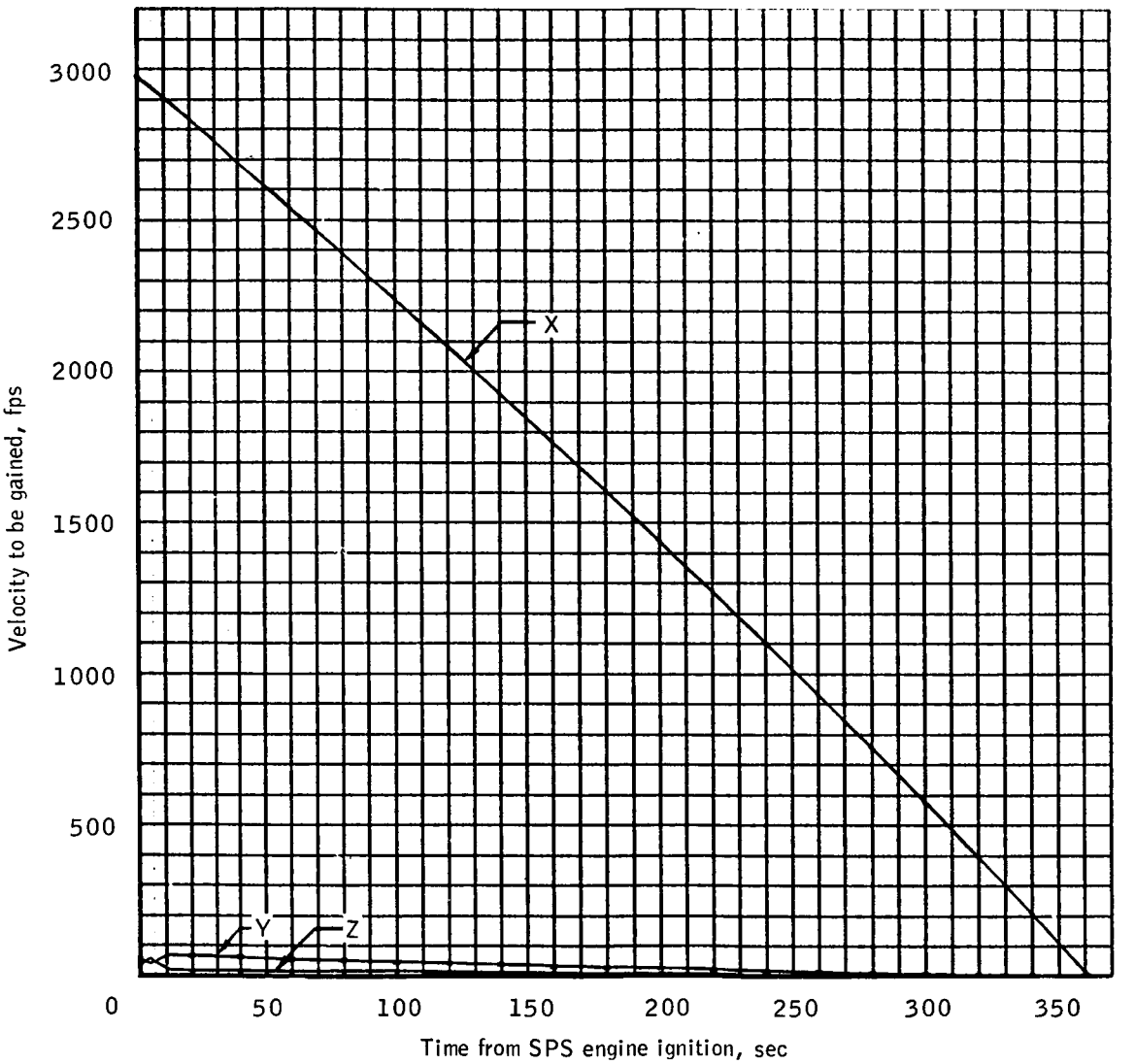

(j) Velocity to be gained in control coordinates.

Figure 3.- Continued.

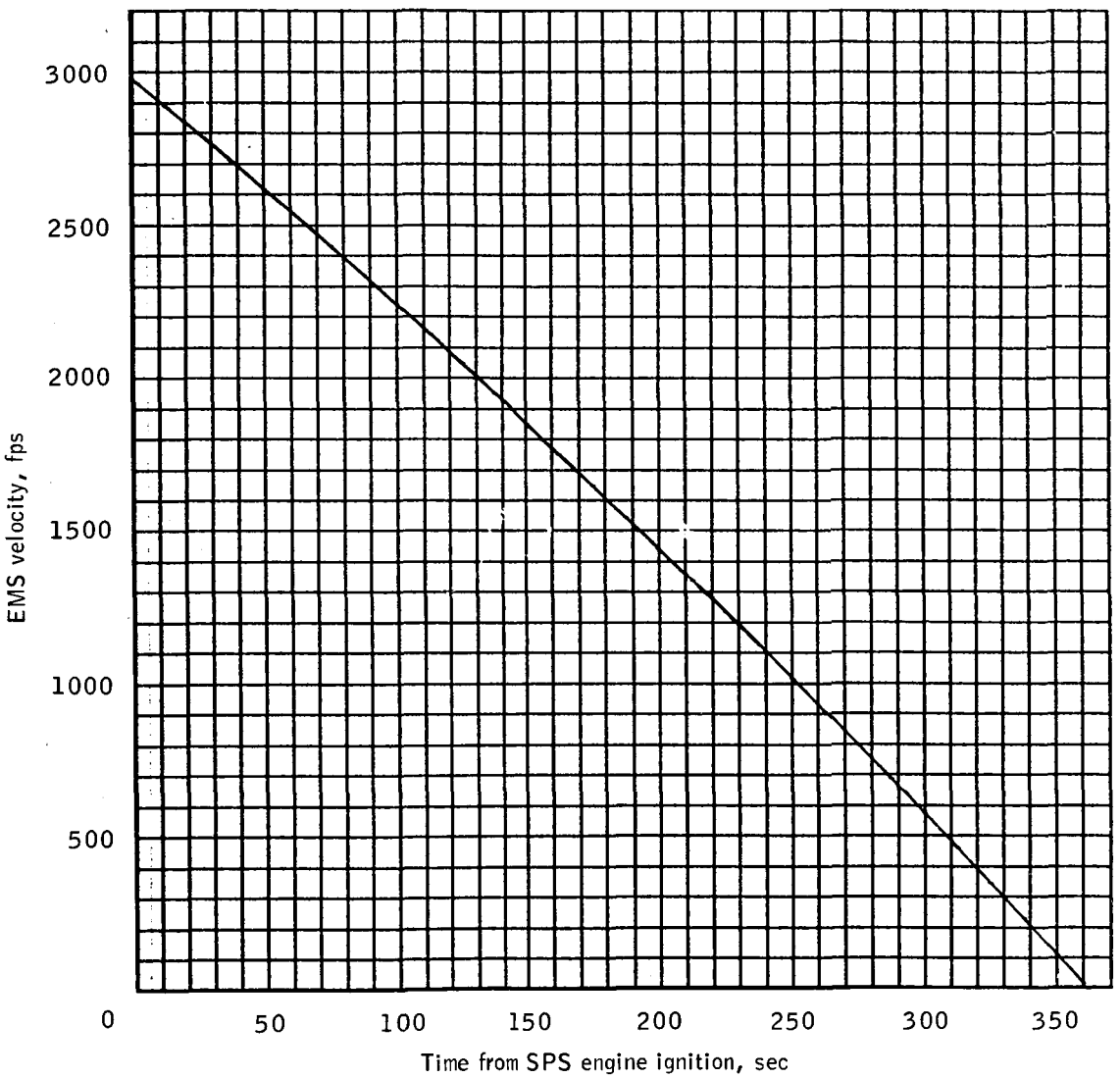

(k) EMS velocity.

Figure 3.- Continued.

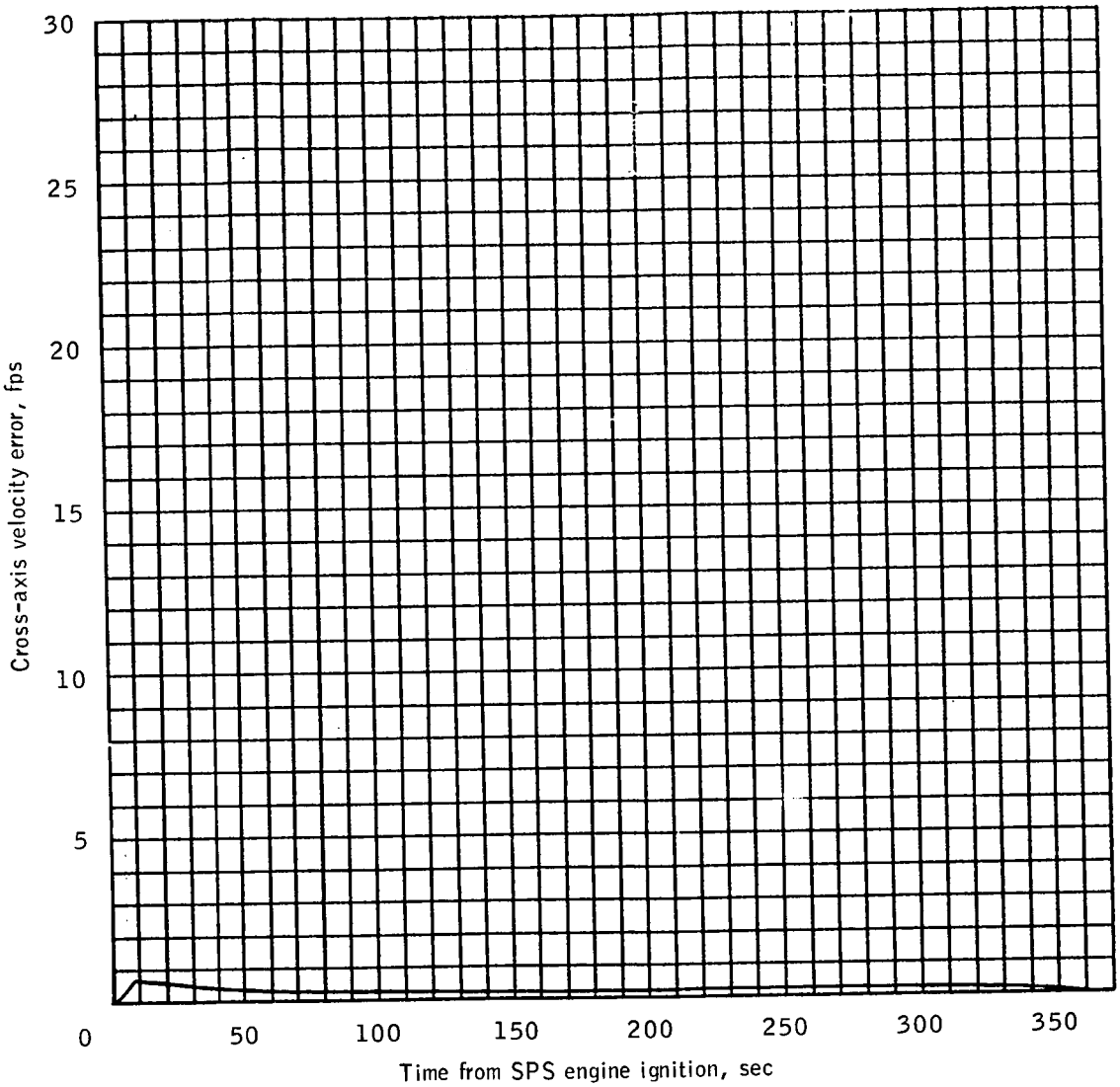

(l) Cross-axis velocity error.

Figure 3.- Continued.

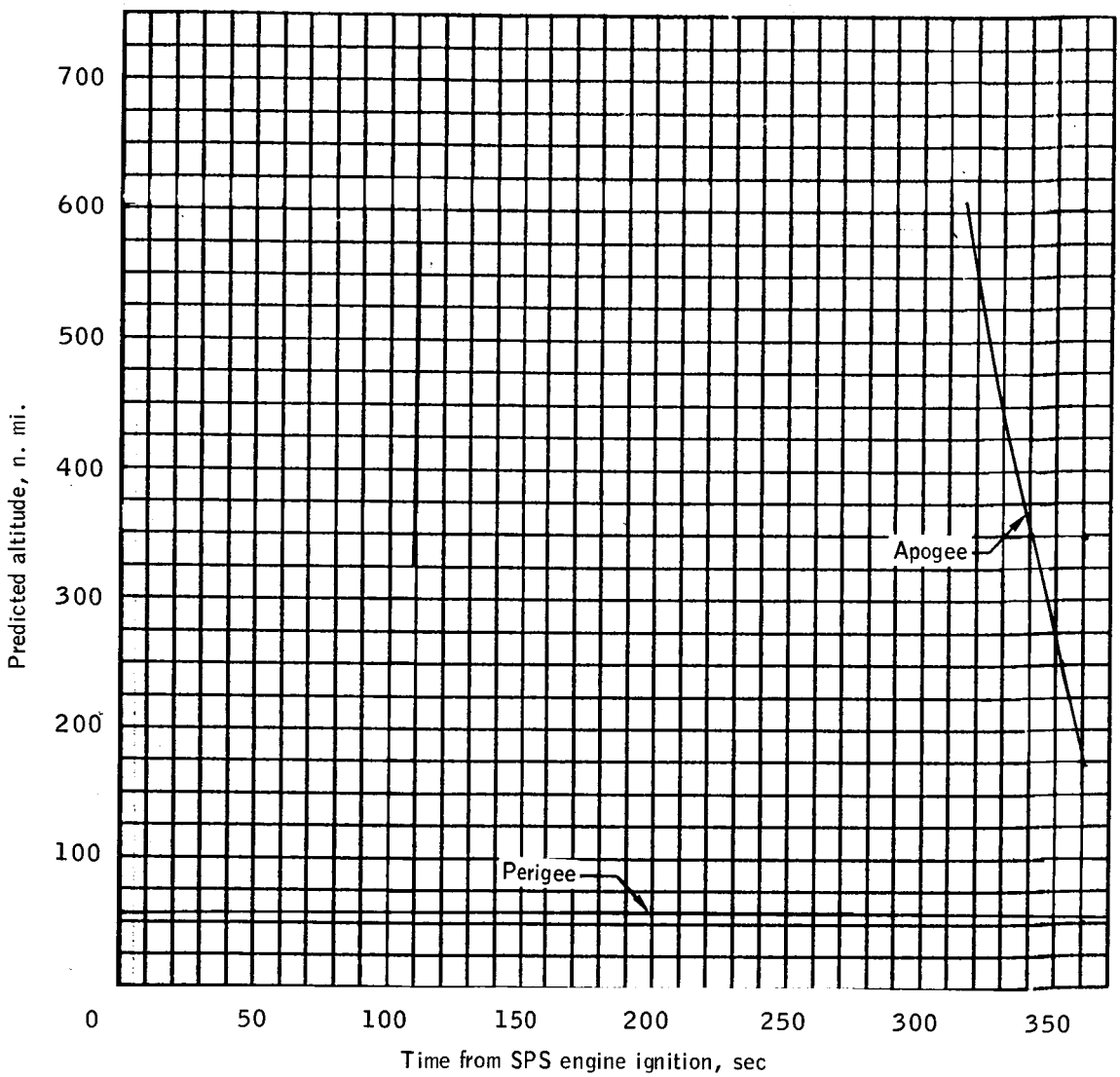

(m) Predicted apogee and perigee altitude.

Figure 3.- Continued.

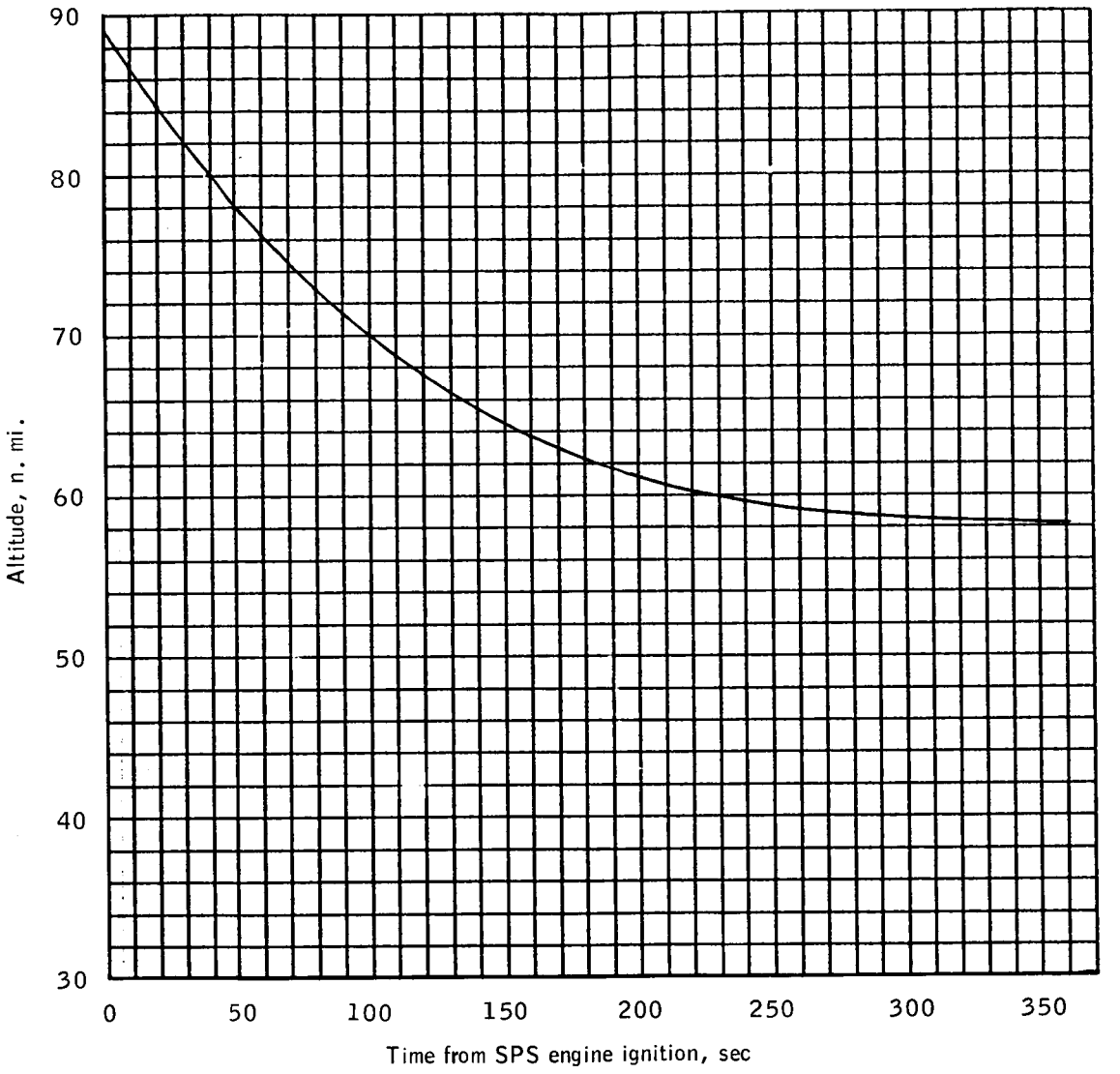

(n) Altitude.

Figure 3.- Continued.

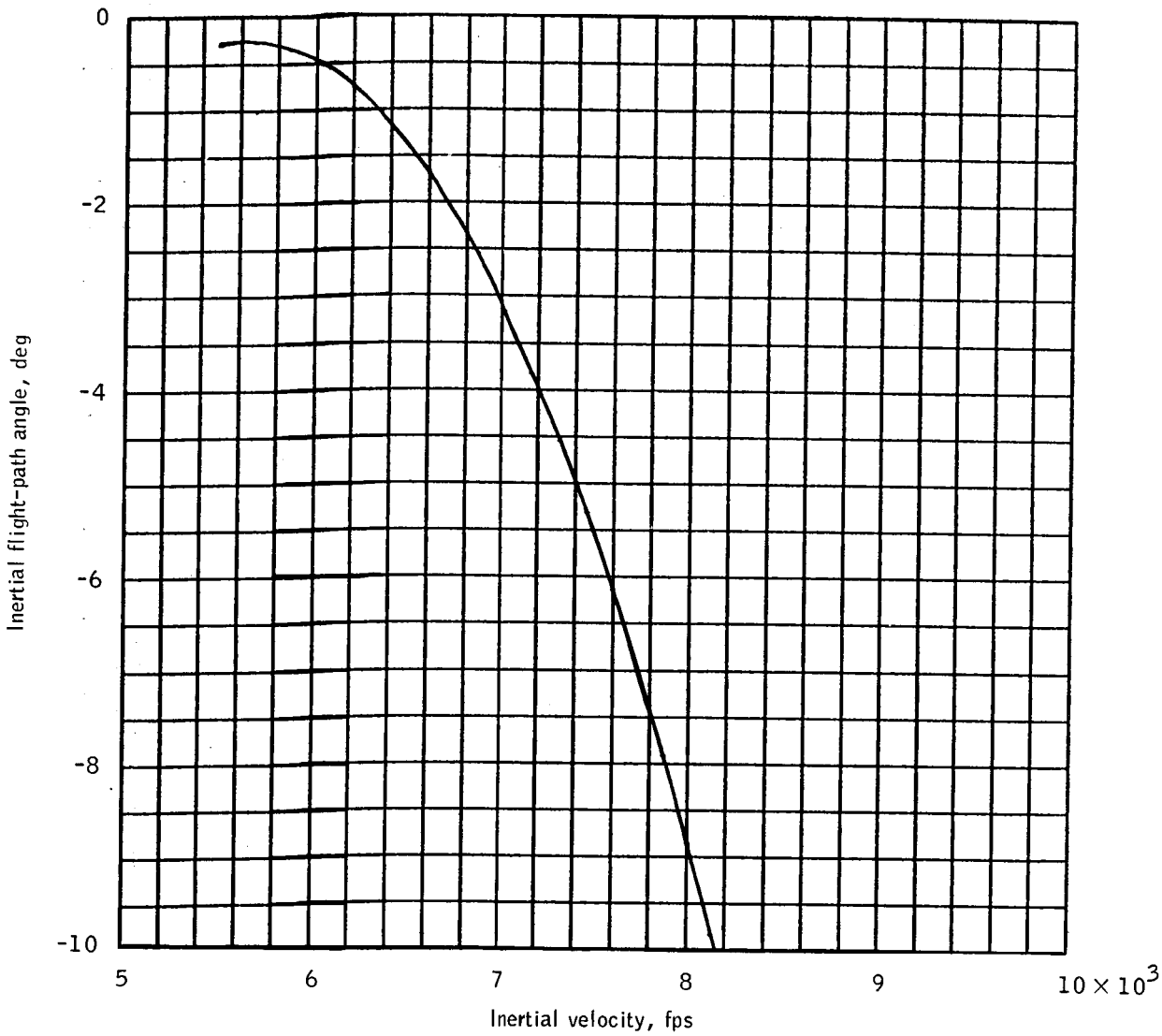

(o) Inertial flight-path angle.

Figure 3.- Continued.

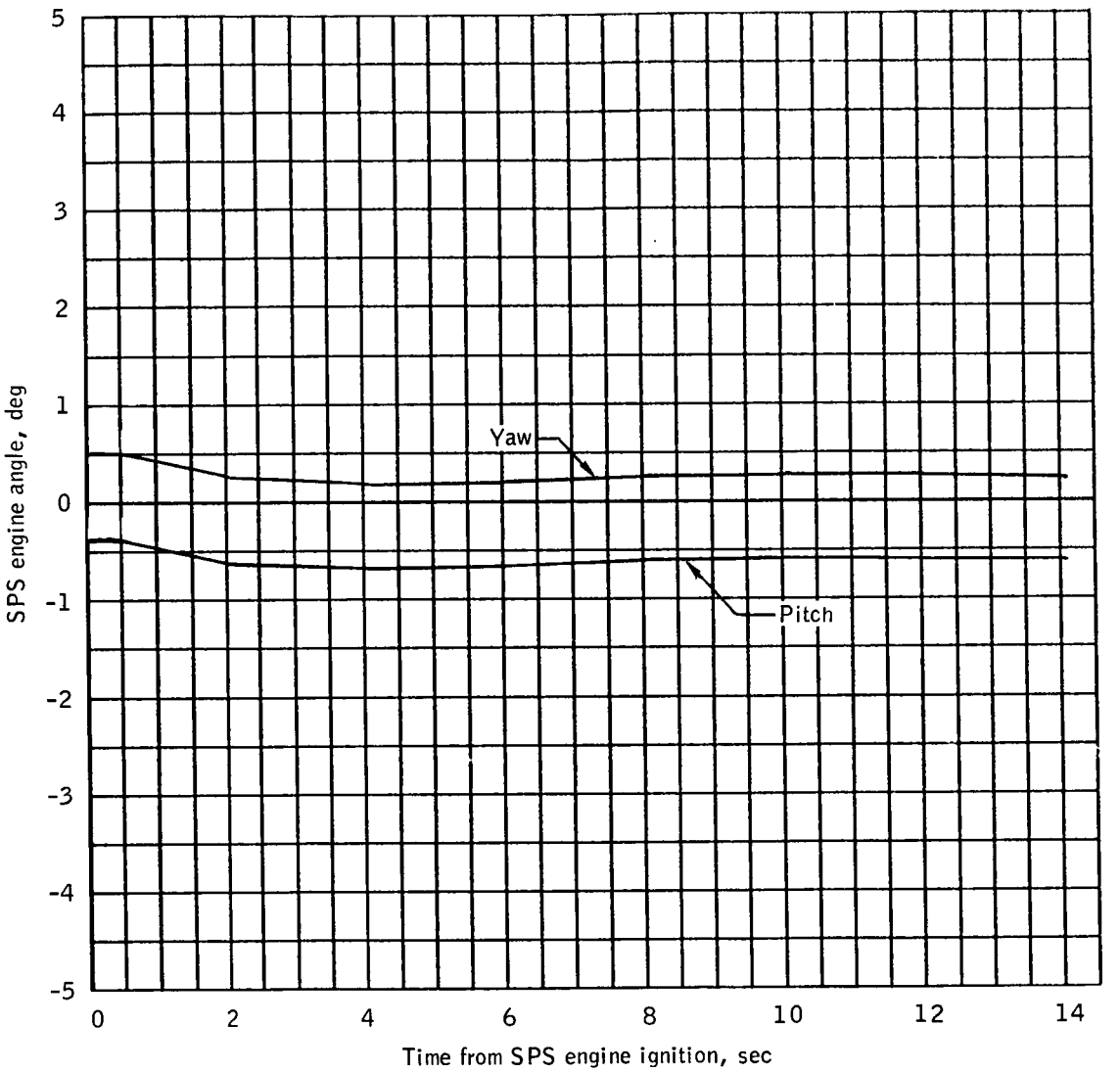

(a) SPS engine angles.

Figure 4.- LOI-2 burn parameters.

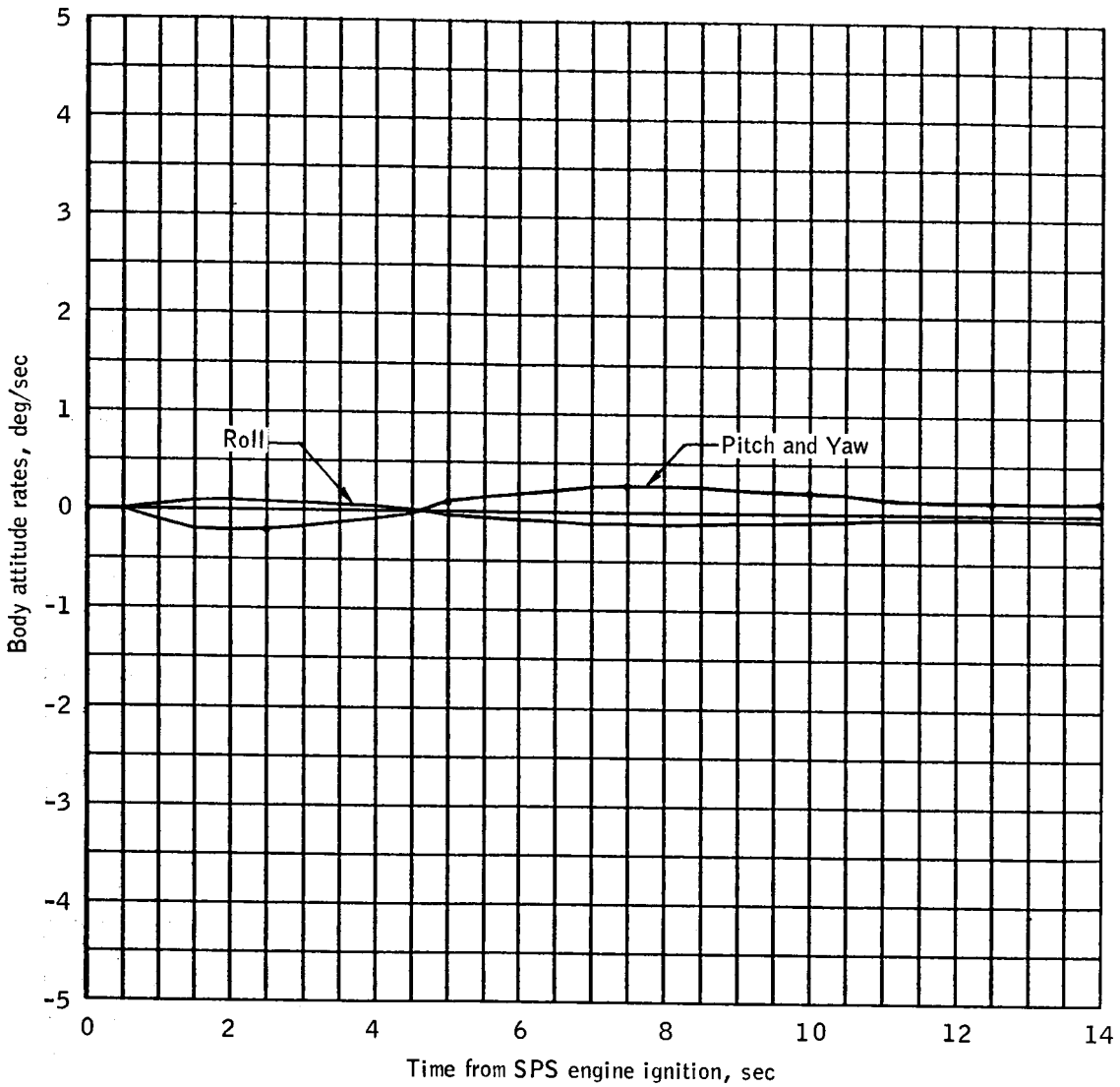

(b) Body attitude rates, FDAI-1.

Figure 4.- Continued.

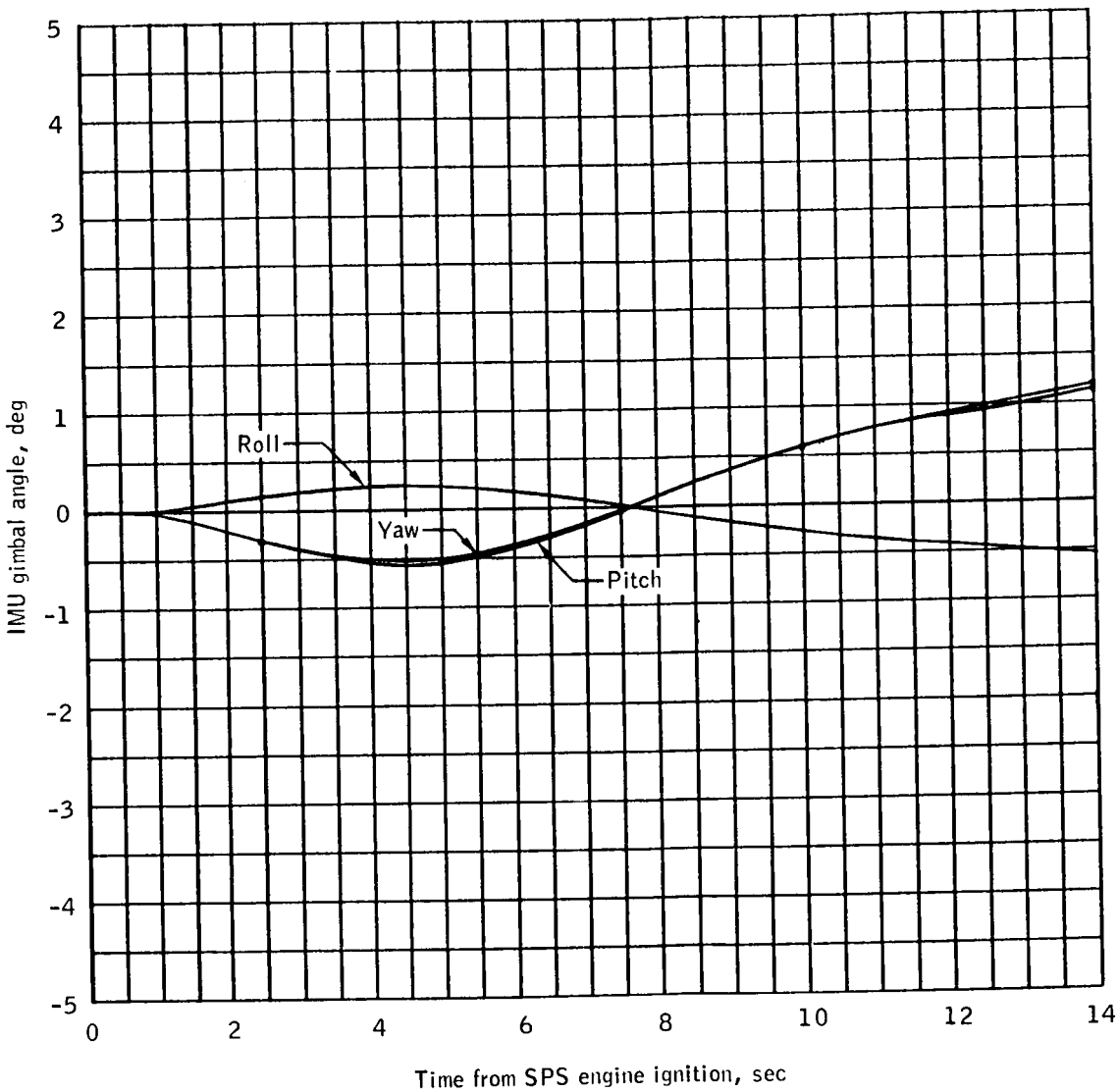

(c) IMU gimbal angles.

Figure 4.- Continued.

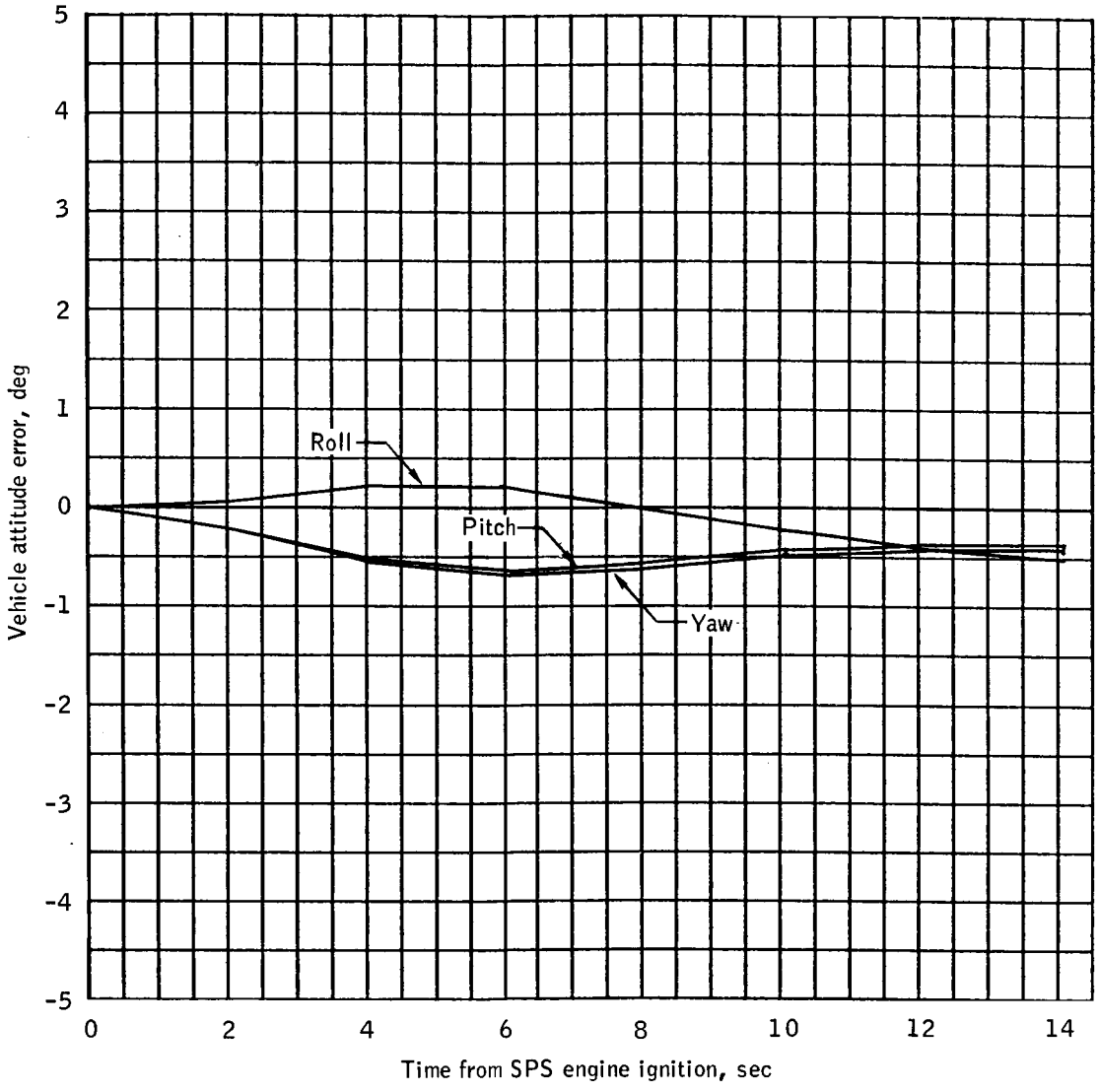

(d) Vehicle attitude errors.

Figure 4.- Continued.

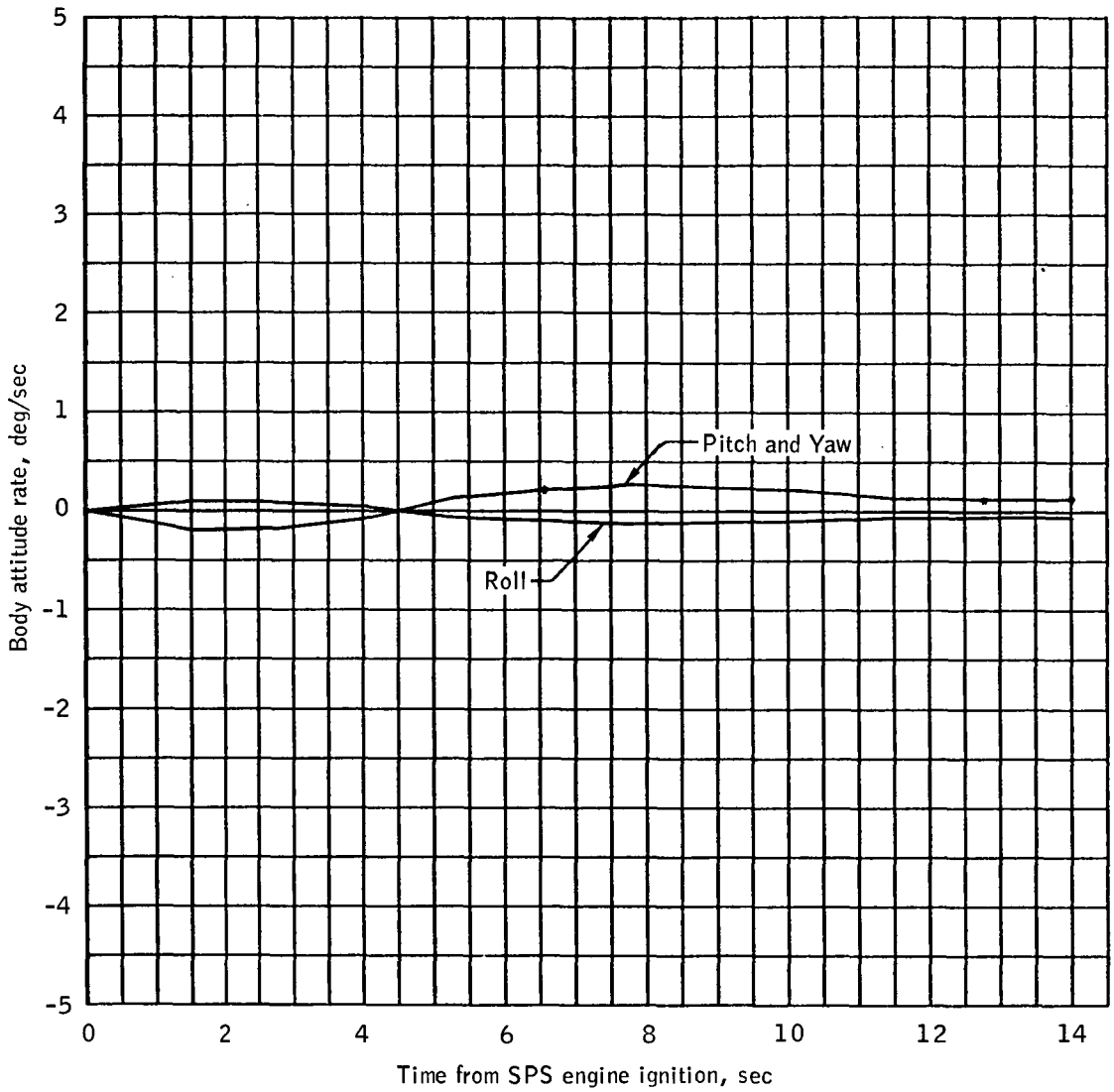

(e) Body attitude rates, FDAI-2.

Figure 4.- Continued.

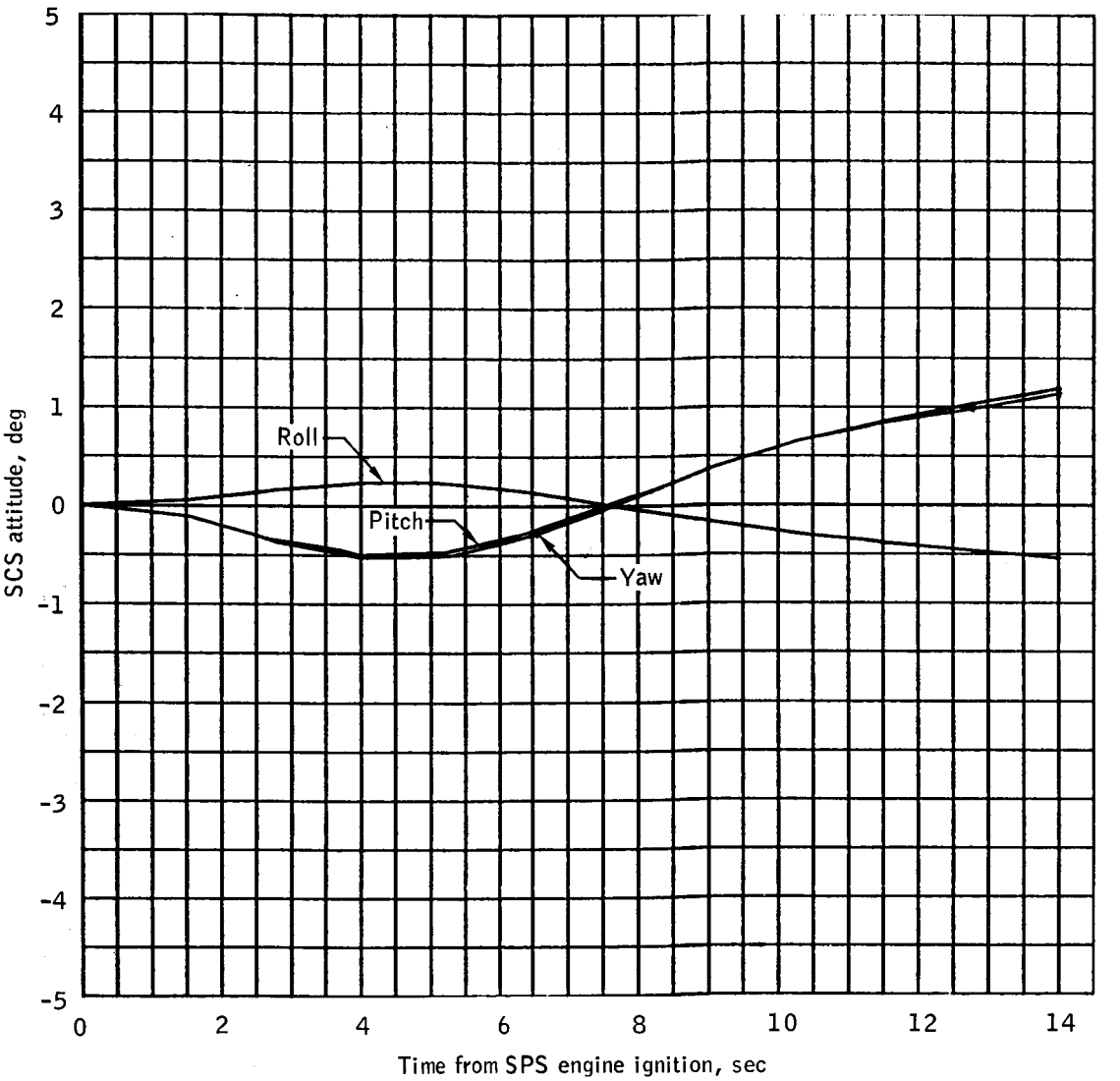

(f) SCS attitudes monitored from BMAGS.

Figure 4.- Continued.

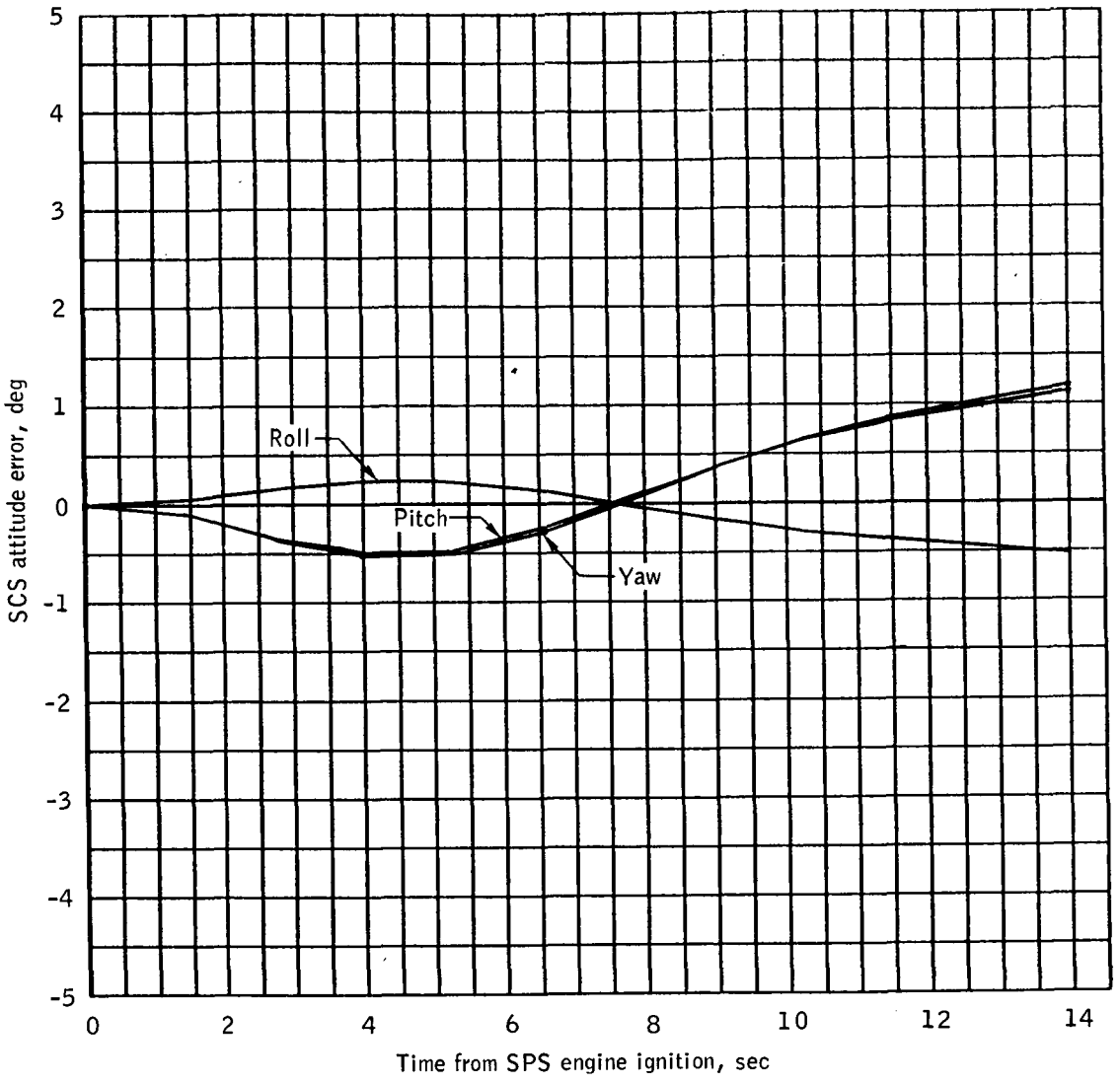

(g) SCS attitude errors monitored from BMAGS.

Figure 4.- Continued.

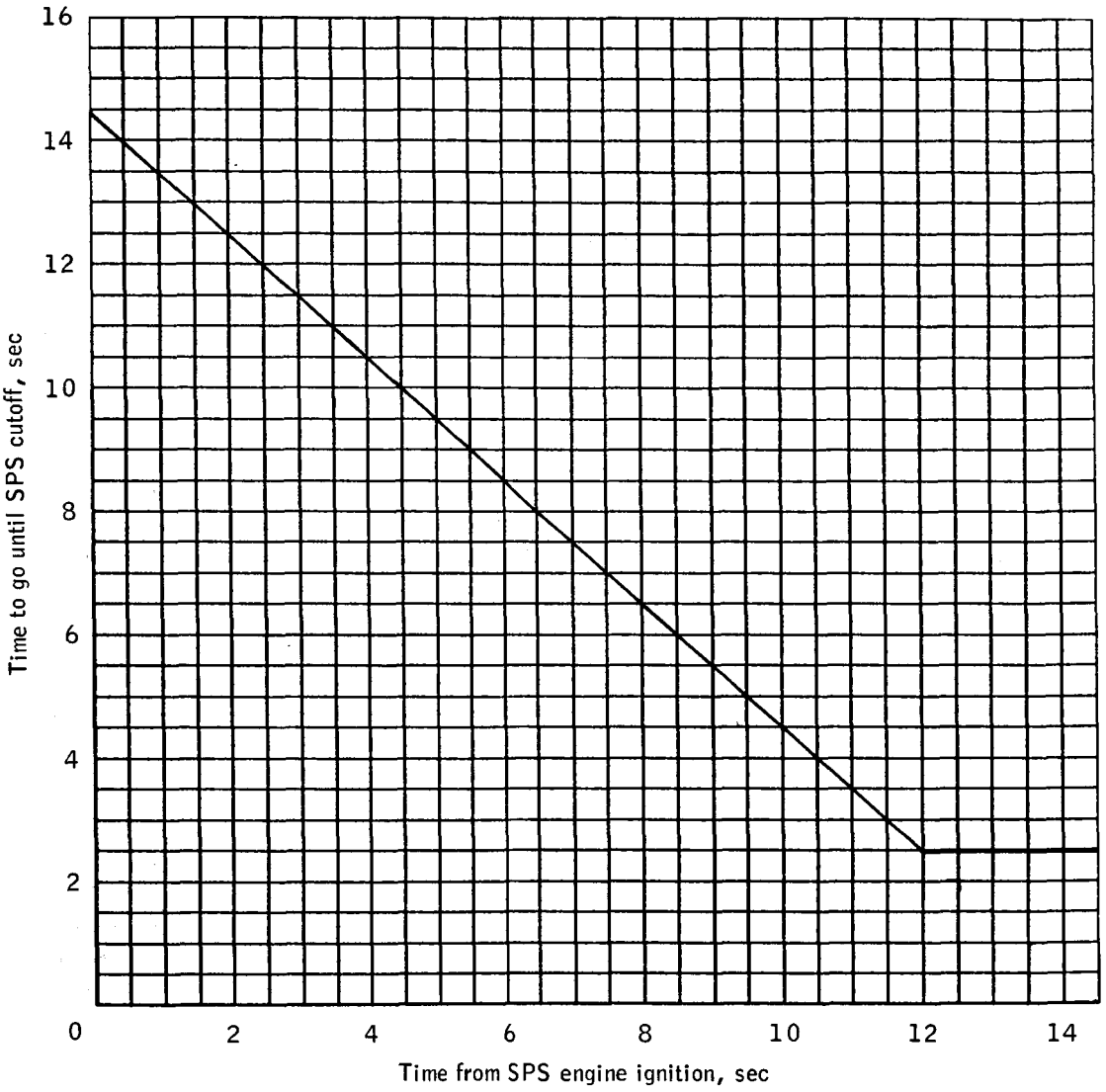

(h) Time to go until SPS cutoff.

Figure 4.- Continued.

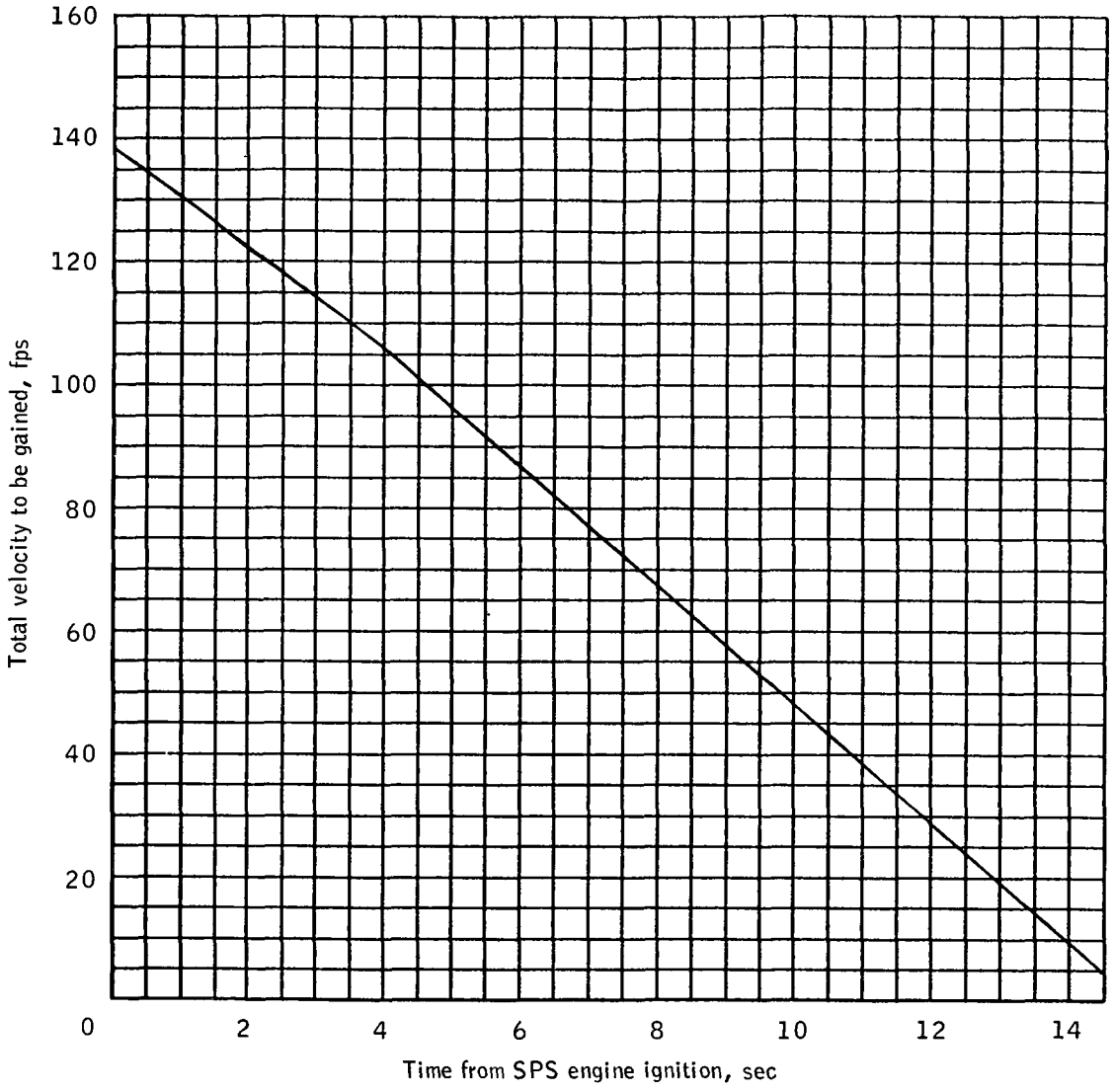

(i) Total velocity to be gained until SPS cutoff.

Figure 4.- Continued.

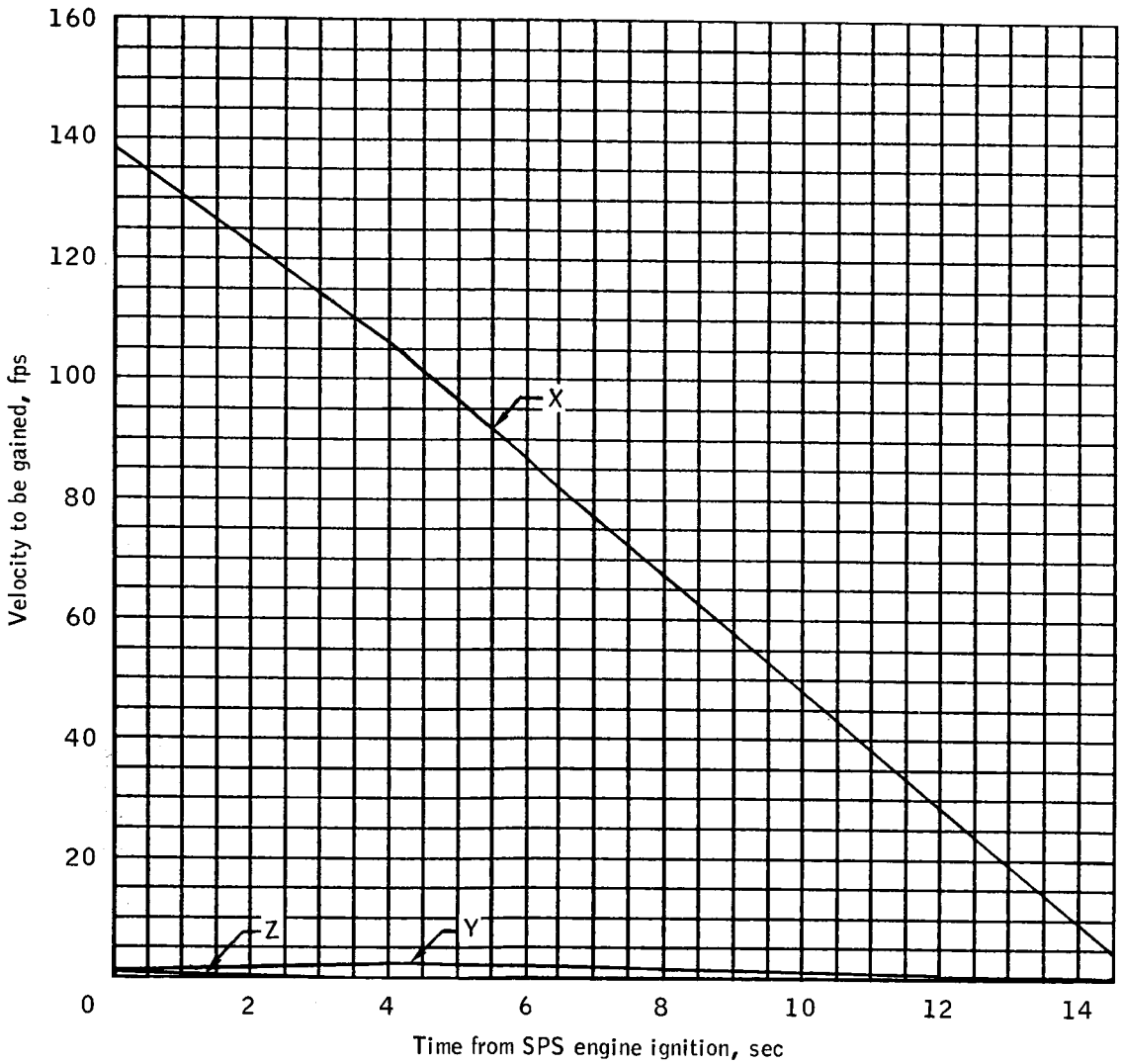

(j) Velocity to be gained in control coordinates.

Figure 4.- Continued.

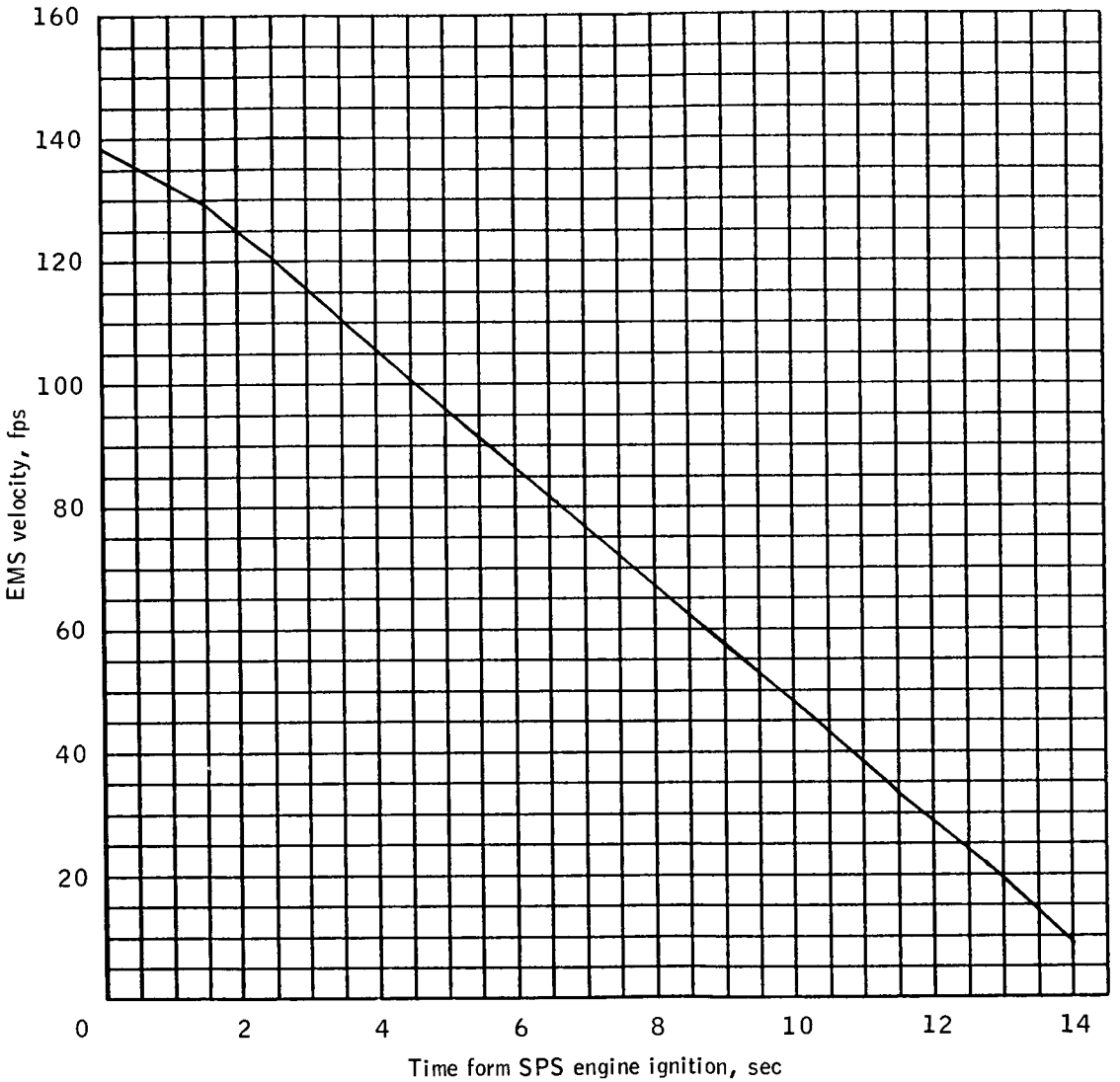

(k) EMS velocity.

Figure 4.- Continued.

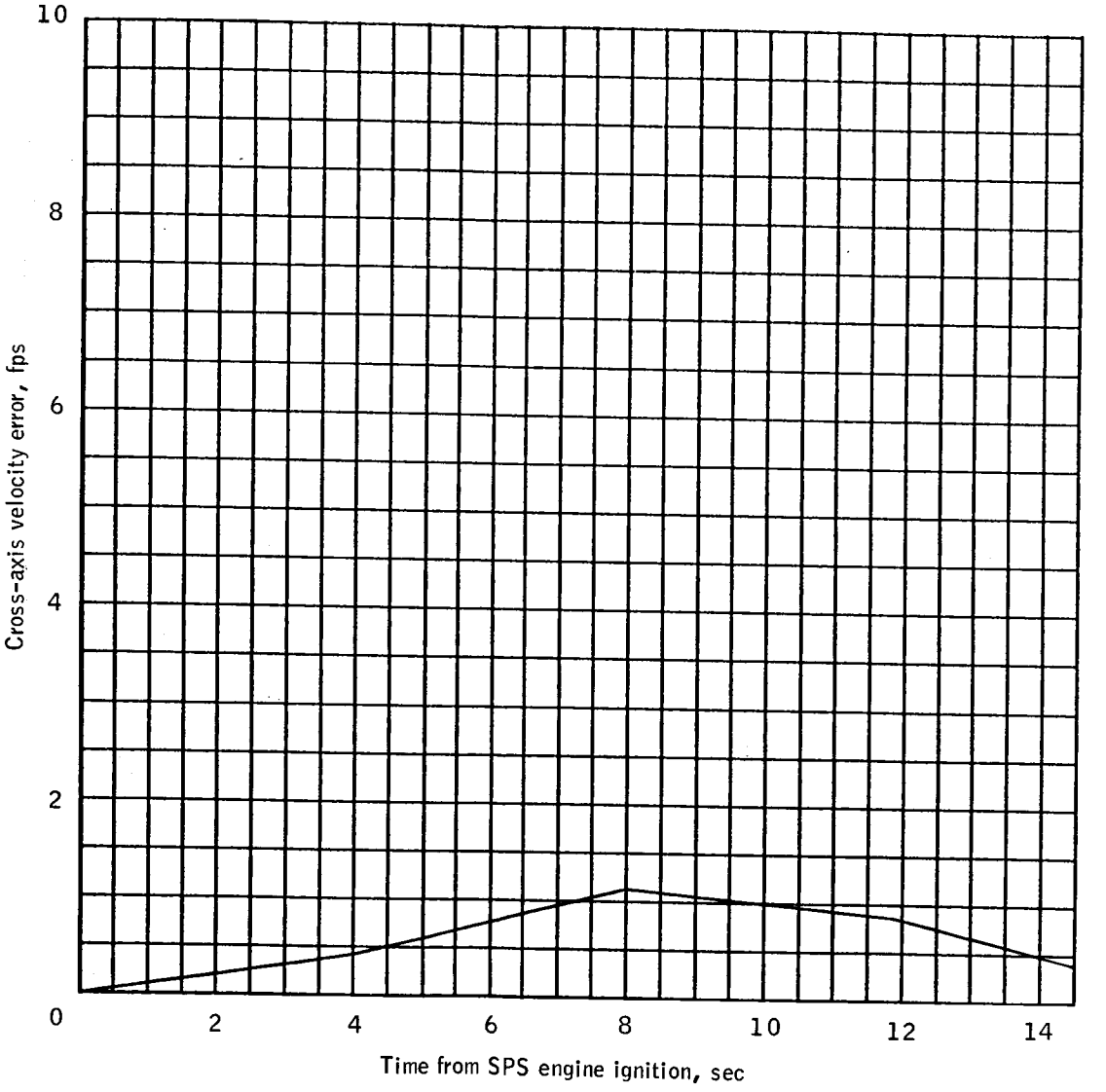

(l) Cross-axis velocity error.

Figure 4.- Continued.

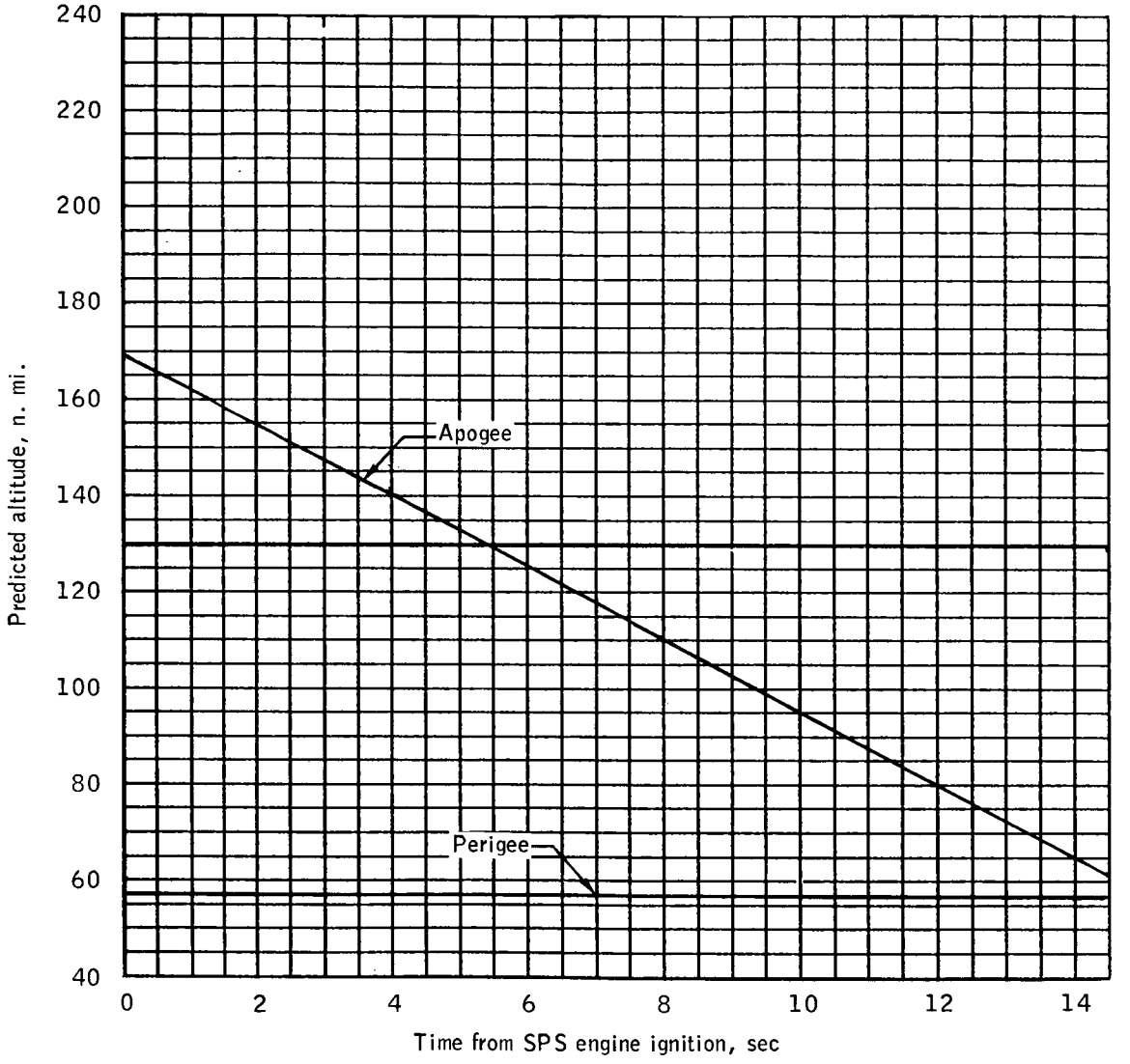

(m) Predicted apogee and perigee altitudes.

Figure 4.- Continued.

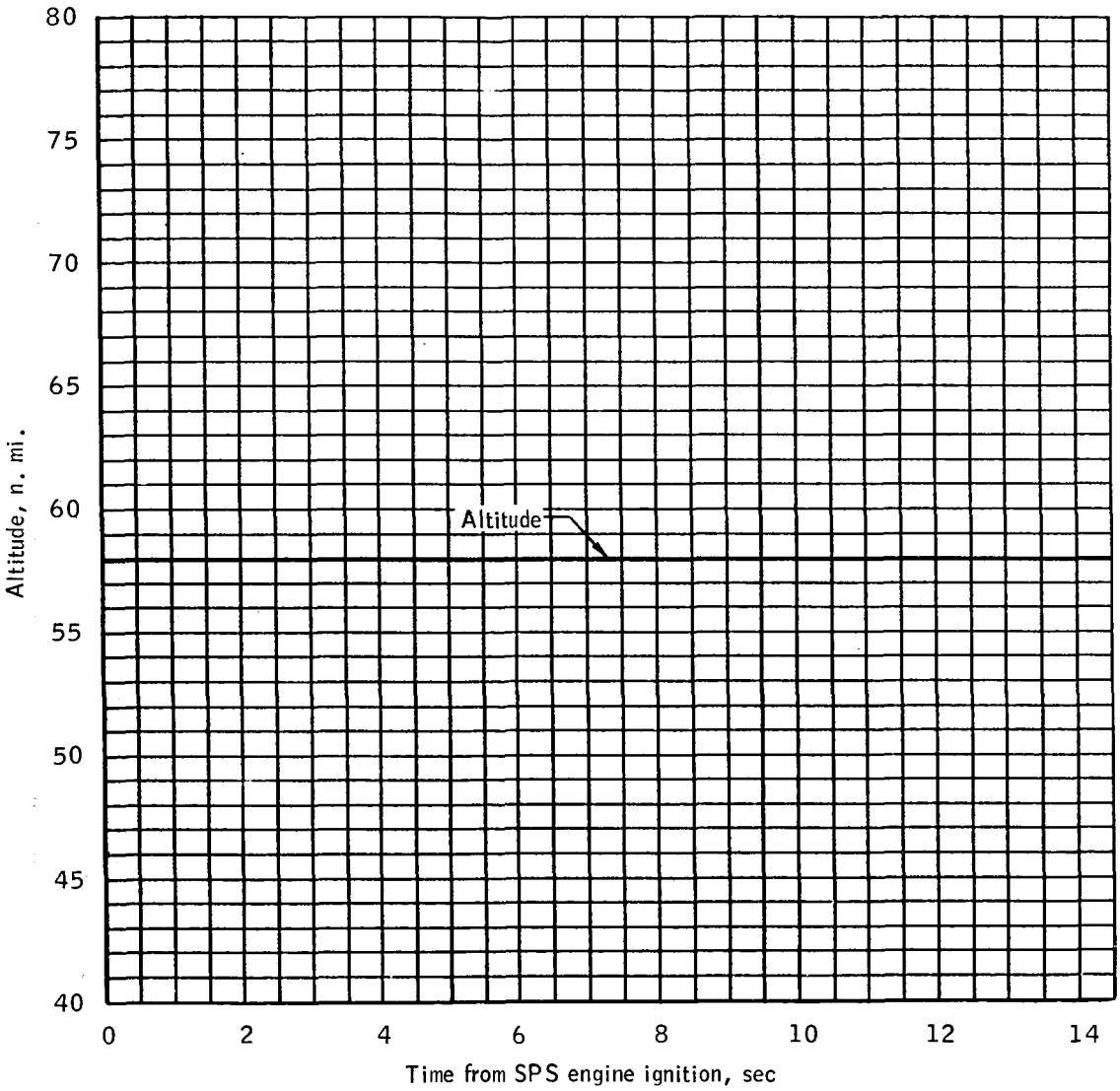

(n) Altitude.

Figure 4.- Continued.

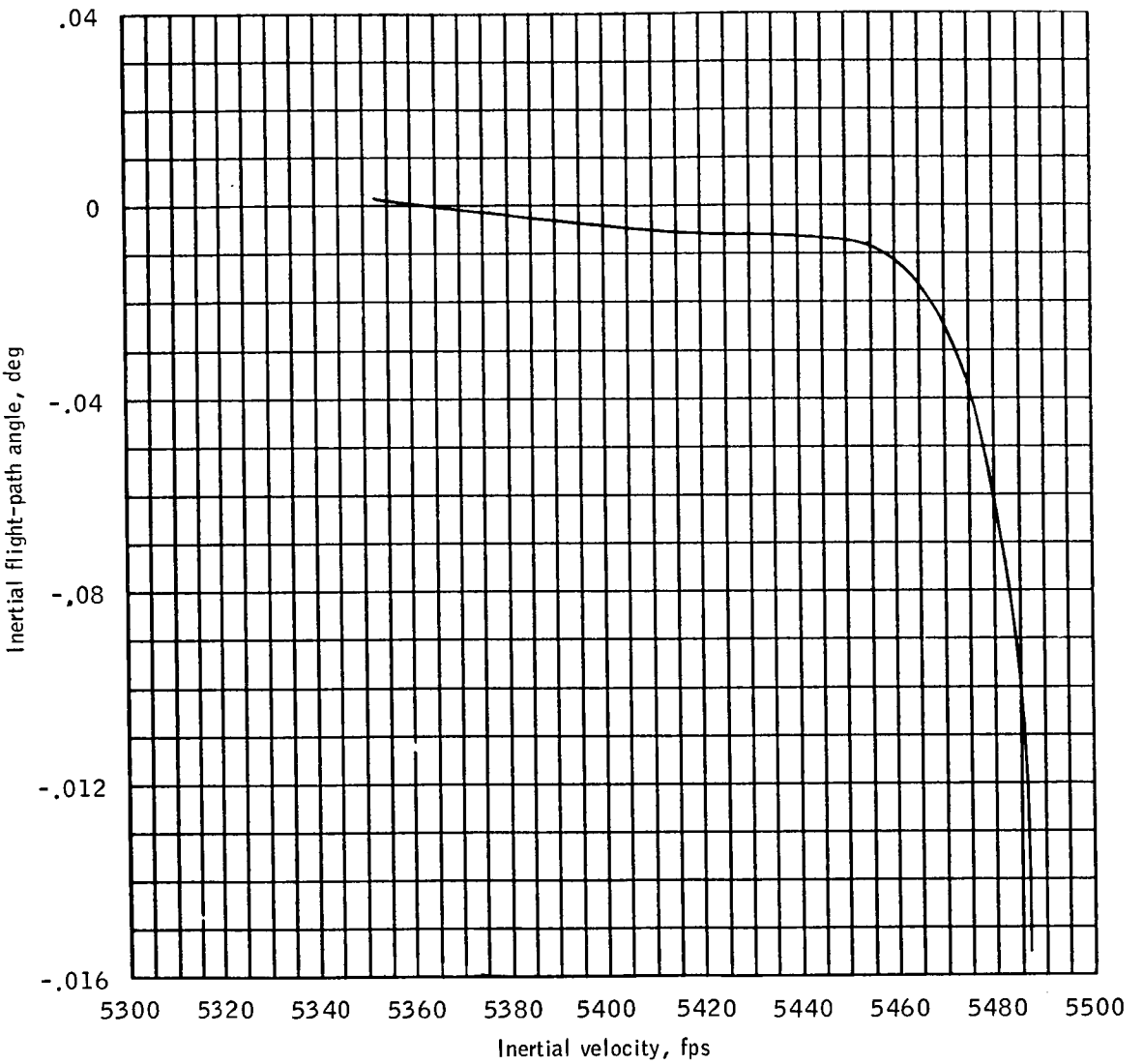

(o) Inertial flight-path angle versus inertial velocity.

Figure 4.- Concluded.

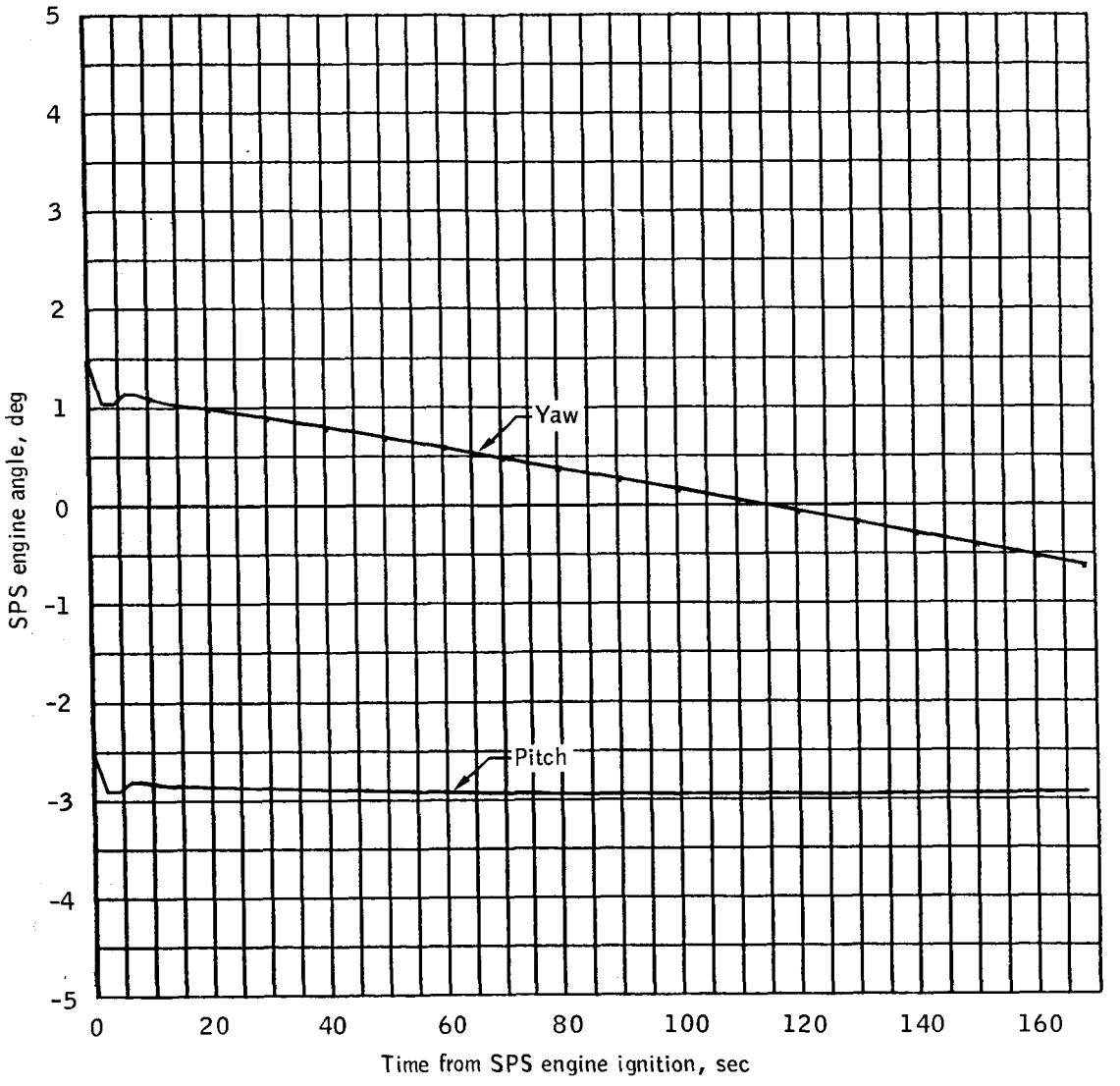

(a) SPS engine angles.

Figure 5.- TEI burn parameters.

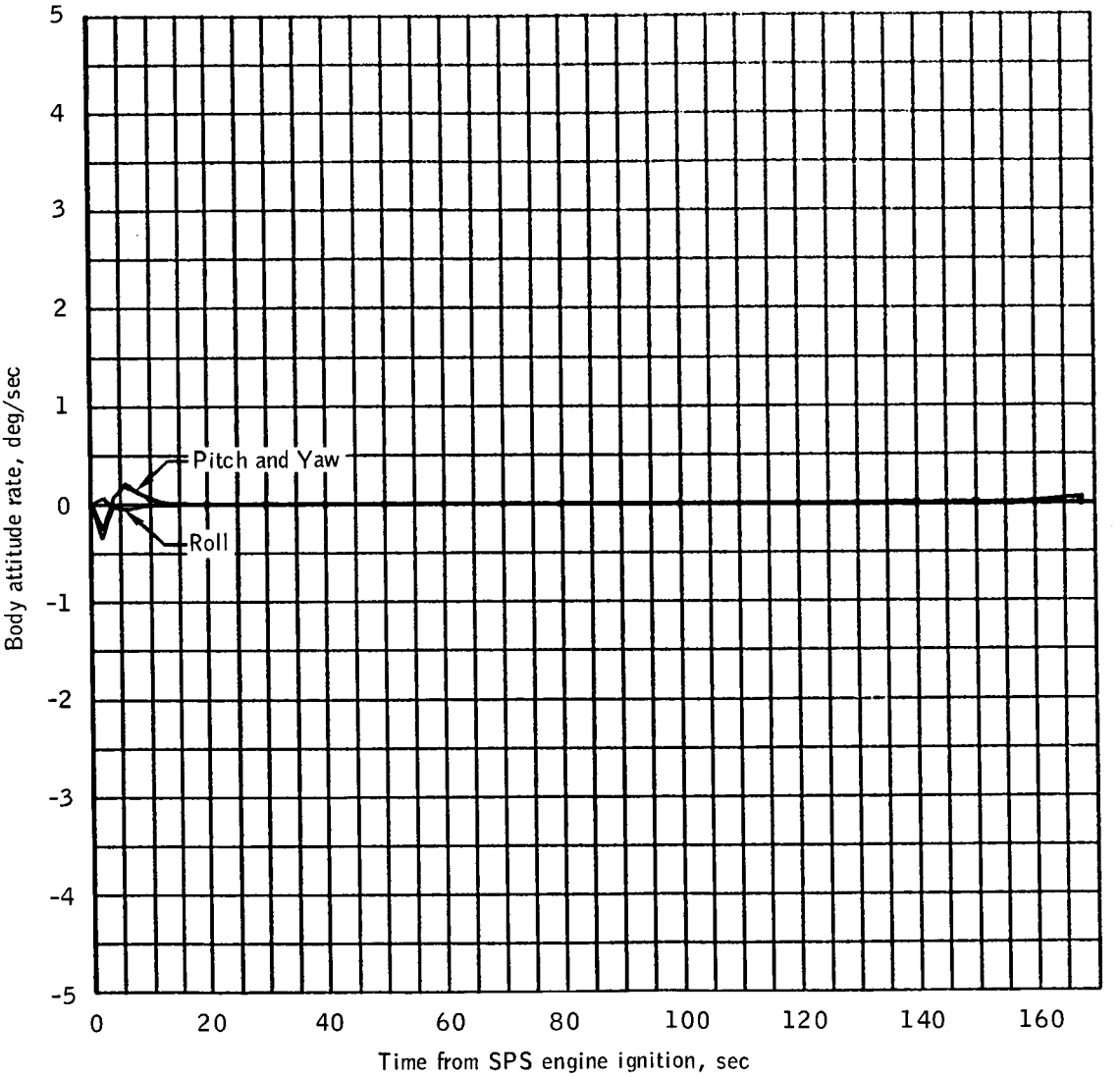

(b) Body attitude rates, FDAI-1.

Figure 5.- Continued.

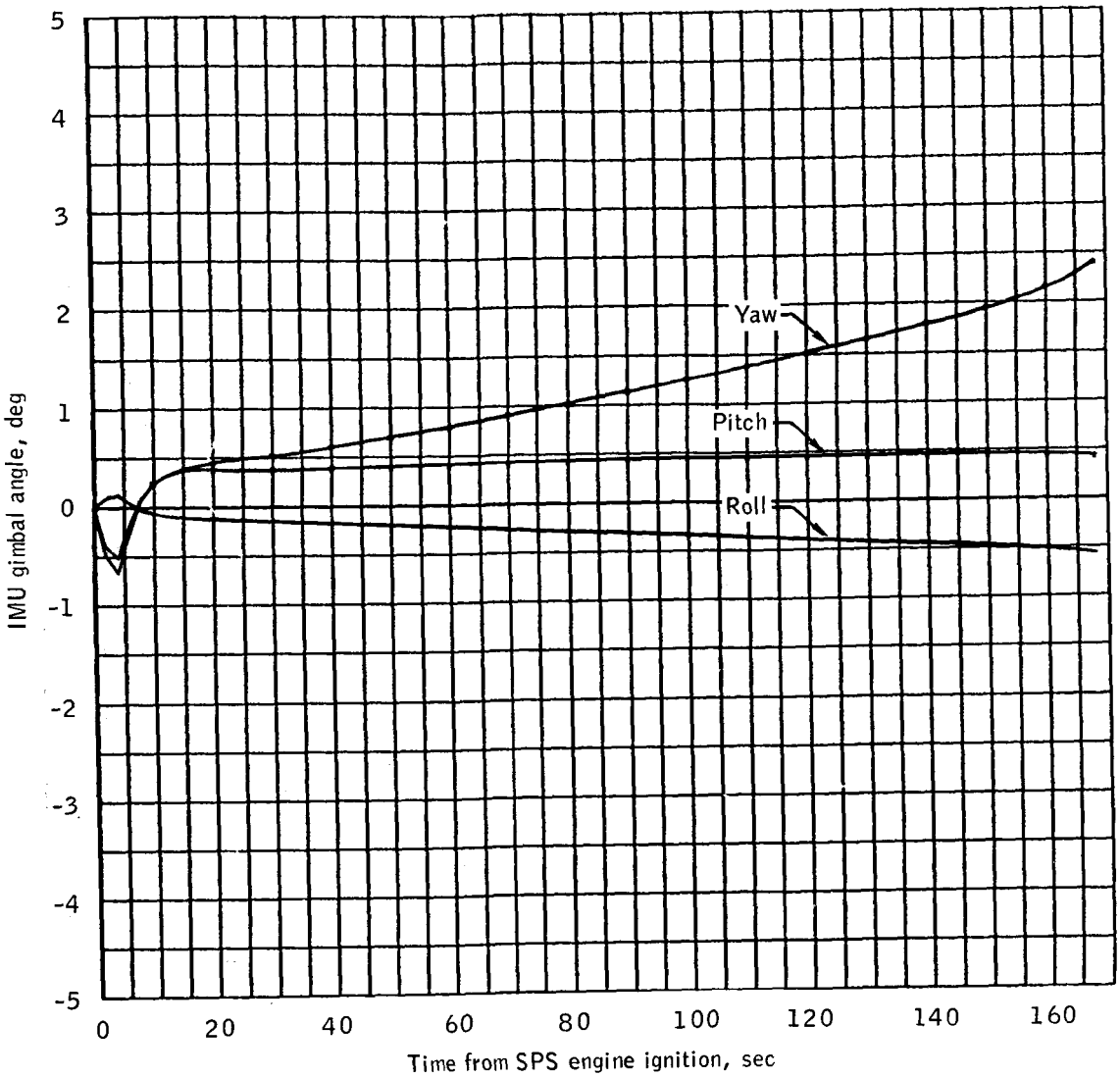

(c) IMU gimbal angles.

Figure 5.- Continued.

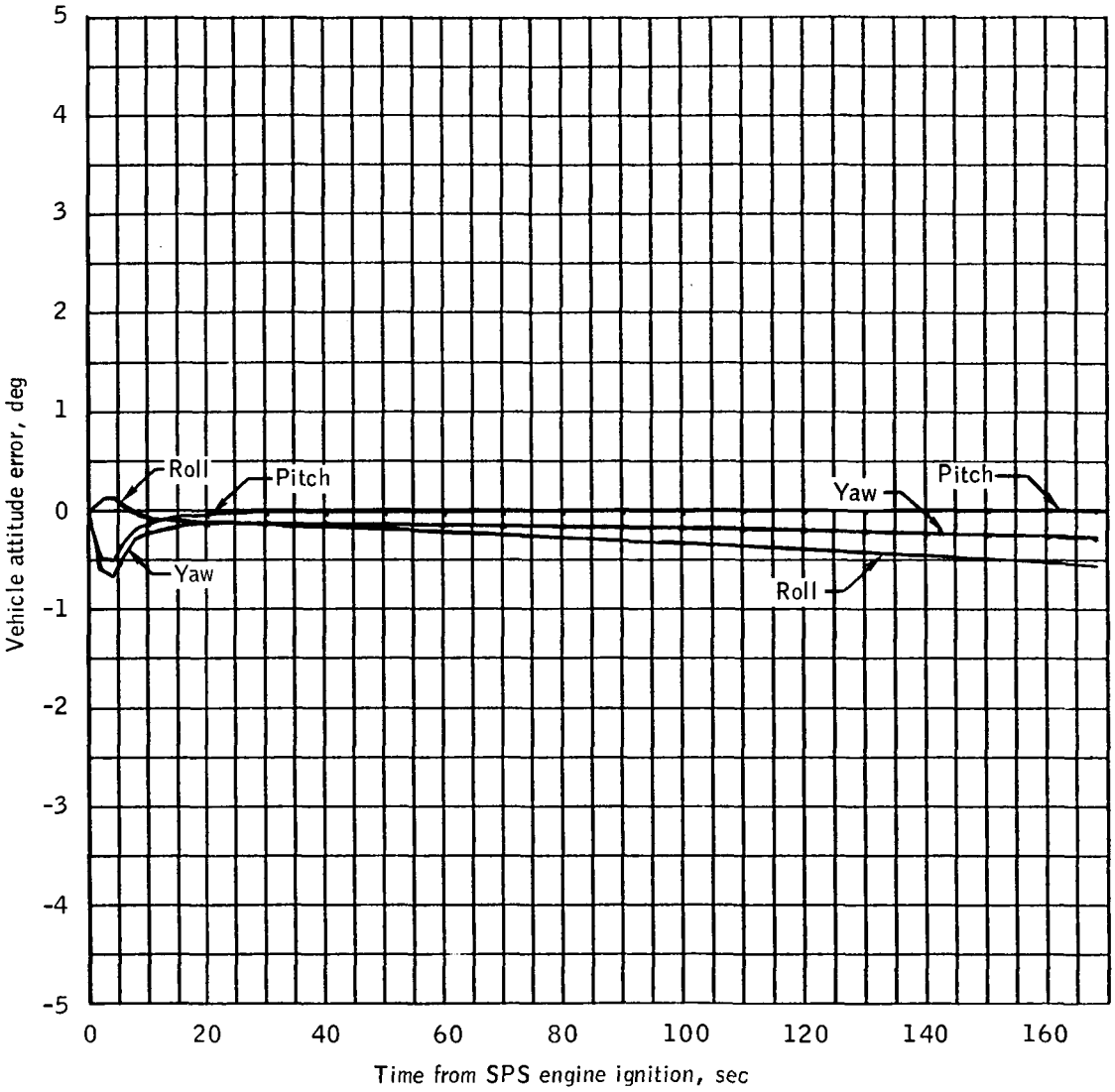

(d) Vehicle attitude errors.

Figure 5.- Continued.

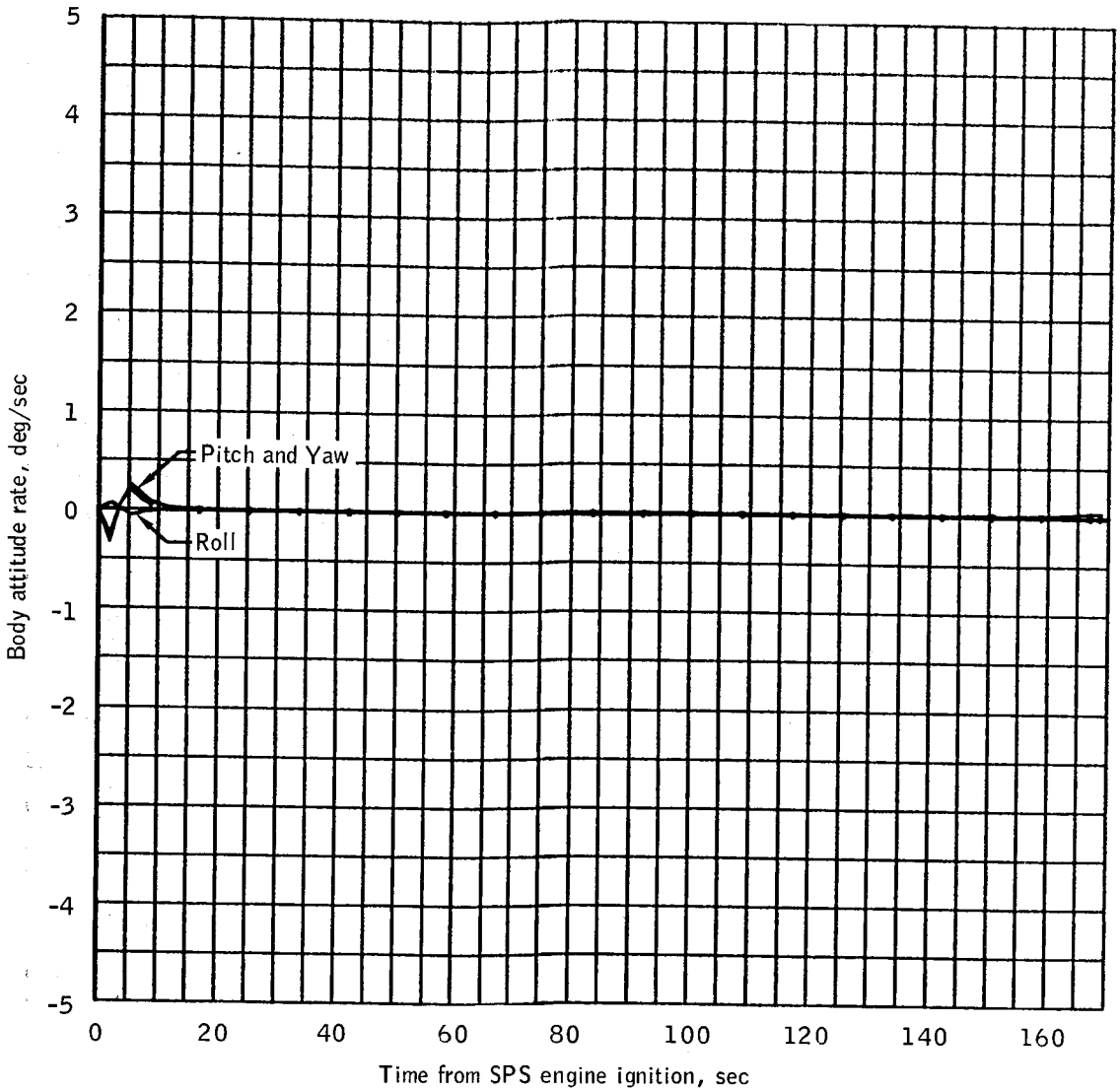

(e) Body attitude rates, FDAI-2.

Figure 5.- Continued.

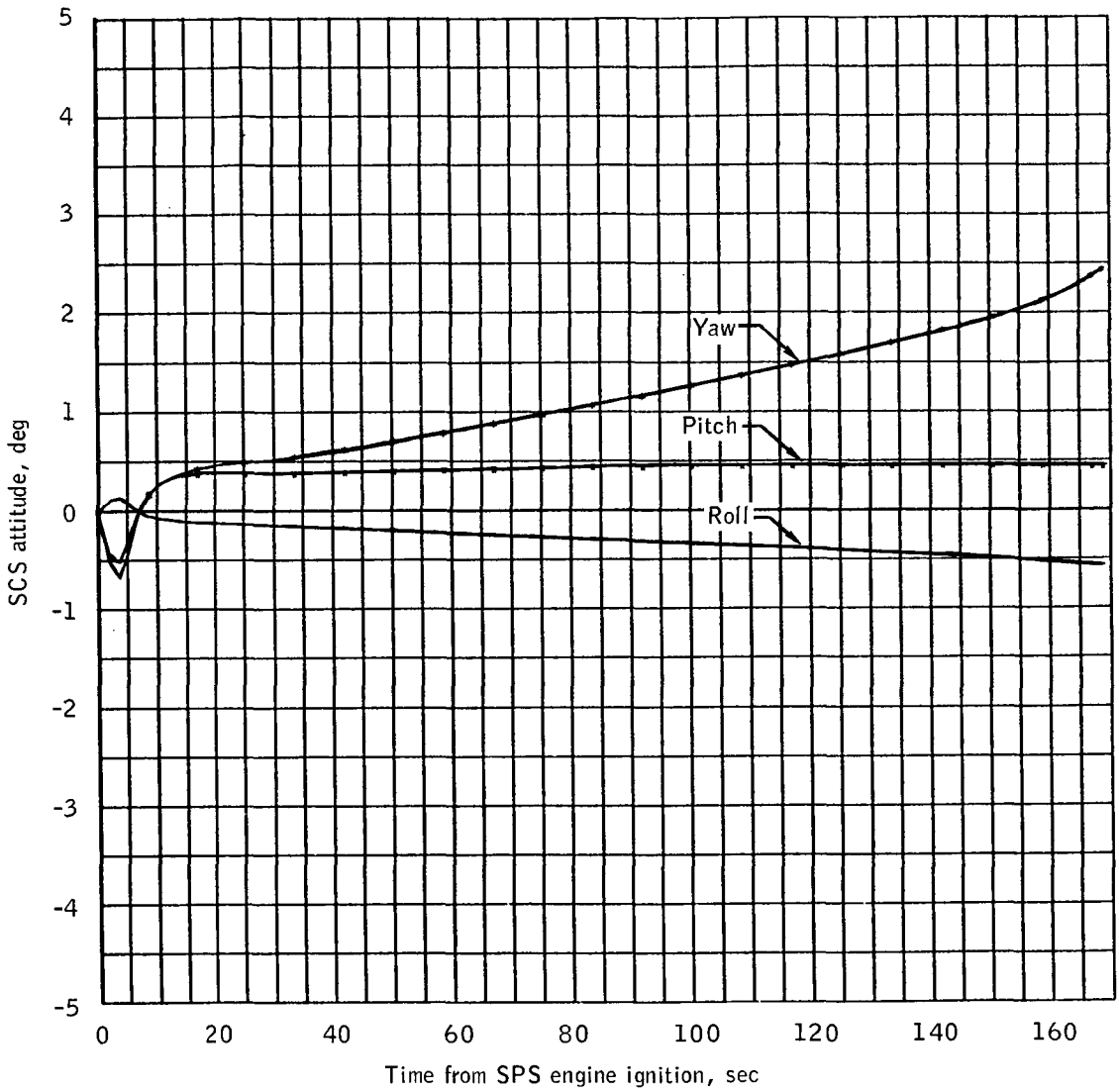

(f) SCS attitudes monitored from BMAGS.

Figure 5.- Continued.

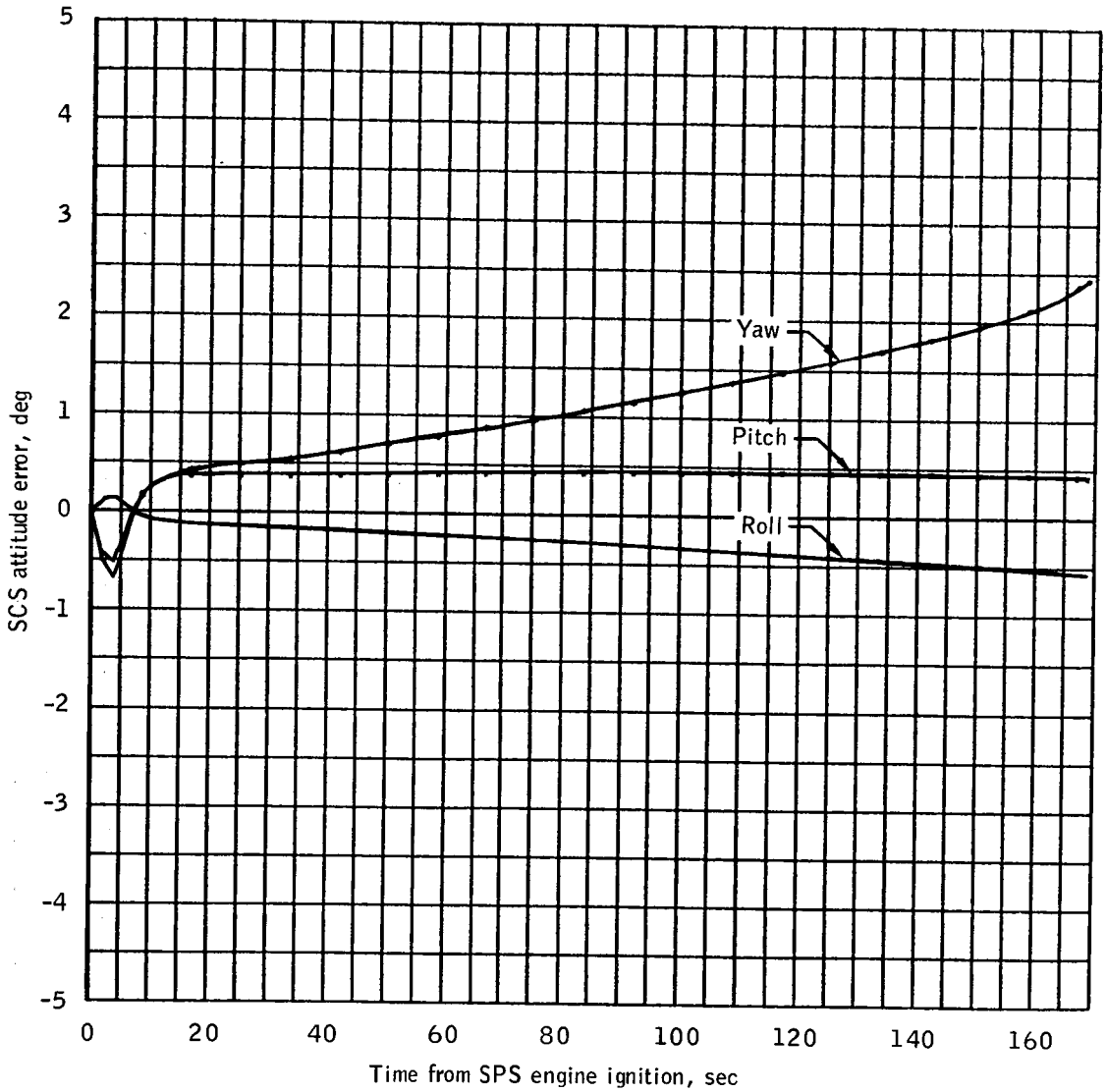

(g) SCS attitude errors monitored from BMAGS.

Figure 5.- Continued.

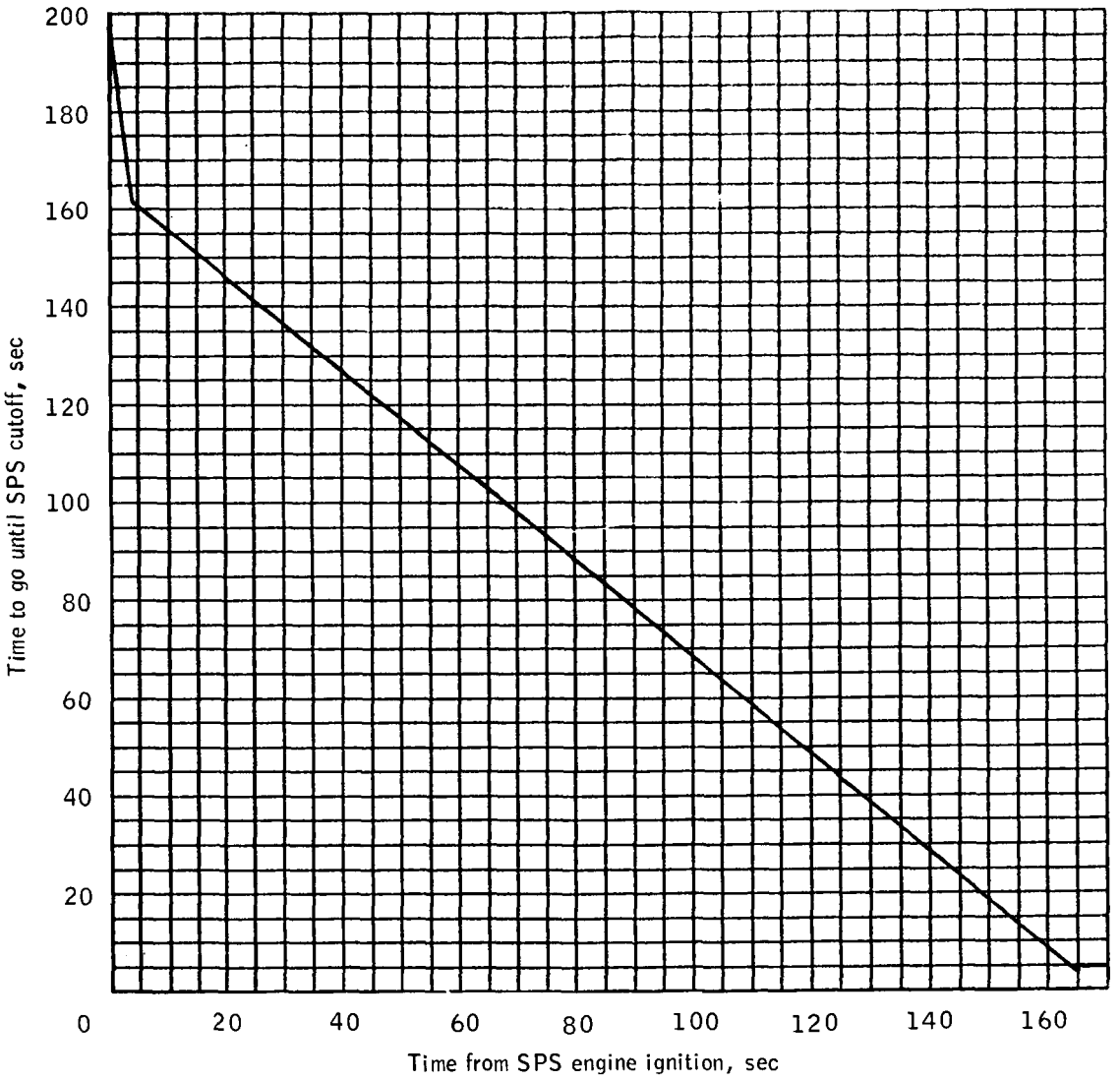

(h) Time to go until SPS cutoff.

Figure 5.- Continued.

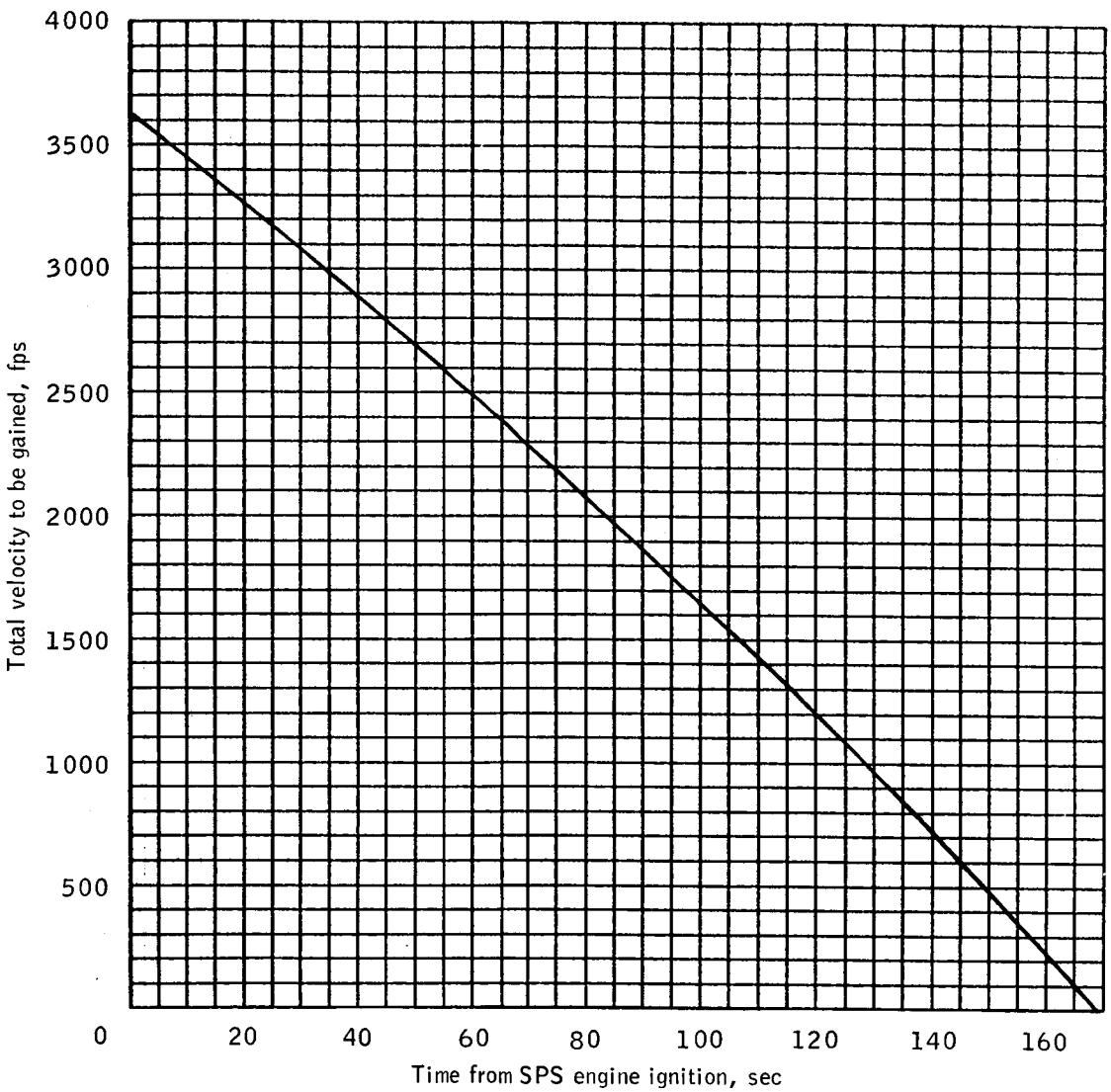

(i) Total velocity to be gained until SPS cutoff.

Figure 5.- Continued.

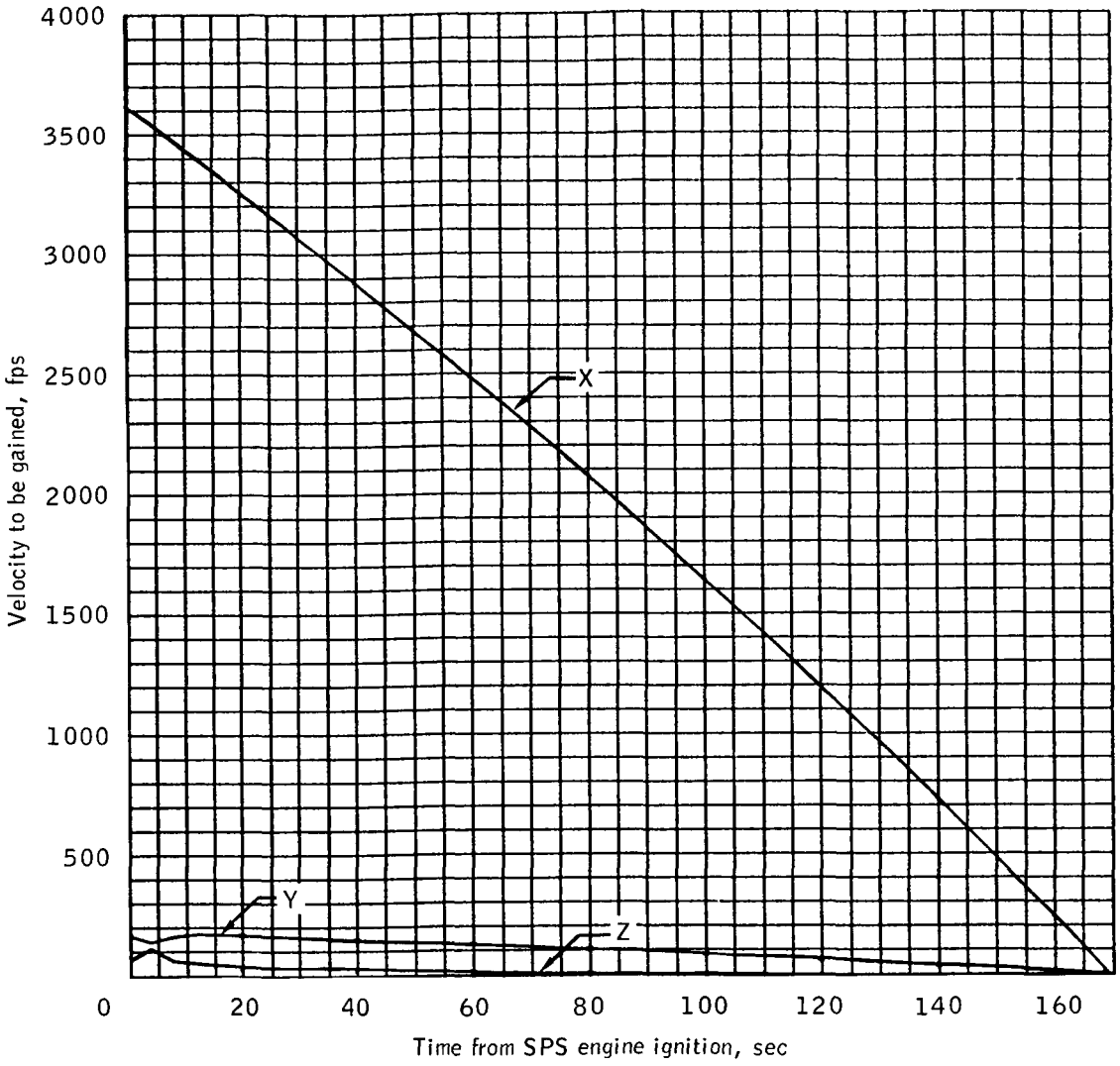

(j) Velocity to be gained in control coordinates.

Figure 5.- Continued.

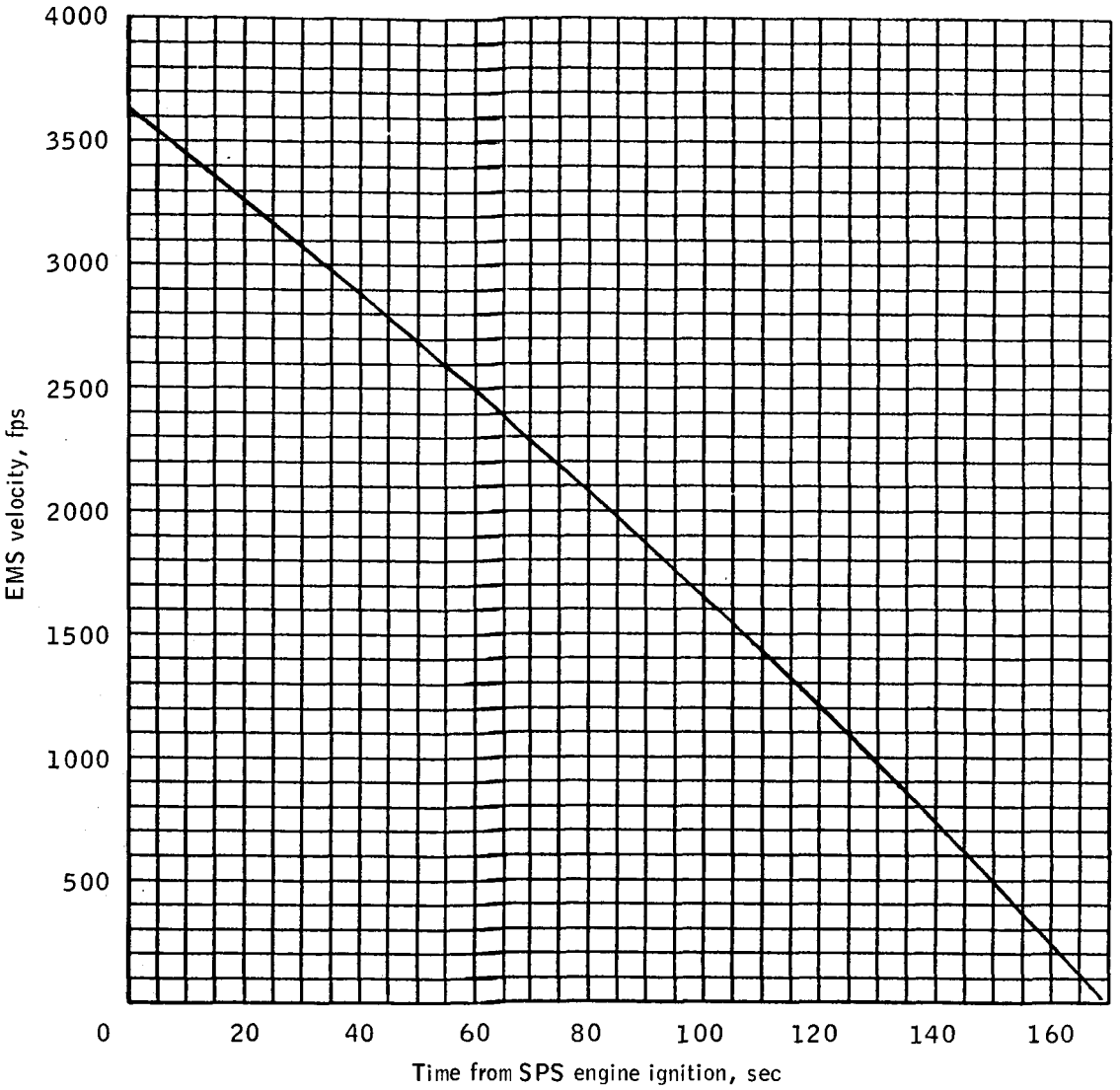

(k) EMS velocity.

Figure 5.- Continued.

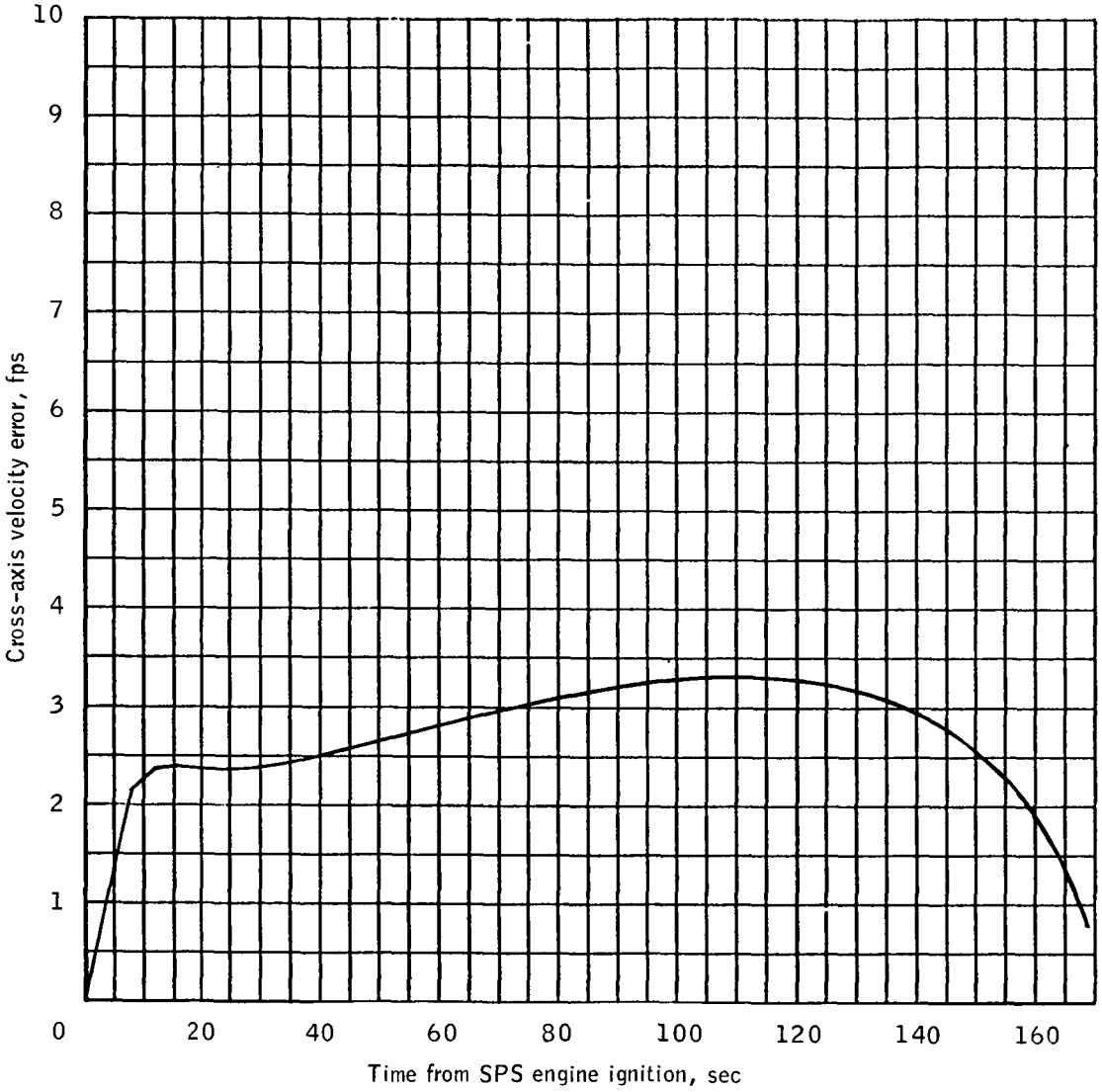

(l) Cross-axis velocity error.

Figure 5.- Continued.

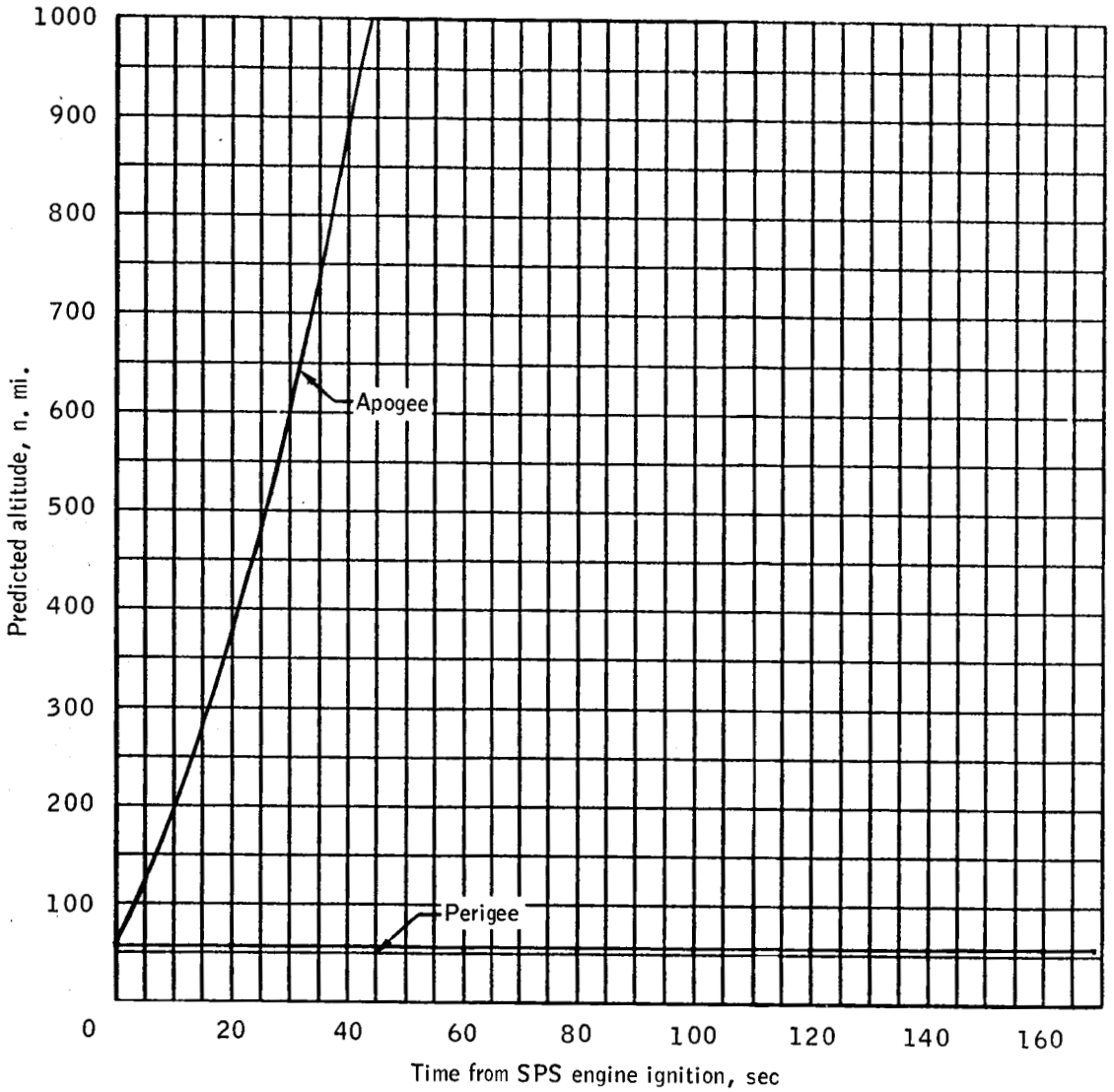

(m) Predicted apogee and perigee altitudes.

Figure 5.- Continued.

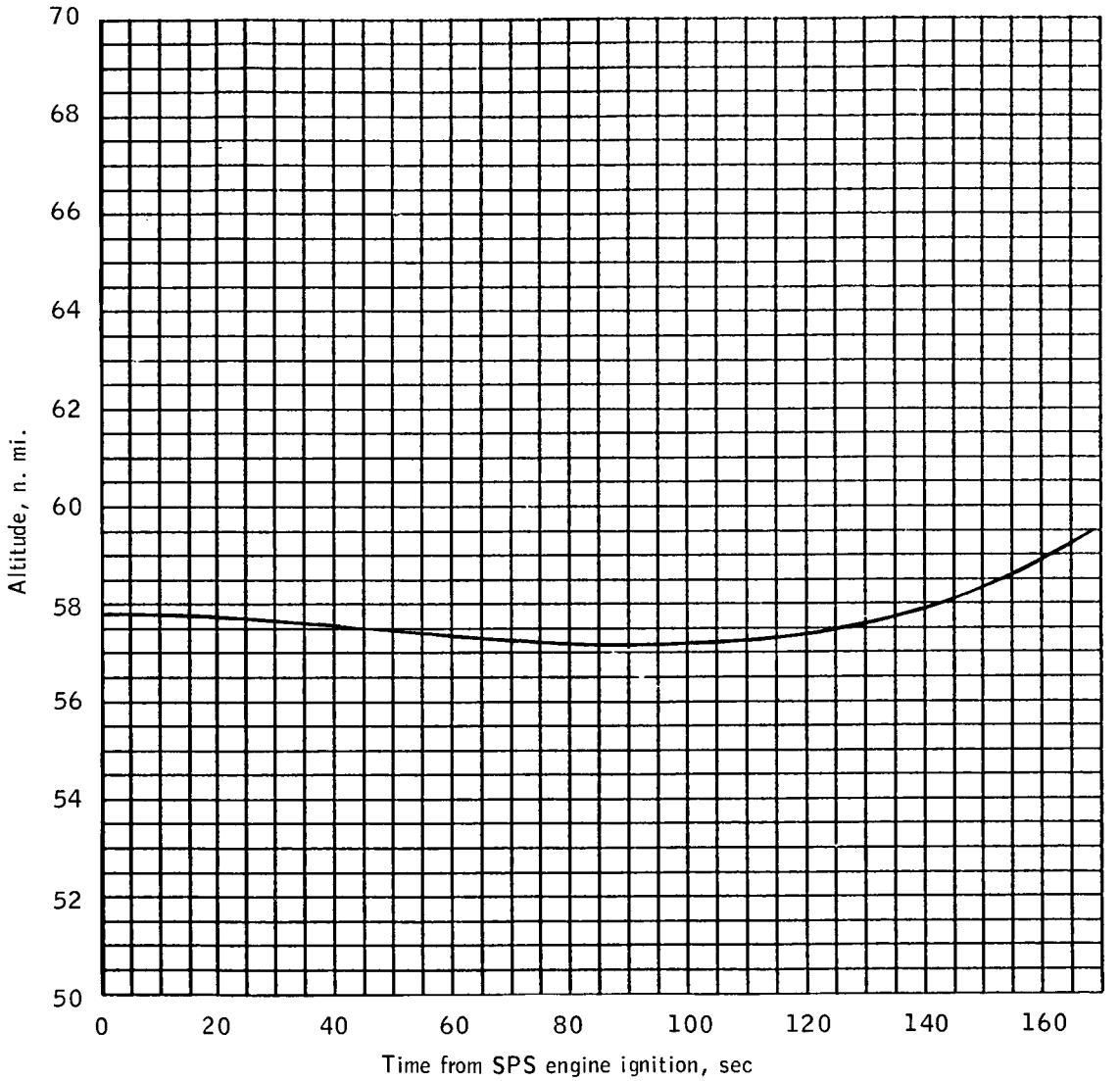

(n) Altitude.

Figure 5.- Continued.

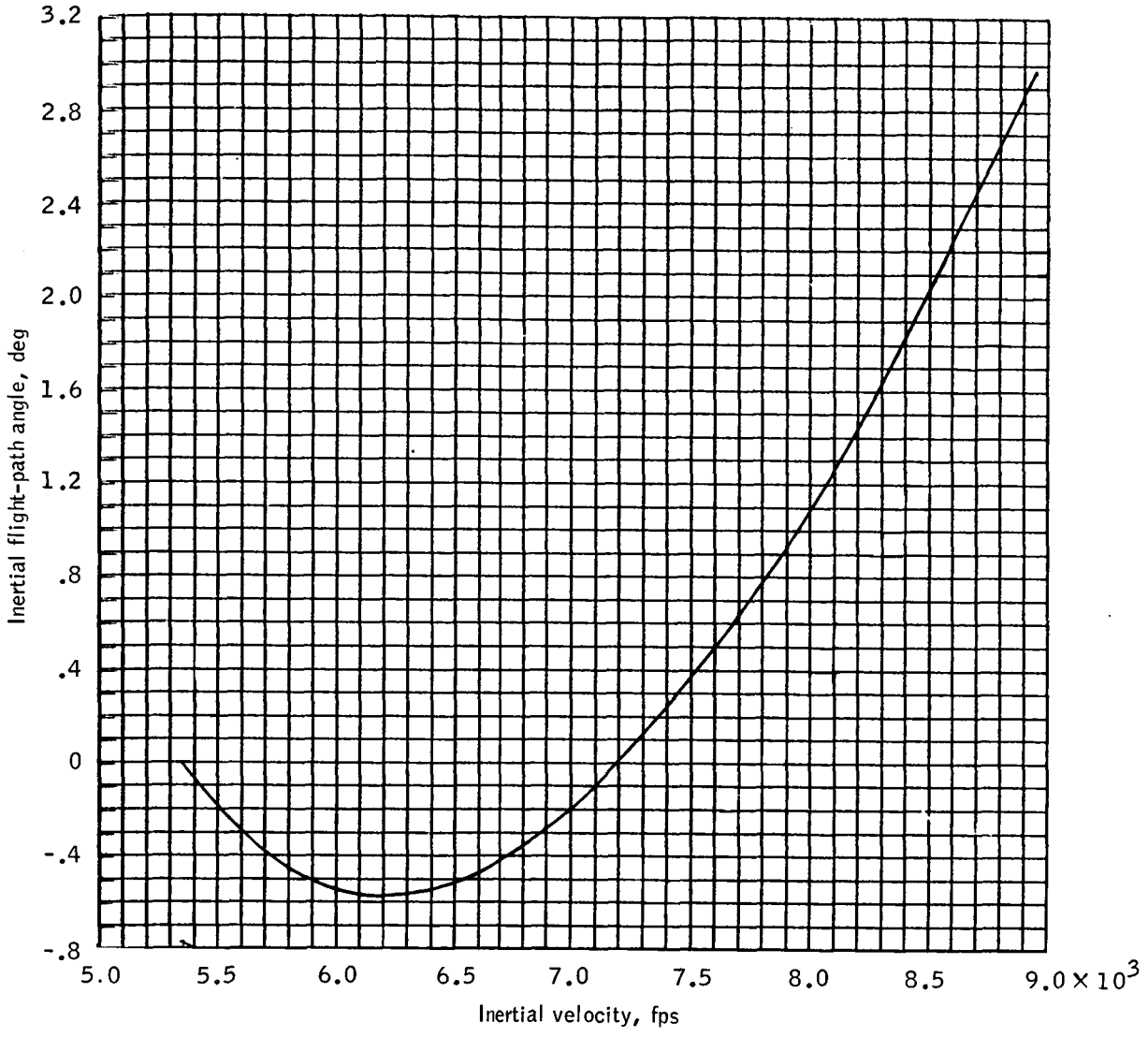

(o) Inertial flight-path angle versus inertial velocity.

Figure 5.- Concluded.

6.0 REFERENCES

1. MIT: Guidance System Operations Plan for Manned CM Earth Orbital and Lunar Missions Using Program COLOSSUS 2 (Comanche Rev. 44), Section 3 Digital Autopilots (Rev. 4). February 1969.

2. MSC: CSM/LM Spacecraft Operational Data Book, Volume III - Mass Mass Properties, Revision 1. (SNA-8-D-027(III), November 1968.

3. Wells, J. L., Jr.: Uncertainty in SPS Thrust Vector Misalinement for AS-205/101 Mission. MSC memo 67-FM7-320, December 1, 1967.

4. Wells, J. L., Jr.; and Beggs, Don R.: Apollo 9 Monitoring Analysis for Each Powered Maneuver. MSC IN 69-FM-54, February 28, 1969.